SYNTHESIS, CHARACTERIZATION AND EVALUATION OF ZEOLITES FOR HYDRO-ISOMERIZATION OF MODEL FEED N-HEXADECANE

A project report

submitted in partial fulfillment of the requirements

for the award of the degree of

MASTER of TECHNOLOGY

in

CHEMICAL ENGINEERING

SPECIALISATION : CATALYSIS TECHNOLOGY

by

SUNIL MEHLA

(CA10M005)

Under the Guidance of

PROFESSOR K.R. KRISHNAMURTHY

DR. B.L. NEWALKAR

PROFESSOR R. RAMNARAYANAN

DEPARTMENT OF CHEMICAL ENGINEERING

INDIAN INSTITUTE OF TECHNOLOGY – MADRAS

CHENNAI 600 036

MAY, 2012

CERTIFICATE

This is to certify that the thesis entitled "**Synthesis, Characterization and Evaluation of Zeolites for Hydroisomerization Applications"**, submitted by **Mr. SUNIL MEHLA (CA10M005)** to the Indian Institute of Technology-Madras, Chennai for the award of the degree of **Master of Technology in Catalysis Technology (Chemical Engineering)**, is a *bona-fide* record of the work carried out by him under our supervision. The contents of this thesis, in full or in parts, have not been submitted to any other Institute or University for the award of any degree.

Co-Guide
PROF. K. R. KRISHNAMURTHY
National Centre for Catalysis Research
IIT-Madras, Chennai 600 036

Co-Guide
Dr. B.L. NEWALKAR
Corporate R&D Centre
Bharat Petroleum Corporation Limited
Plot 2A, Udyog Kendra,
Greater Noida-201 306

Guide

Dr. RAMNARAYANAN
Department of Chemical Engineering
IIT-Madras, Chennai 600 036

Place: CHENNAI

Date : April 30, 2012

ACKNOWLEDGEMENTS

I am very much grateful to my research co-guide **Prof. K.R. Krishnamurthy** for his constant encouragement, thought provoking discussions, critical ideas, support, invaluable suggestions and unfailing guidance at every stage of the research program. It gives me immense pleasure to have been associated with him. I thank him for his patient guidance, open discussions, constant encouragement, unbounded enthusiasm and interest.

I am very much grateful to my research co-guide **Dr. B. L. Newalkar** for his constant encouragement, thought provoking discussions, critical ideas, support, invaluable suggestions and unfailing guidance at every stage of the research programme. It gives me immense pleasure to have been associated with him. I thank him for his patient guidance, open discussions, constant encouragement, unbounded enthusiasm and interest.

I am very much grateful to **Dr. R. Ramnarayanan**, my research guide, for his constant encouragement, support and invaluable suggestions.

I express my sincere gratitude to **Prof. B. Viswanathan** for his inspiring, invaluable guidance, constant encouragement and thought provoking discussions throughout the research work. I am really grateful to him for providing opportunities to learn various aspects in catalysis and material synthesis. I feel privileged to have been associated with him. It is my privilege to express my gratitude to him for introducing me to the field of catalysis.

I express my sincere gratitude to **Prof. S. Sivasankar** for his inspiring, invaluable guidance, constant encouragement and thought provoking discussions throughout the research work. I am really grateful to him for providing opportunities to learn various aspects in catalysis and material synthesis. I feel privileged to have been associated with him. It is my privilege to express my gratitude to him for introducing me to the field of catalysis.

I wish to thank **NCCR, Department of Chemical Engineering, Bharat Petroleum Corporation Limited, BPCL Corporate R&D** and **IIT Madras** for providing opportunity and all facilities to carry out my project.

I express my deep gratitude to **Prof. S. Pushpavanam**, Head, Department of Chemical Engineering and **Prof. B. Viswanathan**, Head, National Centre for Catalysis Research and other faculty members of our departments for the support and facilities provided in carrying out this project work.

I am thankful to **Dr. S. Pai, Dr. Y. Niwate and Mr. Matthew** for their unrelenting support, guidance, help, encouragement and cooperation throughout the span of the project.

I express my sincere thanks to my **Mr. Kishore, Mr. Lalit, Mr. Snehal** for their kindly help, suggestions and support.

I express my sincere thanks to my seniors and colleagues, **Mr. Vamsi Krishna, Mr. Mahendran, Mr. Sankaranarayanan, Mr. Muthu Krishnan, Mr. Prakash,** and **Ms. Vijayashanthi,** for their kindly help, suggestions and support.

I wish to express my thanks to support staff, **Mr. Chandan** and **Mr. Ranjeet** at BPCL, Corporate R&D, Greater Noida, for their kindly help and support.

I am deeply indebted to my father, **Mr. M. S. Mehla,** mother, **Mrs. K. Lakshmi,** sister Ms. **S. Mehla** and friend **Mr. M. Sachan** for their constant support and encouragement whenever needed, without them it would have been impossible for me to complete this work.

ABSTRACT

KEYWORDS: Hydroisomerization, lube oil base stocks (LOBS), bifunctional catalyst, zeolites, ZSM-12 (MTW), ZSM-22 (TON), ZSM-23 (MTT)

The scope of this thesis was to understand the synthesis chemistry of zeolites ZSM-12, ZSM-22 and ZSM-23. The primary focus was the synthesis of ZSM-12. The above mentioned zeolites were evaluated as support material for the hydroisomerization of n-hexadecane. Some conclusions are suggested about zeolite framework type and potential applications.

Significant improvements in oil refining processes due to environmental considerations led to hydroisomerization of n-paraffins as an important and integral part of refining processes for improving the quality of fuels and lube oils. Subsequently, hydroisomerization of n-paraffins had seen significant improvements both in terms of catalyst design and processes. Hydroisomerization of long chain paraffins to iso-paraffins, to obtain Grade II and Grade III lube oil based stocks (LOBS) with excellent cold flow properties and superior yields, had depicted an immense growth owing to the emergent demand for high quality lube oils for automobile and industrial applications. Hydroisomerization for conventional diesel dewaxing and renewable diesel dewaxing had boosted the yields of diesel fuels to meet the ever rising demand.

Typically hydroisomerization of n-paraffins was done over bifunctional catalysts containing mild acid sites for skeletal isomerization via carbenium ions and metallic sites for hydrogenation and dehydrogenation function. Zeolites were an important class of materials for use as a support in the hydroisomerization reaction because of their inherent acidity and molecular sieving property. Among the available 201 zeolite frameworks, only certain frameworks, with desired acidity, pore size and textural properties were useful in the hydroisomerization application. Specifically medium pore zeolites with mild acidity (high Si/Al ratios) had potential for the hydroisomerization application.

The synthesis of zeolites was another interesting aspect indirectly related to the performance of a zeolite as support in the hydroisomerization reaction. The zeolites were characterized and compared in terms of certain properties which had a direct correlation with the performance of the zeolite. These properties of zeolites like acidity, BET surface area, crystal size and morphology could be tailored via synthesis methods. Since the above properties had a direct effect on the performance of a zeolite, a thorough understanding of the synthesis methods was necessary to have good control over the desired properties.

TABLE OF CONTENTS

CHAPTER 1 **INTRODUCTION AND LITERATURE SURVEY**

CHAPTER 2 **EXPERIMENTAL METHODS**

***CHAPTER 3* RESULTS AND DISCUSSIONS**

***CHAPTER 4* SUMMARY AND CONCLUSIONS**

LIST OF FIGURES

Title **Page No.**

LIST OF TABLES

Title **Page No.**

ABBREVIATIONS

API	American Petroleum Institute
BET	Brunauer Emmett Teller
BPR	Back Pressure Regulator
BTMACl	Benzyltrimethylammonium Chloride
FID	Flame Ionization Detector
GC	Gas Chromatography
GRM	Gross Refinery Margin
HPLC	High Performance Liquid Chromatography
IZA	International Zeolite Association
LOBS	Lube Oil Base Stocks
MFC	Mass Flow Controller
MTEABr	Methyltriethylammonium Bromide
PAO	Poly Alpha Olefins
PG	Pressure Gauge
RGA	Refinery Gas Analyzer
SAPO	Silica Alumino Phosphates
SAR	Silica Alumina Ratio
SDA	Structure Directing Agent
SEM	Scanning Electron Microscopy

TCD	Thermal Conductivity Detector
TEABr	Tetraethylammonium Bromide
TEAOH	Tetraethylammonium Hydroxide
TEA^+	Tetraethylammonium Cations
TIC	Temperature Indicator Controller
TPD	Temperature Programmed Desorption
VI	Viscosity Index
WHSV	Weight Hourly Space Velocity
XRD	X-ray Diffraction
ZSM	Zeolite Socony Mobil

NOTATIONS

Å	Angstrom
θ	Angle (degrees)
λ	Wavelength
hr	hour
min	minutes
°C	Degree Celsius
T	Temperature
X	Conversion
S	Selectivity
P	Pressure
V	Volume
P/P_0	Relative Pressure
I/I0	Relative Intensity
cm	centimeter
mm	millimeter
µm	micrometer
µmol	micromoles

Si/Al	Silicon to Aluminum molar ratio
OH/Si	Hydroxyl ion to Silicon molar ratio
Na/Si	Sodium ion to Silicon molar ratio
H_2O/Si	Water to Silicon molar ratio
R/Si	Organic Structure Directing Agent to Silicon molar ratio
Multi/Mono	Percentage of multibranched to percentage of monobranched isomers ratio

CHAPTER 1

INTRODUCTION AND LITERATURE SURVEY

1.1 INTRODUCTION

The operation of modern refinery was becoming more and more complex to meet the stringent transport fuel specifications as well as to answer the increasing global environmental concerns. Hydroisomerization based dewaxing emerged as the preferred route for the production of lube oil based stocks (LOBS) in the nineties owing to the futuristic demands for base oils in terms of high purity, high viscosity index, lower volatility and longer life. (Sequeira, 1994). Lube base oils produced by hydroisomerization based dewaxing in conjunction with hydrofinishing and severe hydrocracking, offered the following attractive features:

- Very high viscosity index (100-130)
- Low volatility
- Superior oxidation resistance
- High thermal stability
- Excellent low temperature fluidity
- Low toxicity

In terms of composition, the above features were obtained by increasing the iso-paraffins and maximizing saturates by means of hydroisomerization and hydrofinishing steps respectively. Table 1.1 summarized the effect of type of hydrocarbon on the properties of lubricants and the desired amount of that hydrocarbon in the lubricant composition (Sequeira, 1994). The above mentioned features gave as good performance characteristics to finished lubricants as synthetic lubricants such as poly alpha olefins (PAO). To classify the various lubricants in order of their performance the American Petrochemical Institute had established a base oil classification, given in Table 1.2.(API publication 1509, 1996)

Table 1.1: Lube oil components and their properties (Sequeira, 1994)

Hydrocarbon Type	Viscosity	Viscosity index	Pour point	Stability	Value in lube oil
n-Paraffins (wax)	Low	High	High	High	Very low
i-Paraffins	Medium	High	Medium	Medium	High
Naphthenes	High	Low	Low.	Medium	Medium
Aromatics	High	Low	Low	Low	Very low

Table 1.2: API classification of base oils (API publication 1509, 1996)

Group	Saturate wt %	Sulphur wt %	Viscosity Index
I	< 90 and/or	> 0.03	> 80 to < 120
II	≥ 90 and	≤ 0.03	≥ 80 to ≤ 120
III	≥ 90	≤ 0.03	≥ 120
IV	All poly alpha olefins (PAOs)		
V	All base stocks not included in Groups I-IV		

The study of hydroisomerization of long chain paraffins was relevant to the lubricant oil dewaxing process aimed to decrease the pour point with viscosity index to remain as high as possible. Similarly understanding of hydroisomerization of n-praffins was required for renewable and conventional diesel oil dewaxing processes to reduce the pour point with no limitation on change in viscosity index.

The current hydroisomerization scenario was a result of step by step advances in lube oil processing technologies over the last three decades. This chapter was aimed to understand the chemistry behind the evolution of these processes and catalysts.

1.2 PROCESS THERMODYNAMICS AND CATALYST CHEMISTRY

Hydroisomerization of n-paraffins was a thermodynamic equilibrium governed exothermic reaction with heat changes in the range of -4 kJ/mol to -20 kJ/mol. The reaction occured without any variation in the number of moles and was therefore not influenced by variations in pressure (Leprince, 2001).

The hydroisomerization reaction was always accompanied by a hydrocracking reaction leading to a decrease in the yield of isomerized hydrocarbons. The product distribution was governed by the relative rates of isomerization and cracking reactions. The length of hydrocarbons in the feed was an important factor on which the rates of competitive hydroisomerization and hydrocracking reactions were strongly dependent (Deldari *et al.*, 2005). Cracking of light alkanes such as n-hexane could take place only through the secondary carbenium ions as transition states, leading to a high selectivity towards isomerization. On the other hand, multibranched isomers of long chain paraffins had better adsorption on catalyst surface as compared to the short chain multibranched isomers of C_5 and C_6 paraffins constituting light naphtha (Deldari *et al.*, 2005). Due to better adsorption of multibranched isomers of long chain paraffins on catalyst surface, the time spent near active sites increased, thereby leading to more cracked products and low isomerization selectivity. Thus in order to increase isomerization selectivity, multibranching must be limited at its most optimum level, in the sense that multibranching is feasible but further cracking of hydrocarbons did not take place. Based on the above mentioned criteria, a good hydroisomerization catalyst must favor the hydroisomerization reaction over the hydrocracking reaction.

Typical hydroisomerization catalysts were bifunctional in nature and consist of two functions, a hydrogenating/dehydrogenating function contributed by the presence of a noble metal in metallic state and an isomerization function contributed by the presence of acidic sites on the support surface. The acid function was responsible for the isomerization and cracking of the olefinic intermediates formed over the metal sites. The need for a balance between the two functions was obvious owing to the preference for saturates in the product distribution, controlled by the dehydrogenating and hydrogenating function with a substantial increase in isomerized products compared to cracked products, governed by the strength of acid sites. A perfect balance between acid and metal functions led to an ideal bifunctional catalyst. Over these ideal bifunctional catalysts, hydrogenation and dehydrogenation reactions occurred rapidly and the rearrangements of the hydrocarbon intermediates over the acid sites constituted the rate determining steps. As a consequence, the hydroisomerization and hydrocracking reactions appeared to occur consecutively, with the sequence of products being monobranched isomers, multibranched isomers and then cracked products (Deldari *et al.,* 2005). A pictorial representation of the governing mechanism is shown in figure 1.01.

Figure 1.01: Mechanism behind hydroisomerization and hydrocracking (Deldari, *et al.,* 2005).

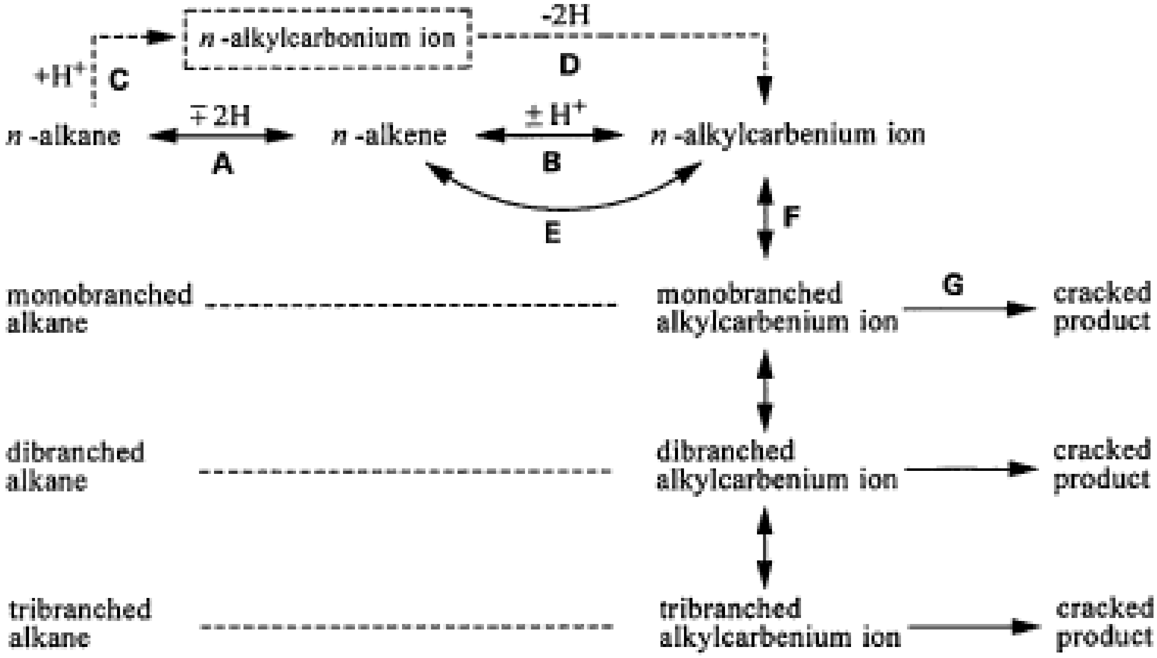

where

A: hydrogenation-dehydrogenation on metal sites

B: Protonation-deprotonation on acid sites

C: Addition of proton to form alkyl carbonium ion on acid sites

D: Dehydrogenation to form alkyl carbenium ion

E: Competitive adsorption-desorption of alkene and carbenium ion on acid sites

F: Rearrangement of alkyl carbenium ion

G: Cracking of alkyl carbenium ion

In view of the above description a successful hydroisomerization scheme was as follows:

- Dehydrogenation on the metal.
- Protonation of olefins on the Brönsted acid sites with formation of a secondary alkyl carbenium ion.
- Rearrangement of the alkyl carbenium ion via formation of cyclic alkyl carbenium type transition state.
- Deprotonation.
- Hydrogenation on the metal.

Thus it was evident that the ideal hydroisomerization catalyst must have an optimum balance between metal and acid functions to favor isomerization. The degree of isomerization in terms of branching was usually dependent on the targeted applications.. For example, in case of long chain n-paraffins mono- and di-branched-paraffins were more preferred as lube oil components in order to meet the pour point and viscosity index parameter for lube oil whereas isomerization to the multibranched level was permissible in the case of renewable and conventional diesel dewaxing where the primary concern was the lowering of pour point and viscosity index parameter was more flexible. Therefore, it was but obvious that catalyst requirements differ for light naphtha and lube/diesel range paraffin isomerization, respectively. Further the choice of catalyst for long chain n-paraffins was governed by the desired application.

1.3 ZEOLITES AS SUPPORT FOR HYDROISOMERIZATION CATALYSTS

Zeolites were three dimensional microcrystalline silicates and aluminosilicates. The basic building blocks of zeolite structures were the silica (SiO_4) and the alumina (AlO_4) tetrahedra joined together by sharing oxygen atoms. However the recent discoveries of materials virtually identical to the classical zeolites but containing oxide structures of elements other than silicon and aluminum had expanded the definition of zeolites.

A three dimensional network comprising only of silicon tetrahedra was neutral. When an aluminum tetrahedra was incorporated in the structure a formal negative charge appeared on the structure which had to be balanced by a positive ion to maintain the neutrality and stability of the structure. When the positive counter-ion was a proton, the zeolite was bound to have acidity, namely bronsted acidity. These protons were lost at high temperatures as water molecules leading to the formation of lewis acid sites. The interconversion of bronsted sites to lewis sites and vice versa is shown in figure 1.02 (Lercher, *et al.*, 2002)

Figure 1.02: Interconversion of bronsted and lewis acid sites (Lercher, et al., 2002)

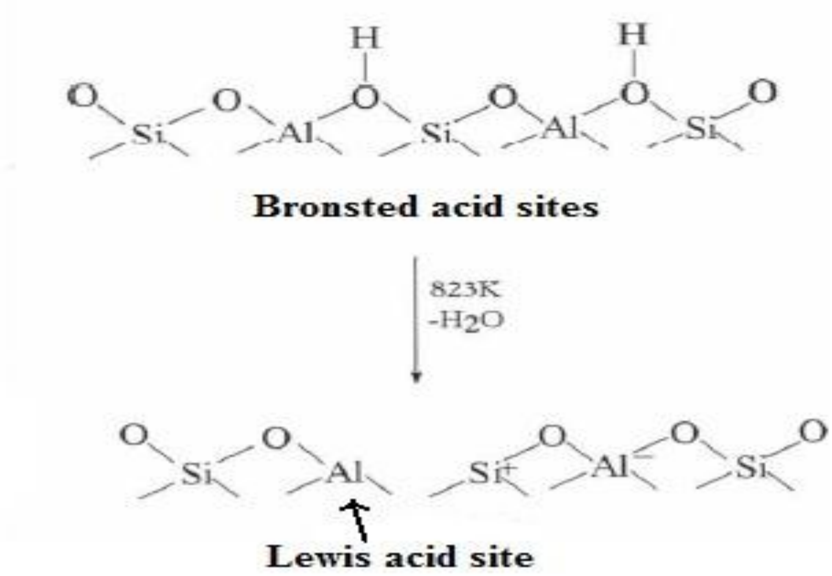

Zeolites were generally classified into three categories namely small, medium, and large pore zeolites (Szostak, 1989). The strength and number of acidic sites in zeolite frameworks was dependent on the framework Si/Al ratio. The framework acidity strength was found to increase with an increase in framework aluminium content. The unique pore size of ~5–7 Å for medium pore zeolites offered shape selectivity in terms of reactant, product, and transition state selectivity, as displayed in Fig. 1.3 (Trap *et al.,* 2000 and Sugi *et al.,* 1994).

Figure 1.03: Molecular shape selectivity in zeolites (Sugi *et al.,* 1994)

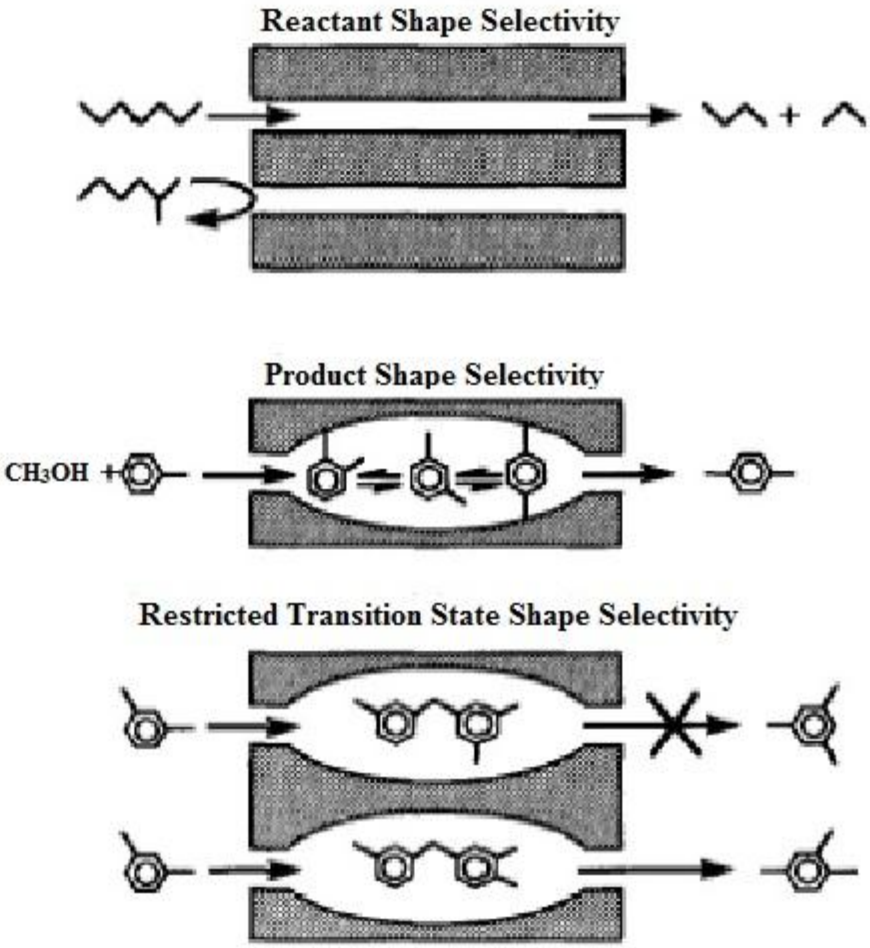

Initially alumina supports were mostly used in the industry for various applications. However difficulties were faced in controlling the acidity of the catalyst which led to undesired cracked products and reduction in life of the catalyst by coke deposition. The advent of zeolite technology was initially inspired by the inherent molecular sieving properties of these materials. Together with this inherent shape selectivity, the hydrophobic nature of high silica zeolites, well defined porous networks, low coke deposition and easy regeneration rendered zeolite into popular supports for various refinery catalysts, including hydroisomerization.

The advantages of using zeolite as supports for hydroisomerization catalysts therefore were:

- controlled acidity levels by tuning Si/Al ratio
- molecular shape selectivity
- low coking tendencies
- high hydrophobicity with an increase in Si/Al ratio
- high aromatic, organic nitrogen, and sulfur resistance
- easy regeneration ability;

1.4 HYDROTHERMAL ZEOLITE SYNTHESIS

Efforts to synthesize zeolites in the laboratory could be traced back to St Claire Deville in 1862 (Deville, 1862). However zeolite synthesis in the form we understood today was inspired by the works of Richar Barrer and Robert Milton in late 1940s where they worked on the conversion of known mineral phases at high temperatures (170°C-200°C) under the action of strong salt solutions (Barrer *et al.,* 1948). The initial research in the field of zeolite synthesis was focused on the synthesis of new structures under thermal conditions. The major breakthrough occurred in 1961 when two groups of workers described the effect of introducing quaternary ammonium cations into zeolite synthesis. Barrer and Denny described the amine associated routes to zeolites A and X (Barrer *et al.*, 1961) whilst Kerr and Kokotailo published data on the silica rich version of zeolite A using tetramethylammonium (TMA) cations (Kerr *et al.,* 1961 and Kerr, 1966). Since then, zeolite science had grown tremendously marked by the application of zeolites in fields ranging from industrial catalysis to detox applications in the field of medicine.

Figure 1.04: Hydrothermal synthesis of zeolites, (Cundy *et al.,* 2005)

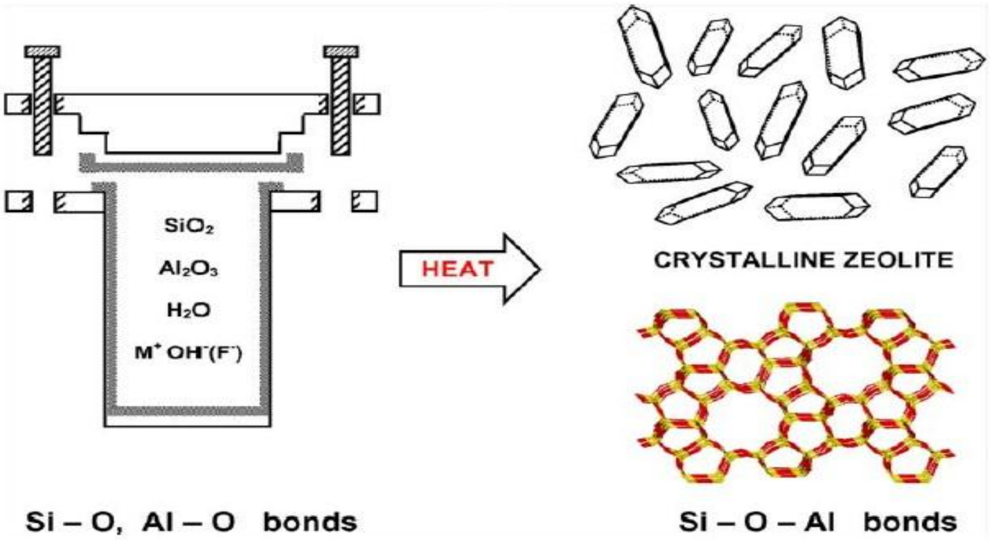

A typical hydrothermal zeolite synthesis was best described by Cundy and Cox in a synthesis review as follows (Cundy *et al.,* 2005):

1. Amorphous reactants containing silica and alumina were mixed together with a cation source, usually in a basic (high pH) medium.
2. The aqueous reaction mixture was heated, often (for reaction temperatures above 100^{o}C) in a sealed autoclave.
3. The reactants remained amorphous for some time after reaching the synthesis temperature.
4. After the above ‘‘induction period’’, crystalline zeolite product could be detected.
5. Gradually, essentially all amorphous material was replaced by an approximately equal mass of zeolite crystals (which were recovered by filtration, washing and drying).

The role of organic cation in zeolite synthesis had been investigated by various researchers. The organic cation could act as a structure directing agent (template) or simply as a pore filling agent. The role in particular could vary from zeolite to zeolite and might vary with synthesis conditions. The role played by the cations was highlighted in detail in the section 1.5

1.5 MECHANISM OF ZEOLITE SYNTHESIS

The total time period of zeolite synthesis was divided into three zones, induction period, nucleation and crystal growth. The induction period (τ) was the time period between the notional start of the reaction to the time where crystalline product first appeared. The induction period was further divided into three parts, the relaxation time (t_r), the time to form a stable nucleus (t_n) and the time for nucleus to grow to a detectable size (t_g). Thus

$$\tau = t_r + t_n + t_g$$

The relaxation time was the time required "for the system to reach quasi-steady-state distribution of molecular clusters" or basically the time during which equilibration of different species took place inside the gel. The induction period was an important phase during zeolite synthesis as this was primarily the phase where zeolite synthesis took place. Subotic and coworkers had shown that the activation energy corresponding to this induction period was essentially the activation energy of the entire synthesis (Subotic *et al.,* 1999).

The initial gel formed after mixing of the reactants was amorphous in nature in the sense that the precipitated product if collected would be amorphous when analyzed by X-ray diffraction. Researchers had investigated the nature of this amorphous material in detail using a number of characterization techniques, the discussion of which is beyond the scope of this project. However it was important to understand the existence of two different amorphous phases namely the primary amorphous phase and the secondary amorphous phase. When first prepared the reaction mixture consisted of partly reacted non-equilibrium combination of components. This was the primary amorphous phase. Over the period of relaxation time (t_r) and at elevated synthesis temperature, a redistribution and repartition of the reaction components took place between the solid and the liquid phases. Structure directing cations played an important role at this stage and directed the organization of a solid phase similar in composition to the final zeolite phase, but lacking the long-range, periodical organization which was visible in the final zeolite. This solid was still amorphous under X-ray diffraction observation but a short range order existed in this secondary amorphous phase.

> However, the situation in some zeolite syntheses might be less clear cut, since the different stages in the process may overlap, e.g. nucleation might begin whilst the bulk of the reaction mixture was still far from attaining a steady state (this is more likely to occur in high temperature synthesis). (Akhmedov *et al.*, 2007)

Zeolite nucleation was a discreet event which could be defined as ‘‘a phase transition whereby a critical volume of a semi-ordered gel network is transformed into a structure which is sufficiently well ordered to form a viable growth center from which the crystal lattice can propagate’’ (Cundy *et al.,* 2005). The critical volume referred to the size of the seed structure to be of a certain minimum size, corresponding to the critical radius. The essential features of the nucleation stage were following (Cundy *et al.,* 2005):

- “The establishment of sufficient regular structure within a statistical distribution of ordered sites to enable such structure to propagate”.
- The accumulation of tetrahedral units from the solution, mediated by the associated cations which provided structural organization for assembling the structure.
- The beginning of crystal growth on the established nuclei.
- The chemical mechanism of all the changes was through the reversible condensation/de-condensation reactions which continuously make and break the T-O-T bonds in the dynamic reaction medium of hydrothermal synthesis.

It was important to note that the organization of the primary, secondary and tertiary building units took place during the nucleation step. A schematic representation of the basic mechanism of cation mediated assembly of ordered regions was shown in Figure 1.5

The final step in the zeolite synthesis was the crystal growth process. The significant change observed during this step was the growth of small nuclei obtained during the nucleation step into the final zeolite crystallites. Zeolite crystals appeared to grow slowly than ionic crystals (such as common salt) and molecular crystals (such as sugar). The reason behind this was the need to establish a three dimensional polymer from solubilized TO2 units (T = Si or Al).

Figure 1.05: Basic mechanism of cation mediated assembly during nucleation (Cundy *et al.*, 2005)

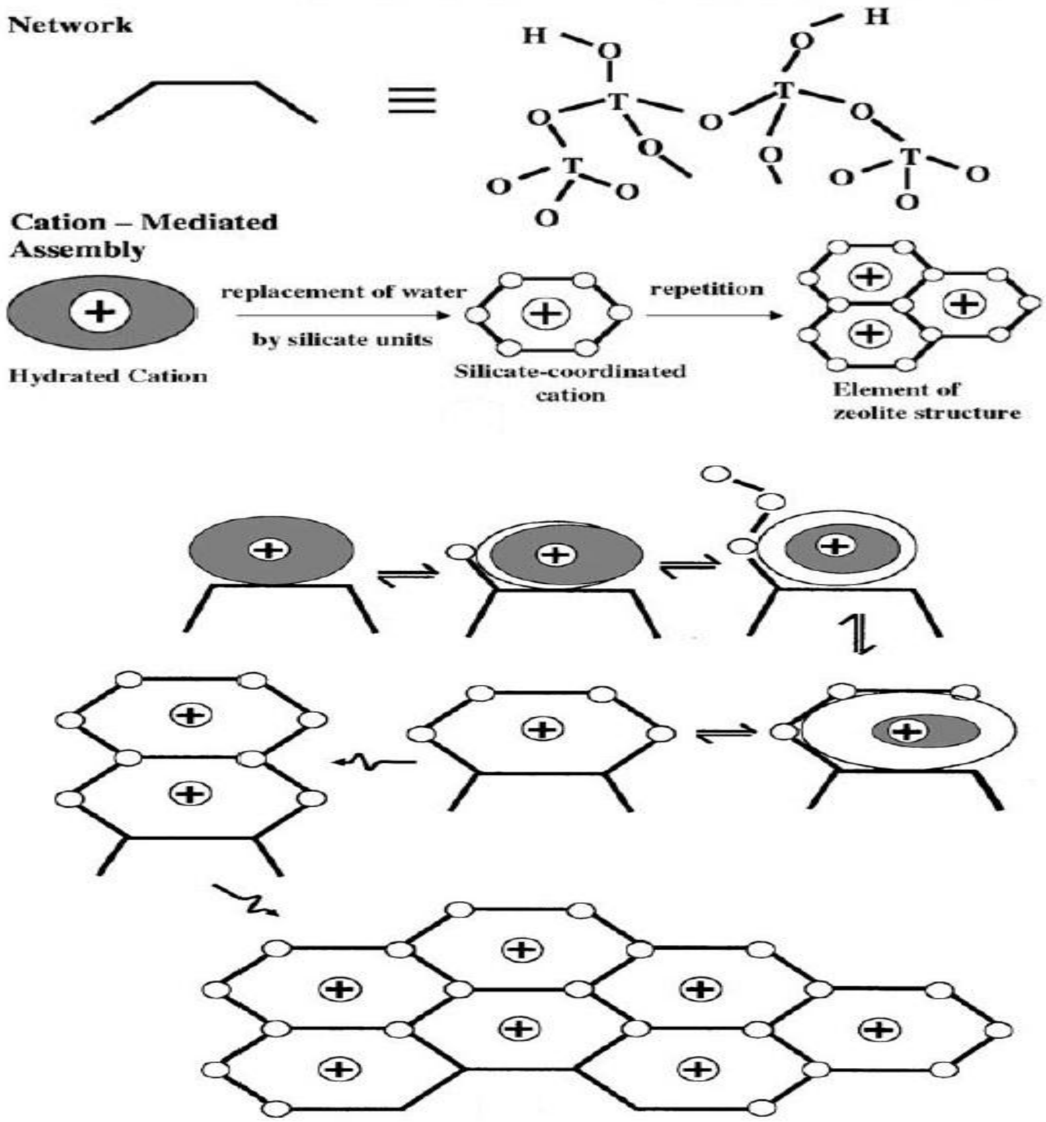

It was important to note that the description of a general mechanism behind the synthesis of all zeolite frameworks was a herculean, if not an impossible task. The different stages in the synthesis process might overlap or occur slowly depending upon the composition and synthesis conditions. For the common researcher more interested in the application of zeolites, zeolite synthesis could be easily understood in terms certain critical factors or critical ratios which controlled the properties of the synthesized zeolite. Regarding the mechanism behind synthesis, it could be summarized that synthesis took place over minute transformations from initial amorphous phase to more ordered structures, particularly through the primary, secondary and tertiary building units. Figure 1.06 illustrated the common building units observed during zeolite synthesis of zeolite ZSM-12 (MTW), ZSM-22 (TON) and ZSM-23 (MTT).

Figure 1.06: Primary, seconday and tertiary building units leading to MTW, TON and MTT strucutres. (Structure Commision, IZA)

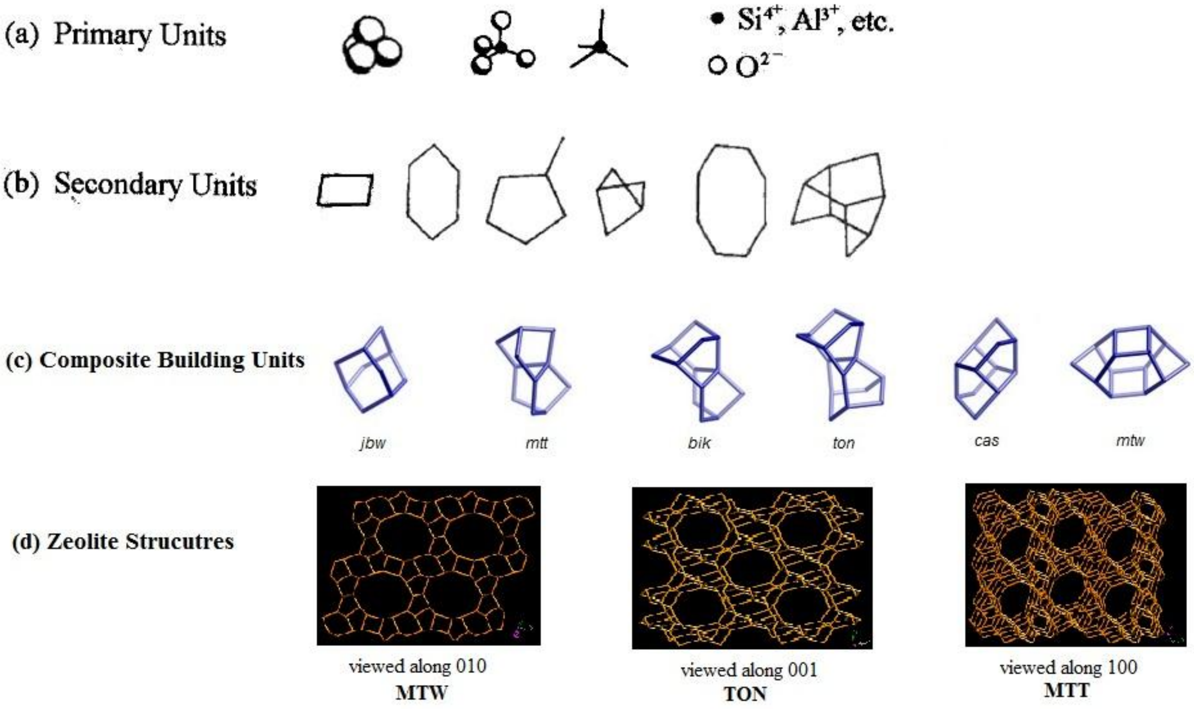

viewed along 010
MTW

viewed along 001
TON

viewed along 100
MTT

A gel with different concentration of ingredients might give rise to different zeolite structures or might fail to crystallize at all. Zeolite synthesis was understood and controlled in terms of certain critical mole ratios which had characteristic influence on a particular property of the zeolite. Table 1.03 gave such a collection indicating the influence of mole ratios on the properties of zeolites. (Byrappa et al., 2001)

Table 1.03: Primary influence of the composition of reaction mixture (Byrappa *et al.,* 2001)

Mole Ratio	Primary Influence
SiO_2/Al_2O_3	Framework Composition
H_2O/SiO_2	Rate, Crystallization mechanism
OH^-/SiO_2	Silicate molecular weight, OH^- concentration
Na^+/SiO_2	Structure, Cation distribution
R/SiO_2	Framework aluminum content

1.6 LITERATURE SURVEY -- HYDROISOMERIZATION CATALYSTS

The catalysts used for the earlier industrial isomerization of light n-paraffins (nC_4-nC_8) were Friedel–Crafts catalysts such as $AlCl_3$ with additives such as $SbCl_3$ and HCl. These catalysts were strongly acidic and very active even at high temperatures (353–390 K) (Leprince, 2001). However, the processes based on these catalysts, did not exist anymore, because of the problems of corrosion of the reactor and the disposal of the spent catalysts. Moreover, these catalysts were very sensitive to poisons such as water, aromatics and sulfur (Leprince, 2001). These disadvantages were the original reasons to search for new and better catalysts in this field.

The 2nd generation catalysts introduced were similar to reforming catalyst having bi-functional role. Typically Pt/Alumina was used. However, these catalysts were found to be effective only in the high temperature range wherein significant cracked product were formed. Thus, such catalysts were prone to rapid deactivation and thermodynamic limitations on conversion per pass (Leprince, 2001).

To overcome these problems, bi-functional catalysts with acidity increased, via halogenation, were introduced to operate at low temperatures. Thus, platinum loaded chlorided alumina was used. Chlorine content was maintained by adding chlorine containing organic compounds, which were continuously supplied during operation to compensate the loss of chlorine on the surface. This catalyst was very active and could operate at lower temperatures

(370 K–470 K) thereby yielding a greater proportion of branched alkanes by taking advantage of the thermodynamic equilibrium.

However, feed pre-treatment became a necessity for such catalyst as they were sensitive to poisons like feed sulfur and in particular water (Leprince, 2001). The feed sulfur was a poison for metal function whereas water reacted with catalyst chloride leading to the formation of HCl. Thus, the continuous injection of chlorine compounds during operation was often found to pose handling and corrosion problems with such catalysts. Therefore, the necessity to develop alternative catalyst in terms of acidic supports was clearly evident. This led to the development of molecular sieve zeolite based catalyst supports.

Solid acids such as zeolites were active for alkane isomerization, though a higher temperature was required compared to Pt/Al_2O_3 based catalysts. In the case of Pt-supported zeolite catalysts, the chlorination (and feed of chlorine-containing compounds) was not required because of higher acidity of zeolites. Also they were found to be highly tolerant for feed contaminants especially water. In fact, Pt-supported mordenite zeolite had been commercially used in early 70s by Shell in a process called Hysomer for C_5-C_6 isomerization.

The catalysts showing good performance in hydroisomerization of light paraffins were not preferred for long chain paraffins because of the increased tendency of multibranched long chain paraffins towards cracking. The logic was explained earlier in section 1.2 (Deldari *et. al.*, 2005). The choice of a catalyst for isomerization of long chain paraffins would depend on chain length as well the desired application of the resulting product. As far as lube oil dewaxing was concerned, catalysts leading to a high yield of mono and di-branched products were preferred. This was because both viscosity and pour point decreased with branching. The multibranched isomers had viscosity index values much lower than their di-branched and mono-branched counterparts. As a result, due to presence of multibranched isomers, the viscosity index of the lubricant oils fell below the minimum desired level and therefore was not desired. On the other hand the primary motive of conventional diesel and renewable diesel dewaxing was the reduction in pour point and the variation in viscosity index was of least importance. Therefore catalysts leading to a high total yield of isomers including mono, di and multibranched isomers would be more suitable for diesel dewaxing operations.

The demand for high quality lube oils with respect to viscosity index, pour point, oxidation stability and need for gross refinery margin (GRM) improvement added impetus to the development of new catalyst chemistry for hydroisomerization in the late 80s. Accordingly, lube oil and diesel oil dewaxing processes underwent step changes from solvent dewaxing to catalytic cracking based dewaxing and finally to hydroisomerization assisted dewaxing process with increased yields vis-à-vis solvent and catalytic cracking dewaxing processes. Unlike, light naphtha isomerization, long chain paraffin isomerization needed to be controlled to an optimum level to achieve desired viscosity index (VI) and pour point, respectively. Furthermore, the position of branching and branching index is found to hold key for the production of lube oil with high viscosity index and desired pour point. The branching at near terminal position of long chain paraffins compared to near center positions was reported to a have a significant impact especially on viscosity index (Miller, 2005).

Thus it became essential to employ a catalyst having a good balance between metal and acid functions to achieve highest isomer selectivity and yield at lowest possible reaction temperature. In order to develop such catalyst system, researchers had focused on understanding zeolites, sulfated zirconia, and mesoporous materials both in terms of their structure and acidity level for improving the isomerization selectivity with an increase in conversion. A brief overview of such efforts was given below:

1.6.1.1 Zeolites (ZSM-23, ZSM-22)

Among the various zeolite frameworks, medium pore zeolites had gained considerable attention for isomerization of long chain paraffins. This was primarily due to the fact that medium pore zeolites favored the formation of methyl branches in the linear aliphatic hydrocarbon chains owing to their restricted pore geometry. In other words, if the pore opening of zeolite was small enough to restrict the larger iso-paraffins from reacting at the acidic sites inside the pore, the catalyst will show good selectivity towards isomerization. The unique selectivity of medium pore zeolites was ascribed to pore mouth / key-lock catalysis mechanism (Martens *et al.,*1995, Claude *et al.,* 2000, Claude *et al.,* 2001). In general, methyl branching increased with decreasing pore width of the zeolite, whereas ethyl and propyl branched isomers that are more susceptible to hydrocracking were obtained from wide pore openings and large cavities (Claude *et al.,* 2001).

Based on the pore mouth / key lock catalysis mechanism, it was apparent that the potential medium pore zeolite should further have the following characteristics for selective hydroisomerization

1. Optimum acid site distribution on the surface
2. Increased external surface area
3. Submicron zeolite crystallite size

With regard to this, Al-framework distribution as a function of Si/Al ratio was judged as an important parameter to control optimum acid strength at pore mouth. Likewise, particle size in the submicron region was viewed to offer a better platform to favor pore mouth / key-lock type mechanism. These aspects for potential zeolites namely ZSM-22, ZSM-23, ZSM-48 and SSZ-32 had been addressed in the patented literature.

Based on the open literature, medium pore zeolites ZSM-22 (TON) and ZSM-23 (MTT), were found to be highly selective for the hydroisomerization of long chain paraffins (Martens *et al.,*1995, Claude *et al.,* 2000, Claude *et al.,* 2001, Souverijns *et al.,* 1998 and Acharya *et al.,* 2004). With ZSM-22/-23 zeolite catalysts, the methyl branches were generated in at very specific carbon positions along the alkane chains as revealed in conversions model for n-alkanes with carbon numbers up to n-C_{24} (Claude *et al.,* 2001). Based on the developed model, monobranched isomers with branches at C_2 carbon position were found to be favored over ZSM-22 type zeolite whereas branches at center positions were favored over ZSM-23 type of zeolites (Huybrechts, *et al.,* 2005). Such trend was noticed over Pt (0.3 wt%)/ZSM-22 in hydroisomerization of long-chain n-paraffins in the range of n-decane to n-tetracosane. The maximum yield of total isomers (both monobranched and multibranched isomers) between 77–90 wt% was noticed over ZSM-22 zeolite with maximum yield of monobranched isomers obtained in the range of 55–80 wt.% with the different n-paraffins. Similarly skeletal isomerisation had been investigated on Pt/ZSM-23. Attempts had also been made to fine tune the acidity level of such zeolites. Accordingly, acidity level was tuned by means of steam deactivation for Pt (0.6 wt.%)/ ZSM-48, ZSM-22, and ZSM-23 catalysts for hydroisomerization of n-decane. The tests showed that by steaming the maximum isomerization yield of ZSM-22, and ZSM-23 catalysts could be increased from 50 to 68, and 50 to 72 wt%, respectively (Acharya *et al.,* 2004).

Interestingly, Pt/ZSM-23 was reported to favor monobranching near the centre of the molecule. Such branching pattern was reported to favor an increase in viscosity index (Miller, 2005). In view of this, MTT zeolite was judged to have an edge over TON type zeolite for the production of lube oil with high viscosity index.

1.6.1.2 Zeolite ZSM-12

ZSM-12 was a medium pore zeolite with a pore size of 5.6 X 6.0 A^o formed by twelve membered rings of silica and alumina tetrahedra. Researchers had investigated the use of platinum loaded ZSM-12 based catalyst for light naphtha isomerization as well as light naphtha isomerization with simultaneous saturation of benzene. (Smirniotis *et al.,* 2003) Pt-ZSM-12 showed better isomerization yields than zeolite Y and zeolite BETA. ZSM-12 based catalysts also showed good resistance against deactivation by coking.

Recently Liang *et al.* studied the hydroisomerization of n-dodecane on SAPO-11, SAPO-41, ZSM-22 and ZSM-12 based catalysts. Activity of the catalyst was observed to be dependent on the acid strength of the zeolites. Selectivity towards isomerization was reported to be dependent on channel structure of the zeolites and a ten membered channel was reported as ideal for hydroisomerization of n-dodecane. Figure 1.07 illustrated the pore structure of ZSM-12, ZSM-22 and ZSM-23 zeolites.

Figure 1.07: Pore structure and dimensions of zeolites ZSM-12, ZSM-22 and ZSM-23 (Structure Comission, IZA)

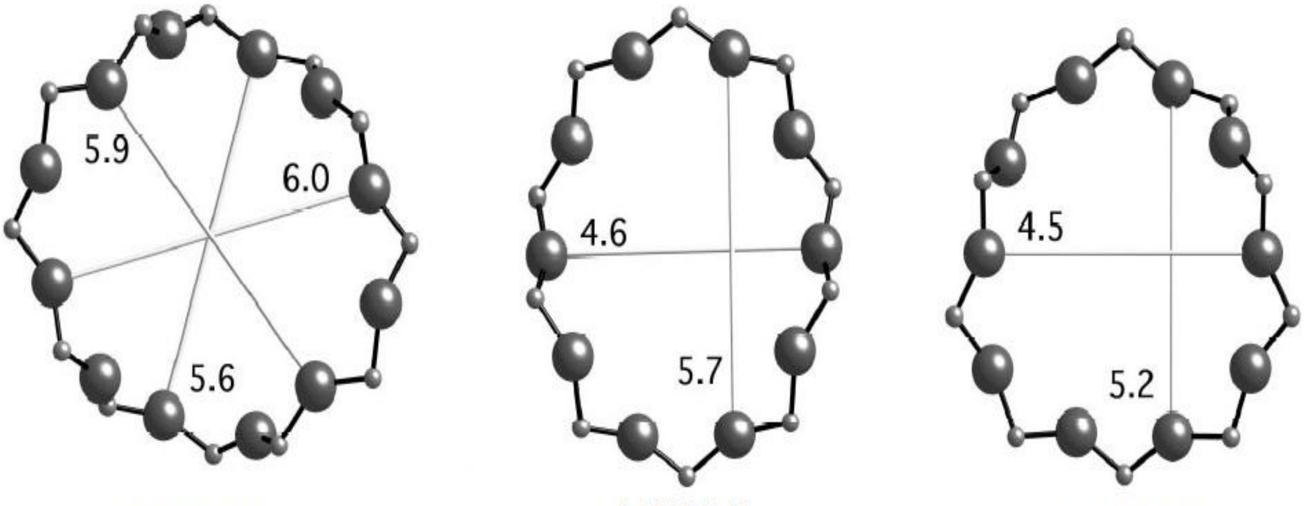

5.6 X 6.0 A°
ZSM-12 viewed along [010]

4.6 X 5.7 A°
ZSM-22 viewed along [001]

4.5 X 5.2 A°
ZSM-23 viewed along [001]

1.6.2 Silicoaluminophosphate molecular sieves (SAPO) (e.g. SAPO-11, SAPO-31, SAPO-41)

SAPO molecular sieves generally had a lower acidity than zeolites. Among SAPO molecular sieves, medium pore SAPOs (SAPO-11, SAPO-31, SAPO-41) had been percepted to be suitable for constituting catalysts for long-chain hydrocarbon isomerization (Maesen *et al.,* 1999). The main SAPO feature was that it resulted in relatively low-branched isoparaffins (Geng *et al.,* 2004). The SAPO framework was created by Si substitution into the $AlPO_4$ framework. There were two mechanisms for this substitution:

- SM2: one silicon substituted one phosphorous;
- SM3: two silicon substituted one phosphorous and one aluminum.

When silicon substituted phosphorous atom, brönsted acid sites were formed whereas if both phosphorous and aluminum were simultaneously replaced by two Si atoms, the tetrahedral framework remained neutral (Szostak *et al.,* 1989).

Among the potential SAPO frameworks, SAPO-11 with AEL type topology was selective for producing monobranched alkanes during hydroisomerization of long chain normal paraffins. Medium pore SAPO-11 was initially employed by M/s Chevron in their Isodewaxing process for selective isomerization of high boiling waxes for the production of high viscosity lube oils.

Hydroisomerization of n-C_{14} over Pt (0.4 wt.%)/SAPO-11 catalyst in a fixed bed reactor showed high isomerization selectivity. Over this catalyst, conversion of n-heptane presented a similar trend, but the values were lower than those of n-tetradecane hydroisomerization at the same experimental conditions. As for the isomerization products, the maximum yield of feed isomers had been 55% for n-heptane hydroconversion. A maximum yield of more than 80% was obtained for n-C_{14} hydroconversion. Also, SAPO-11 based catalyst when evaluated for hydroisomerization of n-hexane, n-octane, n-hexadecane showed the least activity for n-hexane conversion and was the most reactive for n-hexadecane. This result showed that the SAPO catalysts were adequate only for long chain n-paraffins (Ernst *et al.,* 1989, Weitkamp *et al.,* 1987 and Huang *et al.,* 2003). The performance of Pt/SAPO-11 was found to enhance with doping of tin. Isomerization of n-dodecane over Pt-Sn/SAPO-11 catalysts showed more than 90% at 90% n-dodecane conversion whereas only 85% isomerization selectivity at 87% n-dodecane conversion over Pt/SAPO-11 had been obtained. The results indicated that, on SAPO-11 based catalysts, n-dodecane (a long-chain n-paraffin) could intensively isomerize with very limited cracking. The better hydroisomerization performance of the former catalyst had been attributed to the addition of tin to the metallic catalyst composition (Ernst *et al.,* 1989, Weitkamp *et al.,* 1987 and Huang *et al.,* 2003). Like other zeolite catalysts, the performance of SAPO based catalyst was reported to be influenced by metal dispersion and surface area of the catalyst. In order to achieve higher acidity, attempts had been made to incorporate silica by SM2 mechanism. Such mechanism was found to prevail when SAPO-11 was prepared using water-cetyltrimehtlammonium bromide-butanol phase (Sinha *et al.,* 1998 and Blasco *et al.,* 2006).The crystallized SAPO-11 framework was reported to have more brönsted acid sites and smaller crystallite size. Such SAPO-11 support was found to be more active than the conventionally prepared framework (Sinha *et al.,* 1998 and Blasco *et al.,* 2006). SAPO-11 with small crystal size was expected to decrease the effect of diffusion; carbenium intermediates thus easily desorbed from acid sites and further isomerization and cracking was expected to decrease.

Among SAPO-11, SAPO-31, and SAPO-41 with identical acid strength the hydroconversion activity for n-octane decreased in the order SAPO-41 > SAPO-11 > SAPO-31. The low activity of SAPO-31 was ascribed to its framework structure i.e. it has 12-membered ring one-dimensional circular channel. On the other hand SAPO-41 and SAPO-11 had 10-membered ring one dimensional elliptical channel which was found to be effective for hydroconversion owing to their shape selectivity as described earlier. However, SAPO-41 was reported to be more active than SAPO-11 due to its slightly larger pore size which in turn was expected to offer less diffusion constraints for reacting molecules as compared to SAPO-11.

1.6.3 Mesoporous materials (MCM-41, AlMCM-41)

Since the discovery of the new class of mesoporous materials such as MCM-41 in 1992, there had been a growing interest in their potential catalytic applications [Kresge *et al.,* 1992]. Because of their relatively mild acid sites and the possibility to vary the Si/Al ratio over a wide range without significant changes in pore structure, these materials were very attractive catalysts for transformation of bulky compounds, especially for the hydroisomerization of long-chain n-paraffins (Fang *et al.,*2004 , Elangovan *et al.,* 2002 and Lin *et al.,* 2002). Thus, n-decane hydroconversion on bifunctional catalysts comprising Pt, Pd and bimetallic Pt–Pd supported on an Al-MCM-41 (Si/Al = 23) was investigated. The results of this investigation are shown in

Table 1.04. The catalytic activity of all catalysts containing bimetallic clusters was observed to increase in comparison with the values of monometallic catalysts (Elangovan *et al.*, 2002).

On the other hand, Pd (0.35 wt%)/AlMCM-41 catalyst at 623 K in the hydroisomerization of n-tridecane was found to have increasingly better selectivity with a lowering framework Si/Al ratio (Table 1.5). The observed trend suggested a more critical balance was needed between the acid function of MCM-41 and metal function for simultaneous increase in isomer selectivity and selectivity at lowest possible temperature.

Table 1.04: Maximum isomer yields of Pt, Pd, and Pt-Pd/AlMCM-41 catalysts in hydroisomerization of n-decane (Elangovan *et al.*, 2002)

Metal compound	T_{max} (K)	Conversion (wt %)	Maximum isomer yield (wt%)
0.5 wt.% Pt	628	81	53.8
0.27 wt.% Pd	653	74.3	54.5
0.375 wt.% Pt–0.068 wt.%Pd	593	77.4	44
0.25 wt.% Pt–0.135 wt.% Pd	573	58.6	38.2
0.125 wt.% Pt–0.203 wt.%Pd	583	69.6	37.3
0.125 wt.% Pt–0.068 wt.%Pd	603	82.4	32.4
0.5 wt.% Pt–0.27 wt.% Pd	583	73.3	48.9

Reaction conditions: P_{H2} = 1 MPa, $P_{n\text{-}C10}$ = 10 kPa, H_2/n-C_{10} mole ratio=100, W/F = 400 gh/mol.

Table 1.05: The results of hydroisomerization of n-C_{13} over different Pd/AlMCM-41 catalysts (Lin *et al.*, 2002)

Total acid amount (mmol/g)	Si/Al ratio	n-C_{13} conversion (wt.%)	i-C_{13} selectivity (wt.%)
0.135	100	59.3	86.4
0.161	75	59.8	88.7
0.164	50	60.2	86.5
0.198	25	59.5	91.8

Reaction conditions: T = 623 K, Pt = 3.5 MPa, H_2/n-C_{13} = 600, WHSV = 1.5 h^{-1}

1.6.4 Tungstate-promoted zirconia (WO_x-ZrO_2):

Anion-modified metal oxides, such as sulfated zirconia (SO_4/ZrO_2) and tungstated zirconia (WO_3/ZrO_2), had been found to catalyze hydrocarbon conversions under mild conditions. These strong solid acids were environmentally benign and regenerable. Butane isomerization over sulfated zirconia had attracted considerable attention because isobutane was the precursor to methyl-t-butyl ether. Metal-promoted sulfated zirconia was effective for isomerization of short chain paraffins and for hydrocracking of long-chain paraffins including waxes and polyolefins (Yadav *et al.,* 1999). However, loss of activity due to coke formation and sulfur loss, especially under reducing conditions, were obstacles to certain practical uses of sulfated zirconia. Moreover, high isomerization selectivity was difficult to achieve over sulfated zirconia as the chain length increased, even at low conversions. Studies of tungstate-modified zirconia indicated that it was more stable than sulfated zirconia and was promising for hydroisomerization of high molecular weight linear paraffins (Barton *et al.,* 1999, Zhang *et al.,* 2000, Hino *et al.,* 1980, Wen *et al.,* 1990, Keogh *et al.,* 1994 and Keogh *et al.,* 1999).

The performance of Pt (0.5 wt%)/WO_3/ZrO_2 catalyst for hydroisomerization of n-hexadecane in a trickle bed continuous reactor demonstrated high activity and selectivity for hydroisomerization of long chain n-paraffins (Barton *et al.,* 1999). The optimum range of tungsten loading to achieve high isomerization selectivity at high n-hexadecane conversion was found to be between 6.5 and 8 wt% (Barton *et al.,* 1999). The comparison between Pt (0.5 wt%)-/SO_4/ZrO_2 and /WO_3/ZrO_2 (Table 1.06) showed that Pt (0.5 wt%)/SO_4/ZrO_2 catalyst converted 80% of converted n-hexadecane to short-chain paraffins when operated at 423 K since it was very active and was not stable at high temperatures in the presence of hydrogen. On the other hand, Pt (0.5 wt%)/WO_3/ZrO_2 with a comparable n-C_{16} conversion to that Pt/SO_4/ZrO_2 favored the formation of many more C_{16} isomer products (Zhang *et al.,* 1998).

In view of the observed trend, the combination of both i.e. sulfate and tungstate species was expected to play vital role in controlling the surface acidity and acid density for zirconia surface. However, metal function for Pt/WZR was found to be dependent on treatment conditions. The oxidation step during catalyst preparation was found to prevent formation of tungsten-platinum species which commonly lead to low dispersion of platinum in turn demonstrate low activity for isomerization reaction.

Table 1.06: Hydroisomerization of n-C_{16} on of Pt (0.5 wt%)/SO_4/ZrO_2 and Pt (0.5 wt%)/WO_3/ZrO_2 (6.5 wt% W)

Catalyst	Reaction temperature (K)	n-C_{16} conversion (wt%)	i-C_{16} Selectivity (wt%)	i-C_{16} Yield (wt%)
Pt (0.5 wt%)/SO_4/ZrO_2	423	76.7	19.8	15.2
Pt (0.5 wt%)/WO_3/ZrO_2	503	85.9	83.1	71.4

Reaction conditions: Pt = 300 psig, WHSV = 1 h^{-1}, H_2/n-C16 mole ratio = 2

1.7 LITERATURE SURVEY – SYNTHESIS OF ZSM-12

ZSM-12 was first synthesized by Rosinski and Rubin in 1974 from tetraethylammonium cations obtained from a variety of sources (Rosinski *et al.*, 1974). The tetraethylammonium cations were obtained either from salts like tetraethylammonium halides and hydroxides or generated in situ using triethylamine and an alkylating agent like diethylsulfate. The field of ZSM-12 synthesis soon opened up and the original patent was immediately followed by a number of patents for the synthesis of this new zeolite from a variety of structure directing agents. From 1974 to 1993, a period of 18 years, marks an important developmental phase for this particular zeolite and features more than 10 patents on the synthesis of ZSM-12 from a different SDA molecule. Each new patent generally described the use of a different structure directing agent, its corresponding successful gel composition and valid characterization of the zeolite. Table 1.07 tabulated the different molecules which had been used as structure directing agents for the synthesis of ZSM-12.

In the open literature, Ernst *et al.* and Smirniotis *et al.* had studied the synthesis of ZSM-12 synthesis in detail using methyltriethylammonium bromide (MTEABr) and tetraethylammonium cations (TEA^+) respectively (Ernst *et al.*, 1987, Smirniotis *et al.*, 2001, 2003). Ernst *et al.* described the use of sodium silicate and aluminum nitrate as the source of silica and alumina respectively. Sodium cation was observed to play an important role in nucleation and crystal growth process where as MTEABr was observed to serve only as a pore filling agent. Dilution of the synthesis gel was reported to increase the crystal size of zeolite.

Smirniotis *et al.*, had done an exhaustive study on the role of TEA^+ in the synthesis of ZSM-12. The group was able to synthesize ZSM-12 at SAR ratios of 60 for the first time. The concentration of costly structure directing agent was also reduced to a minimum TEA/Si ratio of 0.125. Synthesis of ZSM-12 at low SAR ratios was reported to be highly sensitive to the alkalinity of the synthesis gels. Similar trends were found for the use of TEAOH and TEABr as structure directing agents.

Table 1.07: Tabulation of patented literature, each describing the synthesis of ZSM-12 from a different structure directing agent

Research Group	Patent #	Structure Directing Agent
Rosinski E.J., Rubin M.K., 1974	US 3832449	Tetraethylammonium cations
Rosinski E.J., Rubin M.K., 1983	US 4391785	Dimethyl pyridinium halides, dimethyl piperidinium halides and dimethyl pyrrolidinium halides
Kuehl G.H., 1984	US 4482531	DABCO-C_n-diquat, n=4,5,6 or 10
Kuehl G.H., 1985	US 4559213	DABCO-C_n-diquat, n=4-10
Rubin M.K., 1986	US 4585637	Benzyltrimethylammonium halides
Szostak R., 1986	US 4585639	Linear diquaternary ammonium compounds
Rubin M.K., 1987	US 4636373	Dibenzyldimethylammonium cation
Rubin M.K., 1991	US 5021141	Hexamethyleneimine
Valyocsik E.W., 1992	US 5137705	Bis(methylpyrrolidinium)-DIQUAT-N, N= 4,5 and 6
Moini A., Valyocsik E.W., 1993	US 5192521	Decamethonium cation

1.8 AIMS AND SCOPE OF THE INVESTIGATION

ZSM-22 and ZSM-23 zeolites were reported as suitable candidates for use as a support in hydroisomerization catalysts for long chain n-paraffins. ZSM-12 was a medium pore zeolite investigated for the hydroisomerization of light naphtha and n-dodecane. The zeolite showed good results for light naphtha isomerization but exhibited low total selectivity towards monobranched isomers.

The hydroisomerization studies were aimed to gain a better understanding towards lubricant oil and diesel dewaxing applications. These applications were of considerable relevance to the industry. It was known from the literature survey that monobranched and dibranched isomers of long chain paraffins were desired as the constituents of lubricant oils for desired viscosity index and pour point values. On the other hand, a high total isomerization selectivity was desired for renewable and conventional diesel oil dewaxing applications for desired pour point values.

It was concluded from the literature survey that 10-ring medium pore zeolites ZSM-22 and ZSM-23 zeolites were suitable for lubricant oil dewaxing applications whereas 12-ring medium pore zeolite ZSM-12 had potential for diesel dewaxing applications. In order to establish a suitable benchmark and comparison scale, n-hexadecane molecule was selected as the model feed to compare the results of ZSM-22 and ZSM-23 based hydroisomerization catalysts with other researchers and investigate the results for ZSM-12 based hydroisomerization catalysts. Till now no research work had been published in the open literature on the use of ZSM-12 for hydroisomerization of n-hexadecane.

Finally, the synthesis of zeolites was an area of interest. Zeolite ZSM-12 had been synthesized from a variety of structure directing agents. However, the open literature described the synthesis of ZSM-12 only from MTEABr and TEA^+ cations. As such a gap existed between the patented literature and the open literature. Also no reports are available on the comparison of structure directing agents for the synthesis of ZSM-12. MTEABr and TEAOH were costly structure directing agents and impractical for big scale ZSM-12 production. On the other hand BTMACl was comparatively a much cheaper structure directing agent suitable for scale up operations.

In view of the above discussion “Synthesis, Characterization and Evaluation of zeolites for hydroisomerization of model feed n-hexadecane” was chosen as the topic of research with the following objectives:

1. Understanding the synthesis of zeolite ZSM-12 from MTEABr, TEAOH, TEABr and BTMACl as strcture directing agents.
2. Synthesis of 100% pure ZSM-12 samples at varying silica alumina ratios.
3. Optimization of synthesis conditions for obtaining pure ZSM-12 samples.
4. Synthesis of 100% pure ZSM-22 and ZSM-23 zeolites.
5. Characterization of zeolites ZSM-12, ZSM-22 and ZSM-23.
6. Synthesis of platinum loaded hydroisomerization catalysts using ZSM-12, ZSM-22 and ZSM-23 as supports.
7. Evaluation of zeolite based hydroisomerization catalysts for isomerization of n-hexadecane.
8. Study the effect of variation in reaction parameters like pressure, temperature and WHSV on global reactivity patterns.
9. Making suitable conclusions about the effectiveness of each zeolite type (ZSM-12, ZSM-22 and ZSM-23) for lubricant oil and diesel oil dewaxing applications.

CHAPTER 2

EXPERIMENTAL METHODS

2.1 INTRODUCTION

It is a long journey from an as synthesized zeolite to the finished ready-to-be-used catalyst. The zeolite is stripped and redecorated much like a protagonist being prepared for a grand appearance in the theatre or in our case performing in the reaction. The chapter deals with the various experimental methods used in the preparation of a zeolite based catalyst including everything from synthesis data to the final composition of the ready to perform catalyst.

The synthesis of zeolites has been called an “art” in the past, emphasizing the complexity and the sophisticated nature of transformations taking place during crystallization. However, the continuous addendum of knowledge shared over time has resulted into “taming of this wild beast”. Today zeolite synthesis is understood in terms of critical factors and the characterization techniques used for the complete identification of zeolites.

The science of zeolite synthesis is best described as an experimental science not only because of the extent of experimental work involved but also because of the systematic modifications that can be achieved through logically designed experiments. Zeolite synthesis in the form we understand today began with the investigative works of Richard Barrer and Robert Milton in the 1940s where they worked on the conversion of known mineral phases under the action of strong salt solutions at fairly high temperatures ($150^{o}C$ – $270^{o}C$) (Barrer, 1948, Barrer *et al.*, 1953, Barrer *et al.*, 1961). Zeolite science has made a great progress since then. Today we have more than 201 (IZA, Dec, 2011) different zeolite framework types ready to be applied in fields ranging from medicine to catalysis.

2.2 EXPERIMENTAL WORK

The experimental methods concerning the research work include the following:

1.) Synthesis of Zeolites.
2.) Template removal from synthesized zeolite.
3.) NH_3 ion exchange of template free zeolite.
4.) Calcination of the NH_3 exchanged zeolite.
5.) Optional ion exchange with Group II base metals.
6.) Platinum loading of the calcined zeolite.
7.) Preparation of extrudates.
8.) Activation of extrudates.

The following grades of reagents were used in the experiments:

Silica Sources

Sodium Silicate	(25.5-28.5) wt% SiO_2, (7.5-8.5) wt% Na_2O	Merck
Colloidal Silica (30%)	Ludox-AS30	Aldrich
Colloidal Silica (40%)	Ludox –AS40	Aldrich
Precipitated Silica	Hi-Sil-233	PPG Industries

Structure Directing Agents

MTEABr	99 wt%	Aldrich
TEABr	99 wt%	Aldrich
Aq. TEAOH sol.	35 wt%	Aldrich
BTMACl	99 wt%	Aldrich
Pyrrolidine	98 wt%	Aldrich
1,6 diaminohexane	98 wt%	Aldrich

Aluminium Sources

$Al(NO_3)_3.9H_2O$	99 wt%	Merck
$Al_2(SO_4)_3.16H_2O$	98 wt%	Qualigens
$Al_2(SO_4)_3.18H_2O$	98 wt%	Acros Organics
$NaAlO_2$	51 wt% Al_2O_3, 31 wt% Na_2O	Merck
Pseudo Bohemite	70 wt%	SASOL

pH modifiers

NaOH	99 wt%	Aldrich
Na_2CO_3	99 wt%	Aldrich
Conc. H_2SO_4	98 wt%	Aldrich
Aq. TBAOH sol.	20 wt%	Fischer Scientific

Other Reagents

NH_4NO_3	95 wt%	Qualigens
$[Pt(NH_3)_4](NO_3)_2.2H_2O$	99.9 wt%	Aldrich
Puralox SCFA-230	98 wt%	SASOL
Aq. Nyacol (AL-20) sol.	20 wt%	Nyacol Nano Technologies Inc.

2.2.1 Synthesis of Zeolites:

A typical zeolite synthesis procedure consists of contacting a silica solution with a structure directing agent. Subsequently an aluminum source is added and the pH of the resulting gel is adjusted to the desired value. The resulting gel is set for crystallization in the temperature range of 150-180^{o}C.

2.2.1.1 Synthesis of ZSM-12

a) The typical procedure for preparing a desired gel composition (0.3 Na_2O **:** 0.0083 Al_2O_3 **:** SiO_2 **:** 0.4 MTEABr **:** 42 H_2O) was as follows (SAR 120):

16.18g sodium silicate was first mixed with 16 g deionized water. To this solution, a solution of 6g MTEABr in 20g deionized water was added slowly followed by an addition of 0.48g aluminum nitrate in 6g deionized water. Finally 0.94g concentrated sulfuric acid taken into 6g deionized water was added to the above solution. The resulting gel was allowed to stir for 2-3 hours at room temperature and then transferred in a 120 ml stainless steel auto-clave with a Teflon vessel at 160^{o}C for 7 days. After 7 days, the auto-clave was removed and allowed to cool to room temperature. Good crystallization was indicated by transparent liquid at the top and white solid at the bottom of auto-clave. The product was recovered by filtration, washed with water several times and allowed to dry overnight at 100^{o}C.

b) The typical procedure for preparing a desired gel composition (0.053 Na_2O **:** 0.0084 Al_2O_3 **:** SiO_2 **:** 0.465 TEABr **:** 42 H_2O) was as follows (SAR 120):

26.875g of LUDOX AS-30, a 30% colloidal silica solution was taken in a plastic beaker. To this solution 0.45g NaOH and 0.221g $NaAlO_2$ (53% Al_2O_3, 42.5% Na_2O) dissolved in minimum amount of water were added dropwise. The resulting solution was allowed to stir for 30 minutes. Now 13.125g TEABr dissolved in 20ml water was added to the above solution and allowed to stir for 30 minutes. Finally a 6.25ml 30% aqueous NH_3 solution is added to the above gel and allowed to stir for 2 hours. Now the gel is transferred in a 120 ml stainless steel autoclave with a Teflon vessel and allowed to crystallize at 140^{o}C for 10 days. Good crystallization was indicated by the presence of a transparent liquid at the top and a white dense precipitate at the bottom. The product was recovered by filtration and washed with water several times to remove soluble impurities.

c) The typical procedure for preparing a desired gel composition (0.015 Na_2O **:** 0.0083 Al_2O_3 **:** SiO_2 **:** 0.238 TEAOH **:** 14 H_2O) was as follows (SAR 120):

24.948g of tetraethylammonium hydroxide (35 wt% TEAOH) solution was added dropwise to a 50g solution of LUDOX AS30 and allowed to stir for 30 minutes. Now 0.401g of $NaAlO_2$ (53%

Al_2O_3, 42.5% Na_2O) and 0.074g of NaOH dissolved in minimum amount of water were added dropwise to the above solution. The desired amount of water to silica ratio was maintained by adding necessary amount of water. This solution was allowed to stir at room temperature for 2 hours. Now the resulting gel was transferred to stainless steel autoclave with a Teflon vessel and allowed to crystallize at 165^o for 5 days. Good crystallization was indicated by the presence of a transparent liquid at the top and a dense white precipitate at the bottom of the autoclave. The product was obtained by filtration and washed with water several times to remove dissolved impurities.

d) The typical procedure for preparing a desired gel composition (0.1 Na_2O **:** 0.0055 Al_2O_3 **:** SiO_2 **:** 0.4 BTMACl **:** 20 H_2O) was as follows (SAR 180):

0.8g NaOH was dissolved in 18g distilled water. 0.081g pseudo bohemite was added to this solution and the resultant mixture was heated with vigorous stirring at 70^oC for 2 hours. The resulting solution was a clear glassy liquid with no pseudo bohemite particles at the bottom of the container. Now 3.72g benzyltrimethylammonium chloride (BTMACl) dissolved in 18g distilled water was added slowly to the above solution. The resultant mixture was allowed to stir for 30 minutes. Finally 20g of a LUDOX-AS30 solution was added dropwise to the above solution and the resulting mixture was stirred for 2 hours. This gel was now transferred to a 120 ml stainless steel autoclave with a Teflon vessel and allowed to crystallize at 160^oC for 6 days. Good crystallization was indicated by the presence of a transparent liquid at the top and a dense white precipitate at the bottom of the autoclave. The product was obtained by filtration and washed with water several times to remove dissolved impurities.

2.2.1.2 Synthesis of ZSM-23

The typical procedure for preparing a desired gel composition (0.125 Na_2O **:** 0.0083 Al_2O_3 **:** SiO_2 **:** 0.241 Pyrrolidine **:** 20 H_2O) was as follows (SAR 120):

7g Hi-Sil-233 was mixed with 20g distilled water with constant stirring. Now 0.625g aluminumsulfate hexadecahydrate ($Al_2(SO_4)_3.16H_2O$) dissolved in 12g distilled water was added to the above mixture slowly with uniform stirring. Further 0.5g sodium hydroxide (NaOH) and 1g sodium chloride (NaCl) dissolved in a total of 10g distilled water were added to the solution slowly with vigorous stirring. Finally 2g pyrrolidine was added dropwise to the above solution and the solution is allowed to stir for 2 hours at room temperature. The resulting gel was transferred into the Teflon vessel of a stainless steel autoclave and allowed to crystallize at 150^{o}C at a constant rotation of 470 rpm for 3.5 days. After 3.5 days the autoclave was quenched with cold water and the dense white powder is removed by filtration.

2.2.1.3 Synthesis of ZSM-22

The typical procedure for preparing a desired gel composition (0.143 K_2O **:** 0.011 Al_2O_3 **:** SiO_2**:** 0.296 DAH **:** 40 H_2O) was as follows (SAR 90):

15g of LUDOX AS40 colloidal solution was diluted by 26g of distilled water. To this sol, a solution containing 0.73g of aluminumsulfatedodecahydrate ($Al_2(SO4)_3.18H_2O$), 1.625g potassium hydroxide (KOH) and 3.3g of 1,6 diaminohexane (DAH) in 37g water was added dropwise with vigorous stirring for 2 hours. The resulting gel was transferred to a 60ml stainless steel reactor with a Teflon vessel and heated at 160^{o}C with a constant rotation of 50 rpm for 2 days. After 2 days the autoclave was quenched with cold water and the dense white powder is removed by filtration.

2.2.2 Calcination

The template can be removed by solvent exchange by the use of a solvent which can dissolve the template or by the decomposition of template at a high temperature. Decomposition of template in air was chosen as the method of template removal. The removal of template was done by calcination of the sample at 550^{o}C for 10 hours in a mild flow of air using an air pump. A ramp rate of 5^{o}C/min was used till a temperature limit of 150^{o}C where the sample was allowed to stand for one hour. After this drying treatment, temperature was increased at a rate of 3^{o}C/min till 550^{o}C where the sample was allowed to stand for 10 hours.

2.2.3 NH_3 ion exchange

The synthesized zeolite is in sodium form and an ammonia exchange procedure has to be applied to convert it into ammonia form, from where the zeolite can be converted into the protonated form by calcination. For the ammonia exchange procedure, a 100 ml 0.1M ammonium nitrate

(NH_4NO_3, 98%, Qualigens) solution was added to 5g zeolite and allowed to reflux at 90^{o}C with stirring for 6 hours. Now the stirring and heating was stopped and zeolite was allowed to settle at the bottom of the two necked round bottom flask overnight. The aforementioned process is repeated twice. Finally the zeolite is filtered, washed with water several times and dried overnight at 100^{o}C.

2.2.4 Calcination of NH_3 exchanged zeolite

The ammonia exchanged zeolite was calcined at 550^{o}C for 5 hours in mild air flow, using a heating program similar to the one used for template removal, to convert it to the protonated form. The heating program provided an initial ramp rate of 5^{o}C/min till a temperature of 150^{o}C where the sample was allowed to dwell for 1 hour. Now a ramp rate of 3^{o}C/min is used till a final temperature of 550^{o}C where the sample is allowed to dwell for 5 hours.

2.2.5 Optional ion exchange with group (II) base metals.

Good hydroisomerization selectivity and yield depends on a fine balance between the acid and metal function as explained earlier in section 1.2. One characteristic method of controlling the acidity in a zeolite sample is to vary the Si/Al ratio during synthesis, as low aluminum content will lead to lesser total acidity. However it should be clear that any zeolite catalyst or in fact any heterogeneous catalyst will have a statistical distribution of acid sites of variable strength. Therefore there will exist very strong acid sites much above the average strength, although low in number as there will exist very mild acid sites much below the average strength also low in number. These strong acid sites will typically lead to cracked products in a hydroisomerization reaction, unless they are hindered from doing so either by the shape selectivity effect arising from the pore size or from a treatment of the kind which will neutralize the strong acidity of the site.

In line with the above logic, a partial ion exchange of a zeolite with base metals provides another method of controlling the acidity of a zeolite sample besides varying the Si/Al ratio. Group (I) metals like Na, K and Cs etc. are highly basic in nature and are not desired for this purpose of partial neutralization. Ion exchange with transition metals can have pronounced effect on the overall function of the catalyst, study of which is beyond the scope of this thesis. Group (II) metals like calcium and barium have a potential as suitable ions for partial neutralization. A particular advantage of using group (II) metals is the slight change in pore size of the zeolites because of the replacement of a proton by a bulky ion like calcium and barium.

A group (II) metal loading of 0.35wt% was chosen as the required level of partial neutralization based on theoretical neutralization of 60% of acid sites. A variation in selectivity of a catalyst with change in base metal loading is beyond the scope of this thesis. For the base metal loading or the ion exchange procedure required weight of a water soluble calcium salt like calcium nitrate and zeolite were taken in 100ml water and refluxed at $90^{o}C$ for 6 hours. The solid obtained is filtered, washed with excess water and dried at $100^{o}C$ to obtain the partial calcium exchanged zeolite sample.

2.2.6 Platinum loading of protonated zeolite

Tetraamineplatinum(II)nitrate ($[Pt(NH_3)_4](NO_3)_2.2H_2O$, 99.9%, Aldrich) was used for the platinum loading of the zeolite samples. Desired weight of the salt is taken so as to ensure a 0.35 wt% loading in a 50-50 zeolite-support mixture. For a 5g zeolite (and 5g support) 69.47 mg of the salt is taken in 50 ml deionized water. This solution is added to the zeolite and allowed to stir at room temperature for a period of 3 days. To ensure a good loading of the Pt complex a high pH (10-11) is maintained using tetrabutylammonuimhydroxide (TBAOH). Intially 15-20 drops of TBAOH are consumed to reach the desired pH level. The pH of the solution however decreases over time and more TBAOH is added accordingly to keep the pH in the desired range (10-11).

2.2.7 Extrudate formation of Platinum loaded zeolite

The Pt loaded calcined zeolite needs to be loaded on a support before making into extrudates. The support not only provides the necessary strength to the extrudate but also provides a method to control the overall acidity of the catalyst. Different supports with same zeolite might lead to different conversion and selectivities. The chosen support was a mixture of pseudo bohemite (10 wt%) and Puralox SCFA-203(90 wt%) binded with zeolite using NYACOL. Desired amount of these powders are taken along with an equal total weight of Pt-loaded zeolite and grinded uniformly using a mortar-piston. Nyachol is added dropwise and powder is kneaded into a wet mass which can be made into extrudates using a press and a dye.

2.2.8 Activation of extrudates

The extrudates must be activated before they are loaded in the reactor for evaluation. Two modes of activation are needed before the reaction starts taking place. The first mode comprises of treating the extrudates in an oxygen atmosphere where the loaded platinum salt is oxidized to platinum oxide. This mode of activation is necessary because it is easier and more efficient to oxidize the organic platinum salt to the oxide form and then uniformly reduce the platinum oxide to metallic form in the second stage. The second mode of activation is done inside the reactor by providing a hydrogen atmosphere at elevated temperature.

A ramp rate of 1^oC/min in a mild flow of 99% oxygen gas was used for extrudates till a temperature of 130^oC where the sample was allowed to dwell for four hours. After this initial treatment, a ramp rate of 0.15^oC/min under the constant flow of oxygen gas was used till a temperature of 400^oC where the extrudates were dwelled for four hours. At the end of this activation treatment the color of zeolites changed to a grey color (initially white). The intensity of grey color, observed visually, was a function of aluminum content in the zeolite with the extrudates taking a lighter shade at high Si/Al values and a darker shade at low Si/Al values.

For the second mode of activation where the extrudates were reduced under hydrogen atmosphere inside the reactor, an initial drying treatment was done at 120^oC for 12 hours followed by heating at a ramp rate of 1^oC/min till a temperature of 300^oC and allowed to dwell at this temperature for 5 hours.

2.3 CHARACTERIZATION TECHNIQUES

2.3.1 X-ray Diffraction

The X-ray diffraction patterns for the various zeolite samples were collected over a Philips X'pert 1 X-ray diffractometer using a Cu-K_α radiation ($\lambda = 1.54056$ A^o). The X-ray patterns were recorded for a scan step size of 0.02 degrees and a timer per step value of 0.4 seconds for a region of 2θ values between 5.01 degrees to 39.99 degrees. The selected region of 2θ values (5.01 – 39.99) was sufficient to characterize various zeolite phases.

The X-ray diffraction patterns of pure zeolite phases were obtained from the “Collection of Simulated Diffraction Patterns” published by the Structure Commission, International Zeolite Association (Treacy *et al.,* Structure Commission, IZA).

2.3.2 Scanning Electron Microscopy (SEM) Studies

The microscopy studies in the course of this project were done on a TESCAN Scanning Electron Microscope. The samples in the powder form were taken on the carbon tape and mounted on the SEM sample holder and images were recorded. Scanning electron microscopy was used to investigate the morphology of the sample and to obtain the crystallite size of particles present in the sample.

2.3.3 Ammonia Temperature Programmed Desorption (NH_3 TPD)

The ammonia temperature programmed desorption data was obtained on an Altamira AMI-200 instrument. The temperature program used for collection of data was shown in figure 2.01.

Figure 2.01: A typical temperature ramp rate used by the instrument in NH_3 TPD studies

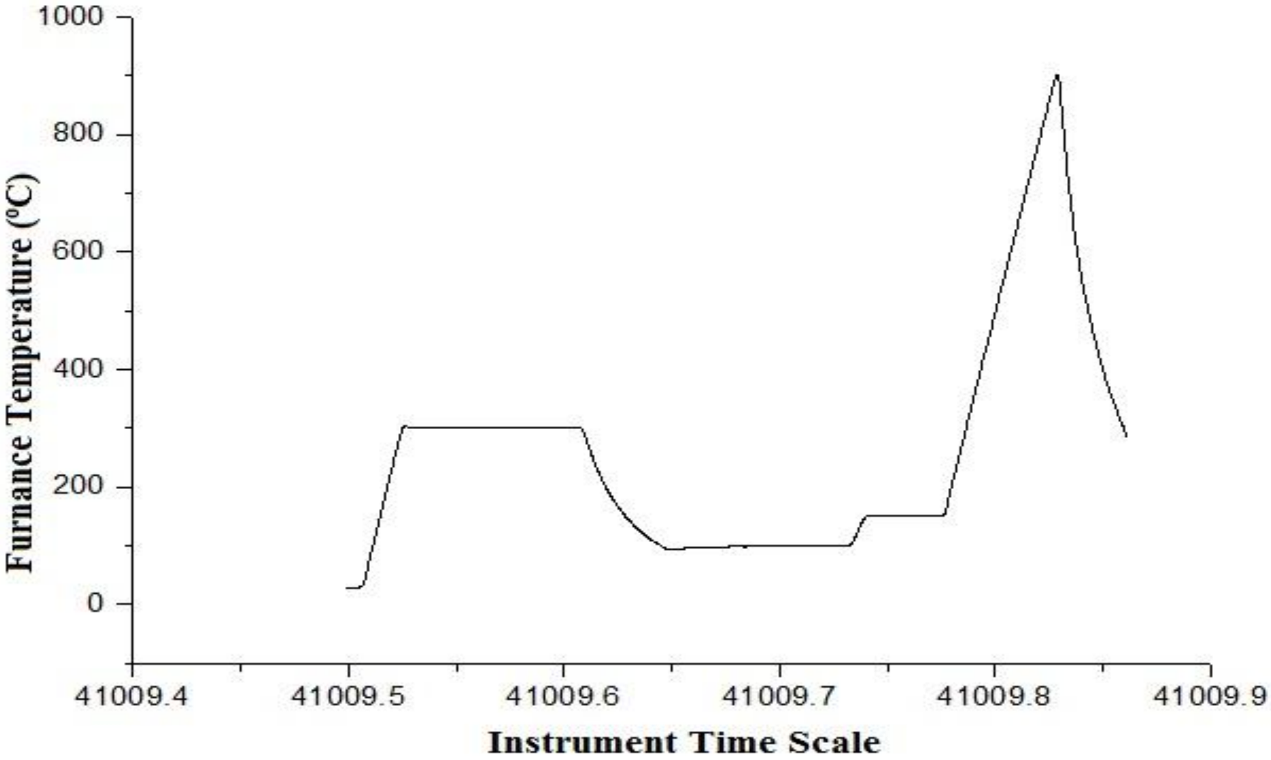

2.3.4 Nitrogen adsorption studies

Nitrogen adsorption/desorption studies were performed on an Autosorb 1 – Quantachrome instrument. The adsorption/desorption data was used to obtain BET surface areas for different zeolite samples. The degassing for all the samples was done at 300^{o}C for at least 6 hours or longer.

2.4 EVALUATION OF ZEOLITES

Bi-functional platinum loaded catalysts prepared from zeolite ZSM-12 as support, synthesized at different Si/Al ratios were evaluated in a fixed bed reactor at high reaction pressure for the hydroisomerization of n-hexadecane. Effect of variations in temperature, hydrogen pressure, WHSV (liquid hour space velocity) and Si/Al ratio of ZSM-12 as support on the conversion of n-hexadecane and selectivity towards hydroisomerization were obtained. Finally a comparison between product distribution obtained from ZSM-12, ZSM-22 and ZSM-23 was done for the hydroisomerization reaction.

2.4.1 Reaction Setup

Experiments were performed using a fixed-bed, up-flow reactor of dimensions 47cm X 1.1 cm ϕ (internal diameter) with a catalyst bed length of 8 cm and equipped with a thermowell (diameter -3mm, length 40mm) for measurement of catalyst bed temperature. The reactor temperature was maintained using ATS split type tubular furnace provided with K-type thermocouples which measured the reactor skin and bed temperature. Catalyst were placed in the reactor so as to have minimum temperature gradient and to have a sufficient layer of inert material towards the input to ensure proper preheating & distribution of feed before it first reacheed the catalyst zone. Catalysts to be evaluated were prepared in the shape of cylindrical extrudates of 1.6 mm diameter and having a length of ~3mm. During the loading process, the catalyst was typically divided into multiple batches. Following each batch of the catalyst, 80-120 mesh sand was packed into the void spaces of the catalyst bed, thus ensuring the uniformity of gas/liquid flow distribution. Around 5 g of extrudate was loaded in the reactor as per the mentioned procedure.

Catalyst loading was followed by pressure testing with N_2 and then by H_2. A minimal leak rate of less than 1 psi/hr was ensured at system pressure of 80 bar. The catalyst drying was carried out under nitrogen flow at 100ml/min for 12 hrs at a temperature of 120°C. Ramping to desired temperature was done at heating rate of 1°C/min. Once the catalyst dry down in nitrogen was completed, the system was switch on to once-through hydrogen gas at flow rate of 100 ml/min using a Brooks mass flow controller. Reactor off gas composition was monitored and when the concentration of hydrogen in the reactor off gas was greater than 90%, the system temperature was ramped to 300 °C at a heating rate of 1°C/min. The catalyst was then reduced for a period of 5hrs. Following this, the system pressure was raised to desired operating pressure and was controlled using a Tescom back pressure regulator. N-hexadecane was pumped in the reactor using a high performance liquid chromatography pump (HPLC pump) at the desired flow rates. A H_2/n-hexadecane molar ratio of 10.9 for was used for the all experiments.

The product from the reactor outlet was cooled using a heat exchanger connected to a chiller and it was further separated into gas liquid phase in a separator. The reactor effluent was passed through a heat exchanger connected to a chiller and cooled to a temperature of 15°C. It was then directed into a 200ml separating vessel kept at room temperature and in which liquid was collected and separated from a gaseous stream. The gaseous stream flow rate was measured using a wet gas meter and was analyzed for its composition using a Perkin elmer 1100 x refinery gas analyzer (equipped with multiple columns , thermal conductivity detector (TCD) and flame ionization detector (FID)). Liquid products were analyzed by a Agilent 6890N gas chromatograph equipped with a FID and a DB-Petro column (100m X 250 µm X 0.5 µm nominal). A 33 minute gas chromatograph program (120°C – 120°C, dwell 2 mins, 120°C – 250°C @5°C/min and 250°C – 250°C dwell 5 mins) was used to analyze the liquid products. A flow diagram for the used reaction setup is shown in figure 2.02.

Figure 2.02: Flow diagram of the reaction setup used for the hydroisomerization reaction

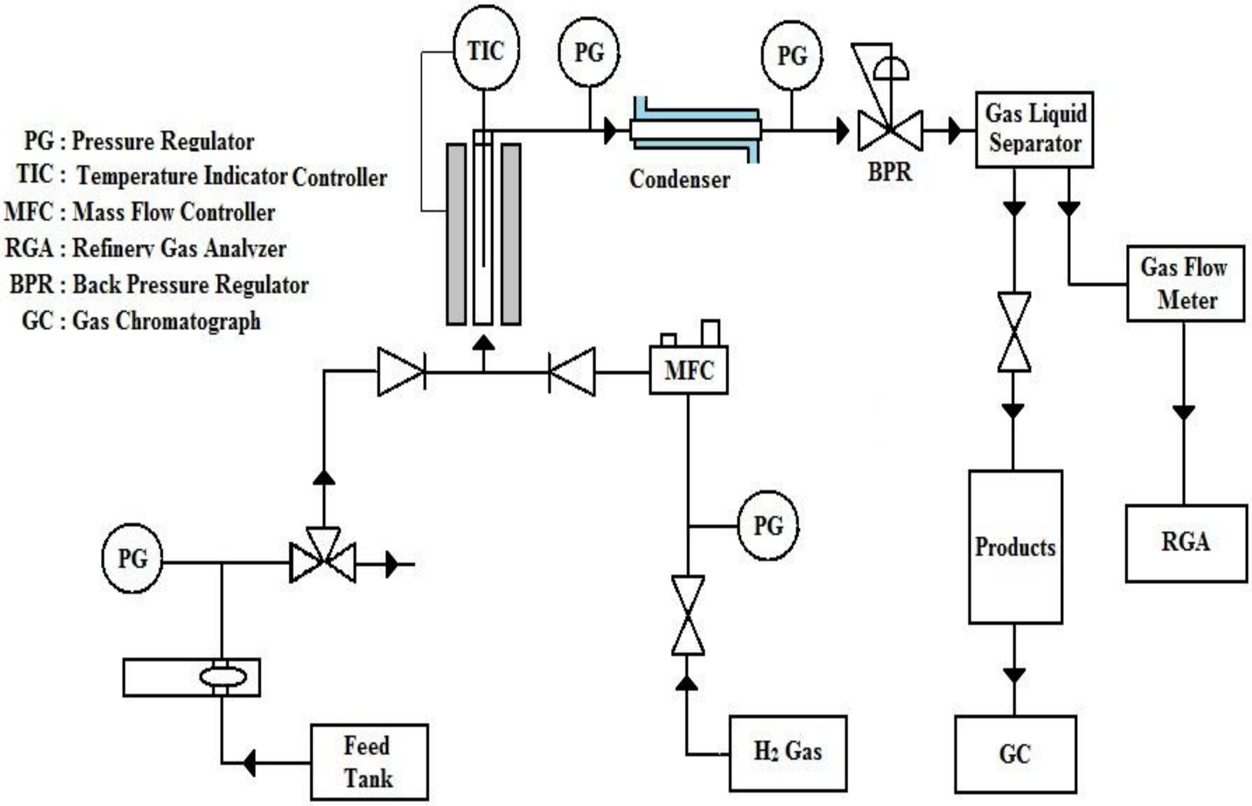

CHAPTER 3

RESULTS AND DISCUSSIONS

3.1 RESULTS AND DISCUSSIONS – ZEOLITE SYNTHESIS

The role of industries and profitable research organizations could hardly be undermined particularly in the case of development of new materials in the latter half of the twentieth century. In the field of zeolite synthesis, more often than not, a novel material was reported by a corporation (mostly Mobil Oil Corporation, thereby giving the name, Zeolite Socony Mobil, ZSM) through a patent instead of an open discussion through a journal. Therefore much information about the synthesis of zeolites remained as trade secrets and became available only later through open literature.

However through a careful study of the available patented literature from this earlier phase of zeolite synthesis and understanding the trends could shed some light, if not enlighten, about the art of zeolite synthesis. These ideas (more precisely the preferred values of critical factors) were further verified and reinforced by comparison with the knowledge that was shared later in the upcoming years (Ernst *et. al.*, 1984 and Smirniotis *et. al.*, 2001) by other researchers.

ZSM-12 was first synthesized by Rosinski and Rubin in 1974 from tetraethylammonium cations obtained from a variety of sources (Rosinski *et al.*, 1974). The tetraethylammonium cations were obtained either from salts like tetraethylammonium halides and hydroxides or generated in situ using triethylamine and an alkylating agent like diethylsulfate. The field of ZSM-12 synthesis soon opened up and the original patent was immediately followed by a number of patents for the synthesis of this new zeolite from a variety of structure directing agents. From 1974 to 1993, a period of 18 years, marked an important developmental phase for this particular zeolite and features more than 10 different patents on the synthesis of ZSM-12. Each new patent generally described the use of a different structure directing agent, its corresponding successful gel composition and valid characterization of the zeolite.

As stated earlier in section 1.5 in chapter 1, zeolite synthesis can be easily understood in terms of maintaining certain critical factors which control the crystallization and other properties of the zeolite. These critical factors were:

1. Structure Directing Agent and R/Si value.
2. Gel Si/Al ratio.
3. Alkaline metal concentration or M/Si value.
4. Alkalinity of the gel or OH/Si value.
5. Water content or H_2O/Si value.

Tetraethylammoniumhydroxide (TEAOH), tetraethylammoniumbromide (TEABr), methyltriethylammmoniumbromide (MTEABr) and benzyltrimethylammoniumchloride (BTMACl) were selected as the structure directing agents to study the synthesis of zeolite ZSM-12. The results obtained with these SDA's were discussed in the following sections.

3.1.1 MTEABr as Structure Directing Agent

Chu *et al.* from Mobil Oil Corporation and Ernst *et al.* from Engler-Bunte Institute had both described the synthesis of ZSM-12 using methyltriethylammonium cations in 1984. Chu *et al*. had patented the use of methyltriethylammoniumchloride (MTEACl) as the structure directing agent and the use of precipitated silica Hi-Sil as the source of silica and obtained ZSM-12 at gel Si/Al values between 150 to 300 (Chu *et al.,* 1984). Ernst *et al*. had described in the journal "Zeolites" the use of methyltriethylammoniumbromide (MTEABr) as the structure directing agent and sodium silicate as the source of silica to obtain ZSM-12 between gel Si/Al values of 60 to 120 (Ernst *et al.,* 1984). Also the International Zeolite Association's Synthesis Commission reported the standard method of ZSM-12 synthesis using precipitated silica, aluminum hydroxide and MTEABr as the structure directing agent at 140^{o}C in 6 days (IZA, synthesis commission).

In the present work, Initial experiments were done following the method described by Ernst (Ernst *et al.,* 1984). The synthesis data generated over various experiments and the corresponding results were given in Table 3.01. Ernst *et al.* reported the presence of Cristobalite and ZSM-5 as impurity phases. In our experiments the OH/Si values had been kept at a value of 0.3 which removed Cristobalite as an impurity. Thus in all the experiments with MTEABr only 100% ZSM-12 or ZSM-12 with ZSM-5 as an impurity phase was observed.

Ernst *et al.* concluded that increasing the gel Si/Al ratio enhanced the rate of crystallization for ZSM-12 decreased on increasing the aluminum content of the gel. Thus the incorporation of aluminum in ZSM-12 framework was a difficult process. For these reasons the gel Si/Al value was kept fixed at 60 for initial experiments. Ultimately ZSM-12 successfully crystallized between gel Si/Al values of 45 to 120 (Sample 79 (45), Sample 46 (60), Sample 61 (90) and Sample 75 (120)) when crystallization temperature was kept at 160°C for a period of 7 days. The identification of MTW or ZSM-12 phase was done by X-ray diffraction. The XRD spectra for the above samples are given in Figure 3.01

Figure 3.01: ZSM-12 at different Si/Al values using MTEABr

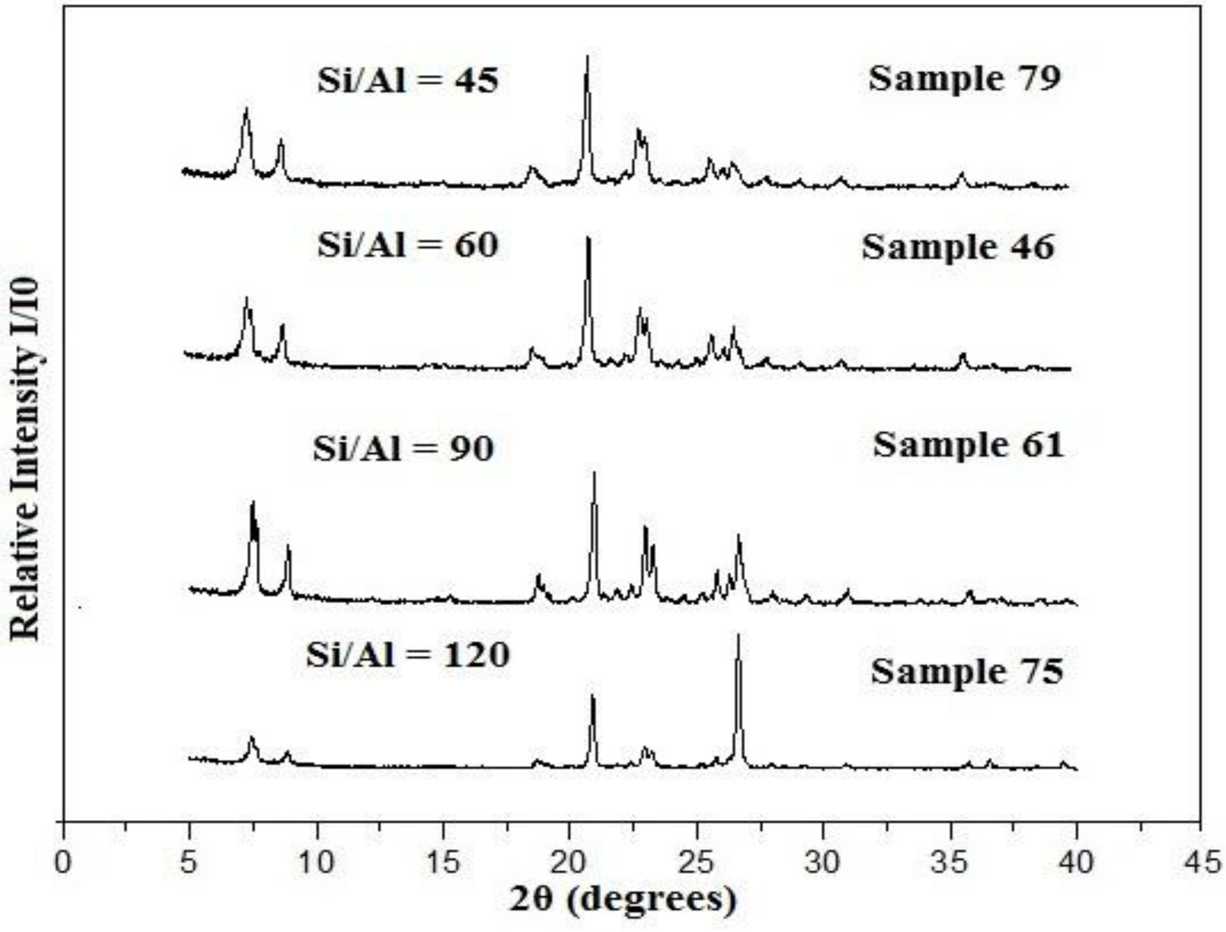

Table 3.01: Synthesis data using MTEABr as SDA

Sample	Gel Si/Al	MTEA/Si	Na/Si	Temperature (^{o}C)	Time (days)	Result
Sample 15	60	0.389	0.596	160	7 days	ZSM-12
Sample 21	60	0.389	0.596	160	7 days	ZSM-12
Sample 23	120	0.199	0.596	160	7 days	Quartz
Sample 24	90	0.299	0.596	160	7 days	ZSM-12 + ZSM-5
Sample 25	60	0.389	0.596	160	7 days	ZSM-12 + ZSM-5
Sample 41	60	0.389	0.596	165	7 days	ZSM-12
Sample 42	60	0.389	0.596	165	7 days	ZSM-12
Sample 43	60	0.389	0.596	165	7 days	ZSM-12
Sample 44	120	0.1993	0.596	160	7 days	ZSM-12 + ZSM-5
Sample 45	90	0.1993	0.596	160	7 days	ZSM-5
Sample 46	60	0.389	0.596	160	7 days	ZSM-12
Sample 48	60	0.389	0.596	160	7 days	ZSM-12 + ZSM-5
Sample 49	60	0.389	0.596	160	7 days	ZSM-12 + ZSM-5
Sample 50	60	0.389	0.596	160	7 days	ZSM-12 + ZSM-5
Sample 52	90	0.299	0.596	160	7 days	ZSM-12 + ZSM-5
Sample 53	90	0.299	0.596	160	7 days	ZSM-12
Sample 54	60	0.389	0.596	160	7 days	ZSM-12 +Impurity
Sample 55	90	0.299	0.596	160	7 days	ZSM-12 + ZSM-5
Sample 61	90	0.299	0.596	160	7 days	ZSM-12
Sample 62	90	0.299	0.596	160	7 days	ZSM-12
Sample 66	60	0.389	0.596	160	7 days	ZSM-12
Sample 67	60	0.389	0.596	160	7 days	ZSM-12
Sample 73	45	0.389	0.596	160	7 days	ZSM-12
Sample 74	90	0.389	0.596	160	7 days	ZSM-12
Sample 75	120	0.389	0.596	160	7 days	ZSM-12
Sample 79	45	0.389	0.596	160	7 days	ZSM-12
Sample 80	45	0.389	0.596	160	7 days	ZSM-12

Ernst *et al.* also asserted that sodium cation played a very important role in the nucleation and crystal growth process of zeolite ZSM-12 and MTEABr acted only as a pore filling agent instead of acting as the structure directing agent. This conclusion indicated that crystallization of ZSM-12 should not be very sensitive to a particular template to silica ratio or the R/Si value of the gel. Instead there should be a comfort zone or a particular range of R/Si values between which successful crystallization of ZSM-12 will take place. A comparison of gel compositions between sample 53 and sample 74 clearly illustrated the above point. The two gels differed only in their R/Si values and both gels crystallized into 100% pure ZSM-12 as indicated by XRD, shown in Figure 3.02. A complete specification of crystallization field in terms of R/Si values for MTEABr was beyond the scope of this thesis. However the above experiments clearly indicated the flexibility in the R/Si values of starting gels.

Figure 3.02: 100% pure ZSM-12 at different R/Si values using MTEABr

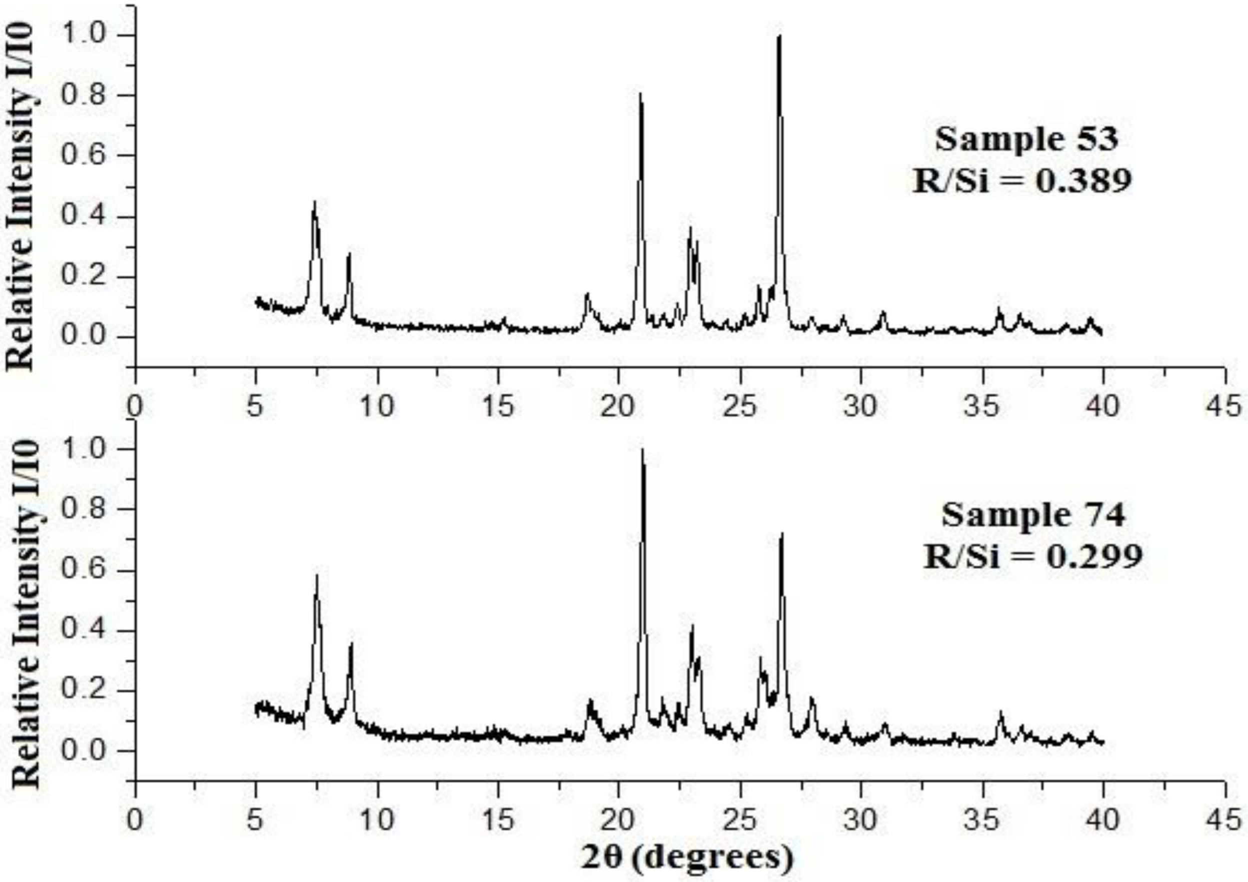

Ernst *et al.* also indicated the importance of OH/Si values of the gel in controlling the nucleation and growth of zeolite ZSM-12. There existed a minimum concentration of OH anions below which the crystallization of ZSM-12 was very slow. Thus an OH/Si value of 0.3 was chosen as the adequate value for all the experiments. This OH/Si value was achieved by neutralization of the excess anions by sulfuric acid. In the performed experiments slight deviations in OH/Si value from 0.3 resulted in a ZSM-5 impurity. Therefore an OH/Si value of 0.3 was recommended for the synthesis of ZSM-12 using MTEABr. When the MTEA/Si values were changed from 0.389 to 0.299 a ZSM-5 impurity was observed for OH/Si values less than 0.3. 100% pure ZSM-12 could only be obtained when the OH/Si values were maintained at a value of 0.3.

Finally Ernst *et al.* concluded that diluting the synthesis mixture increased the crystal size of the precipitated zeolite. To verify the effect of dilution 3 batches were prepared with 3 different levels of H_2O/Si values. A comparison of SEM images and crystal sizes of sample 48 (H_2O/Si=41), sample 49 (H_2O/Si=62) and sample 50 (H_2O/Si=83) clearly indicated a growth in crystal size. The XRD spectra for all 3 samples indicated minute amount of ZSM-5 as an impurity, observed by focusing the feature at 2θ value of 8, the position characteristic of a ZSM-5 XRD spectra. The impurity phase could also be observed in the SEM images, marked by the presence of spherical dots on the surface of prismatic ZSM-12 crystals. In spite of the minute amount of ZSM-5 as an impurity there was significant increase in the prismatic crystals of ZSM-12 with increasing dilution as reported by Ernst. Figure 3.03 clearly illustrates the above findings.

Sodium silicate was an excellent source for the synthesis of zeolite ZSM-12 because the inherent Na/Si ratio was the necessary and sufficient M/Si value desired for successful crystallization. However a 50% dilution of the sodium silicate solution prior to addition of other reagents provided sufficient dilution to avoid any unwanted ramification effects. Ramification or the solidification of gel, usually happened on rapid acid addition instead of a slow dropwise method. The best way to prevent this was to use a 50% diluted conc. sulfuric acid solution. MTEABr and Aluminum Nitrate both were easily soluble in water and could be easily added to the sodium silicate solution without any undesirable effects. The final gel was allowed to stir at room temperature for 2 to 3 hours before transferring into an autoclave for crystallization. However in a hot and dry weather the water content of the gel might alter by small amounts (2 -3 g) observed visually by appearance of dry solid at the gel-air interface. This could easily be tracked by noticing the difference in weight of the container after the final addition to the state ready for crystallization.

Figure 3.03: Effect of increasing dilution for ZSM-12 using MTEABr

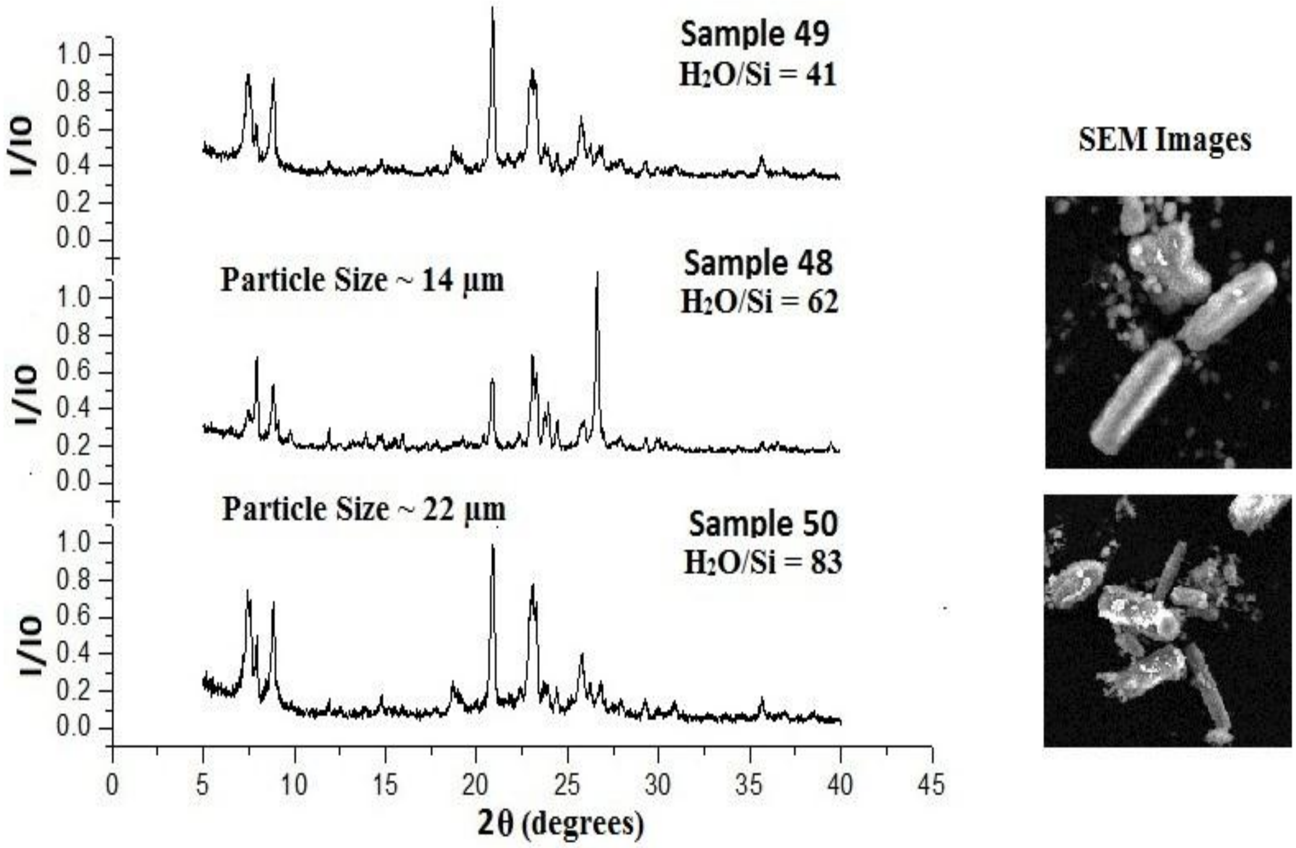

A typical XRD diffraction pattern for zeolite ZSM-12 (Sample 70) compared with the simulated X-ray diffraction pattern given by IZA was shown in Figure 3.07. The peak at 2θ value of 26.4^{o} corresponded to the (206) plane. There was significant variation in the intensity of the peak at this 2θ value. The peak corresponded to a valid zeolite ZSM-12 peak as can be verified by comparison with the simulated pattern. The reason for variation in intensity of this peak was assigned to the minute variations in the water content of the gel. Therefore a short period of stirring after final addition 1-2 hours at best was recommended. Sample 42 (Si/Al 60) and sample 75 (Si/Al 120) had shown a characteristic diffraction pattern where the peak at 2θ value of 26.4° was observed as the most intense peak. These samples were observed in SEM for any elevated growth into any of the planes. There was no such observable change in the shape of the crystals as compared to the other samples where the peak intensity was normal.

3.1.2 TEABr as Structure Directing Agent

Rosinski and Rubin came up with a patent in 1974 focusing at the use of tetraethylammonium cations for synthesis of ZSM-12 (Rosinski *et al.,* 1974). The tetraethylammonium cations were obtained either from tetraethylammoniumbromide salt and tetraethylammonium hydroxide or generated in-situ by the reaction between triethylamine and diethysulfate or any such alkylating agent. The group had given examples with each of these different TEA sources. However the Si/Al range described under the “particularly preferred” column is 45-60 indicating the sensitive nature of this template towards Si/Al value.

Smirniotis *et. al.* had done a thorough study on the synthesis of ZSM-12 from TEABr and TEAOH from 1999 onwards. The group reports aluminum content of the gel, alkalinity (OH/Si) and the concentration of template (TEA/Si) as important factors affecting the crystallization of ZSM-12. Alkalinity was kept a little lower in case of TEABr as compared to TEAOH. The crystallization was found to be faster in the presence of sodium when compared to pottasium.

The group had synthesized ZSM-12 in a wide range of Si/Al values with gel Si/Al values ranging from 30 to 150 and the actual Si/Al values of the products measured by ICP-AES ranged from 30 to 100. The BET surface area of the various samples varied in the range of 260-340 m^2/g with 300 m^2/g plus surface areas obtained in the case of low Si/Al values (<45). The morphology of the particles was reported as cube shaped with particles size less than a micron.

In the current investigation, the experiments using TEABr as structure directing agent were done along the guidelines suggested by Smirniotis *et al*.. However a failure in crystallization of ZSM-12 was observed in most of the samples. Only in the case when ammonium hydroxide was used in the gel as a pH buffer, a ZSM-12 sample with very low crystallinity was obtained at 140°C in

10 days. The XRD spectrum for this product (Sample 60) is shown in figure 3.04. The SEM image of sample 60 indicated cube shaped crystals as reported by Smirniotis *et al.*. However the size of crystals was observed in the range of 2-3 µm. The bigger size of the particles was assigned to the low crystallinity of the sample, which is clear from the XRD indicated by the presence of humps rising into peaks. The density of a zeolitic product phase increaseed with crystallization. A less crystalline sample might contain some fluffy (less dense) amorphous material surrounding the dense and small cube shaped crystals. This can be further confirmed by carefully observing the morphology of sample-60 where the cube shaped particles have blunt edges and might appear spherical. The sample can be best described as “not fully crystallized”.

Figure 3.04: XRD spectrum for sample obtained from TEABr as SDA

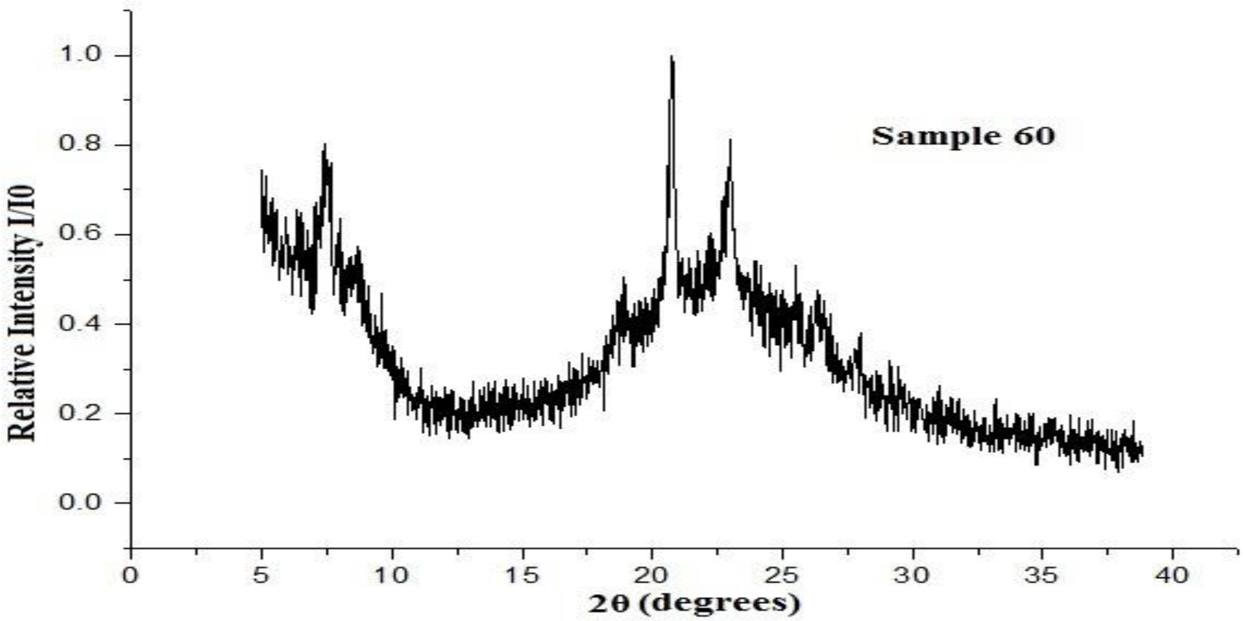

Table 3.02: Synthesis Data for ZSM-12 using TEABr as SDA

Sample	Gel Si/Al	TEA/Si	Na/Si	Temperature (^{o}C)	Time (days)	Result
Sample 14	60	0.465	0.106	140	11	Amorphous
Sample 38	150	0.125	0.059	160	7	Amorphous
Sample 39	80	0.125	0.078	160	7	Amorphous
Sample 40	120	0.125	0.067	160	7	Amorphous
Sample 60	60	0.465	0.106	140	10	ZSM-12
Sample 64	60	0.125	0.082	160	7	Amorphous
Sample 65	60	0.465	0.106	140	10	Amorphous
Sample 71	60	0.465	0.106	150	9	Amorphous
Sample 72	60	0.465	0.106	150	9	Amorphous

The failure in successful crystallization of ZSM-12 from TEABr in most of the samples indicated the high sensitivity of this template to the various crucial factors. The most important of these factors would be the OH/Si ratio of the gel. The little success obtained in the case of sample-60 when ammonium hydroxide was used as pH buffer strengthens the above argument. Smirniotis *et al.* have tried to locate the favorable OH/Si ratios by plotting the OH/Si ratio of gels versus the Si/Al values. The plot indicated a narrow range of OH/Si ratios (0.05 – 0.1) where ZSM-12 was successfully crystallized. In fact the range narrows at low Si/Al values (<45) and high Si/Al values (>80) and was the most broad at medium Si/Al (≈60) values. The particularly preferred Si/Al values (45-60) as reported by Rosninski and Rubin also indicated the same.

Thus the use of TEABr as the structure directing agent for ZSM-12 might have the advantages of cost effectiveness and a low product crystal size but the sensitivity of the template towards OH/Si ratio raised the questions towards repeatability and effectiveness towards scale-up operations because of the difficulty in maintaining uniform and accurate conditions.

3.1.3 TEAOH as Structure Directing Agent

The structure directing TEA cations could be obtained from any source. However a critical issue was faced while using TEAOH as the structure directing agent. The alkalinity of the primary gel in case of TEAOH couldnot be measured or tracked because of the highly basic nature of this template. The pH of the gel always remained at 14.0.

Table 3.03: Synthesis Data for ZSM-12 using TEAOH as SDA

Sample	Gel Si/Al	TEA/Si	Na/Si	Temperature (^{o}C)	Time (Days)	Result
Sample 1	36	0.2	0.0366	160	6	Amorphous
Sample 4	70	0.245	0.0188	160	6	Amorphous
Sample 5	60	0.465	0.0225	160	4	BETA
Sample 6	60	0.245	0.0219	160	4	Amorphous
Sample 7	60	0.125	0.0219	160	4	Amorphous
Sample 8	45	0.245	0.03	180	5	ZSM-5
Sample 12	45	0.245	0.03	170	5	ZSM-5
Sample 13	60	0.2376	0.029	170	5	ZSM-5
Sample 16	60	0.2376	0.029	165	5	ZSM-5
Sample 17	70	0.153	0.0188	165	6	Amorphous
Sample 18	70	0.325	0.0188	160	6	Amorphous

The gel composition reported by Rosinski and Rubin in 1974 was chosen as the starting point. At a Si/Al value of 45 and a crystallization temperature of 180^{o}C for 5 days, the gel resulted in pure ZSM-5. The same gel composition (Sample 12) resulted again in to ZSM-5 at a crystallization temperature of 170^{o}C. A comparison of XRD spectra of sample 12 and 100% pure ZSM-5 in figure 3.05 confirmed this observation. Rosinski reported the importance of relative metal concentration as an important factor. This factor could be measured by measuring the ratio of moles of template to the total amount of cations (R/(R+Na)) present in the gel (Na and R). The synthesis results for a Si/Al value of 60 using the same value of R/(R+Na) as in the above case (0.89) also resulted in similar ZSM-5 samples. A variation in the gel composition to vary the R/(R+Na) in both directions from the above ratio (0.94 and 0.85) resulted in amorphous products.

Figure 3.05: Comparison of product obtained from TEAOH as SDA and 100% ZSM-5

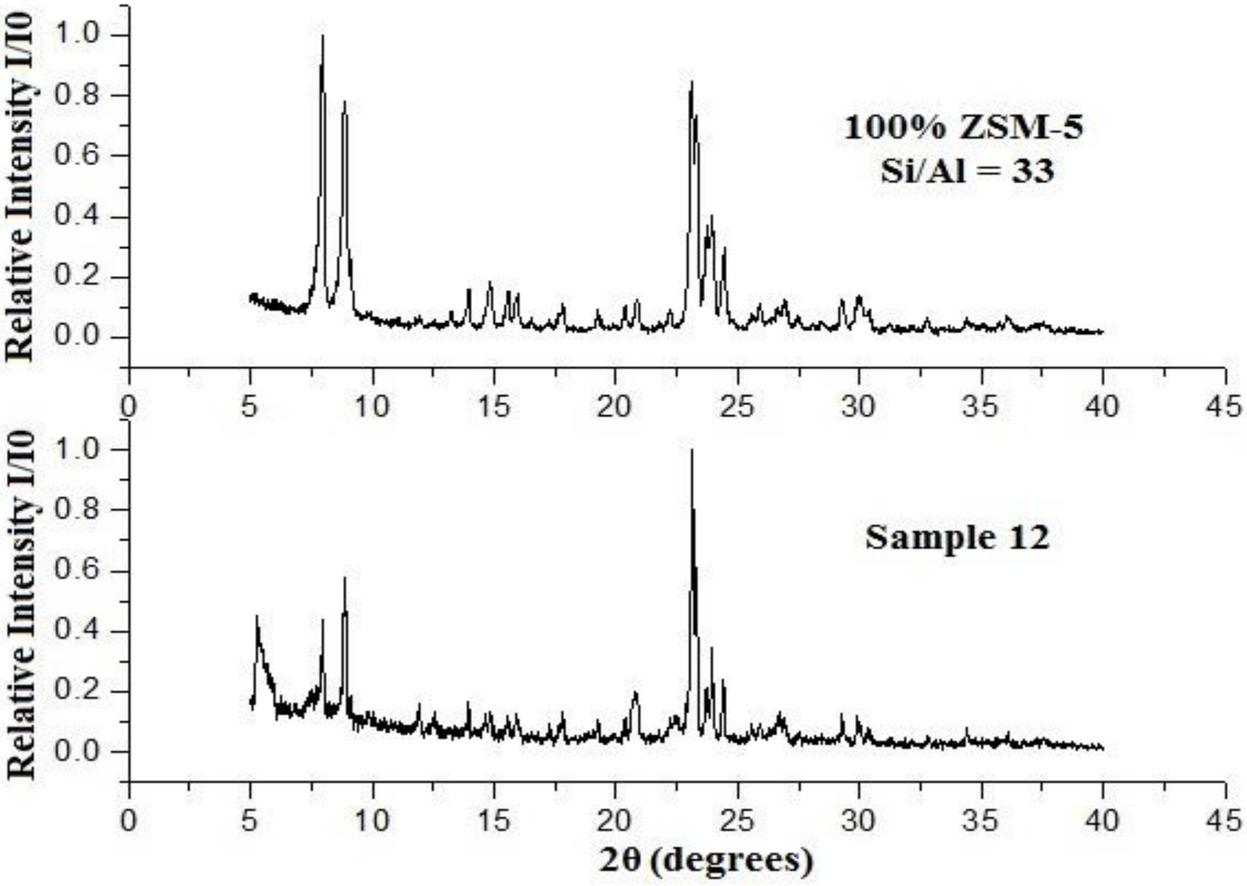

Thus only mixtures of ZSM-5 and ZSM-12 could be obtained from TEAOH under the limited set of experiments. A difficulty was observed in tracking and varying the OH/Si ratio of the gel because of the inherent high alkalinity of TEAOH solutions. The template was highly sensitive to the OH/Si and Si/Al ratios of the gel.

3.1.4 BTMACl as Structure Directing Agent

Benzyltrimethylammoniumchloride was first patented for the synthesis of ZSM-12 by Rubin in 1986 (Rubin *et al.*, 1986). The patent described the synthesis of ZSM-12 from SAR ratio of 137 to ∞ (pure silicalite structure). The molecule therefore had potential as a SDA with great flexibility towards crystallization at variable SAR ratios. Ernst *et al.* had reported the difficult incorporation of aluminum in ZSM-12 at low Si/Al values (Ernst *et al.*, 1984). This observation was verified again by Smirniotis *et al.* and their main achievement was the synthesis of ZSM-12 at Si/Al values up to 30, below which the crystallization did not take place (Smirniotis *et al.*, 2001). The experiments conducted in the project work also had shown a similar trend and ZSM-12 was obtained only at gel Si/Al ratios above 45 using MTEABr. In case of BTMACl ZSM-12 crystallized at even higher Si/Al ratios starting at a Si/Al value of 75.

The experiments conducted had shown a difficulty in crystallization of ZSM-12 at low Si/Al values with BTMACl as the SDA. The successful crystallization occurred at 160^{o}C in a period of 6 days with gel Si/Al values ranging from 75 to 120 (Sample 63 (75), Sample 69 (90) and Sample 70 (120)). The BET surface area for these samples averaged around 260 m^2/g. The morphology of particles was found to be rice shaped crystals of size in the range of 2µm to 3µm. The synthesis data generated for BTMACl as the structure directing agent was shown in Table 3.04.

Two different aluminum precursors, sodium aluminate and pseudo bohemite had been used for the synthesis of ZSM-12. All the experiments using sodium aluminate resulted into amorphous materials whereas the experiments using pseudo bohemite resulted in crystalline ZSM-12. This behavior was found as controversial because the synthesis method using pseudo bohemite used the required amount of pseudo bohemite in a sodium hydroxide solution with heating at 70^{o}C and vigorous stirring. The expected product of this first step was sodium aluminate. Therefore an in situ generated sodium aluminate resulted into successful crystallization compared to the use of synthetic sodium aluminate. Rubin *et al.* had also differentiated in the use of these two aluminum sources in their 1986 patent (Rubin *et al.*, 1986). The patent described the use of pseudo bohemite or alpha alumina monohydrate for low Si/Al ratios (90 - 274) and sodium aluminate as the source of aluminum for very high Si/Al ratios (500- ∞, pure silicalite structures).

Table 3.04: Synthesis data using BTMACl as SDA

Sample	Gel Si/Al	BTMA/Si	Na/Si	Temperature (^oC)	Time (days)	Result
Sample 19	50	0.09	0.215	160	5 days	Amorphous
Sample 20	500	0.09	0.047	160	5 days	Amorphous
Sample 26	137	0.155	0.073	160	7 days	Amorphous
Sample 27	137	0.155	0.123	160	7 days	Amorphous
Sample 28	137	0.155	0.123	160	7 days	Amorphous
Sample 29	137	0.09	0.047	160	7 days	Amorphous
Sample 30	137	0.09	0.09	160	7 days	Amorphous
Sample 31	137	0.09	0.166	160	7 days	Amorphous
Sample 32	137	0.09	0.0486	160	7 days	Amorphous
Sample 33	137	0.09	0.0225	160	7 days	Amorphous
Sample 34	137	0.09	0.01	160	7 days	Amorphous
Sample 63	75	0.2	0.2	160	6 days	ZSM-12
Sample 69	90	0.2	0..2	160	6 days	ZSM-12
Sample 70	120	0.2	0.2	160	6 days	ZSM-12
Sample 76	45	0.2	0.2	160	6 days	Amorphous
Sample 77	60	0.2	0.2	160	6 days	Amorphous
Sample 78	45	0.2	0.395	160	6 days	Unknown

ZSM-12 samples prepared using MTEABr as structure directing agent showed a significant variation in the peak intensity of the peak at 2θ values of 26.4^o. However no such variation in intensity of the peak at 26.4^o took place in the case of BTMACl as the structure directing agent. A typical X-ray diffraction pattern obtained for BTMACl and compared with MTEABr is shown in figure 3.09. The only difference in these two XRD spectra was the difference in intensity of the (510), (206) and (-606) planes. The BET surface areas of samples prepared from BTMACl as SDA averaged around 260 m^2/g.

Thus the use of BTMACl as a structure directing agent for the synthesis of ZSM-12 seemed very promising. The straight forward advantages of using this SDA were the relatively low cost of the SDA (BTMACl) and the small size of ZSM-12 crystals.

3.1.5 1,2 diaminohexane as structure directing agent for ZSM-22

Synthesis of ZSM-22 with 1,2 diaminohexane as structure directing agent was based on the research work by Ernst *et al.* for the study of n-decane isomerization (Ernst *et al.*, 1989). In addition to the typical zeolite synthesis parameters like Si/Al ratio, OH/Si ratio, Na/Si ratio and R/Si ratio, temperature of synthesis and stirring rate had a profound effect on the purity of products obtained. The typical competing phase was a ZSM-5 phase along with pure ZSM-22 phase. The product crystallized in aggregation of needle shaped crystallites of crystallite sizes in the range of 1µm - 2µm. A typical XRD pattern for the product is shown in figure 3.06.

Figure 3.06: Typical XRD powder patterns for ZSM-22 and ZSM-23

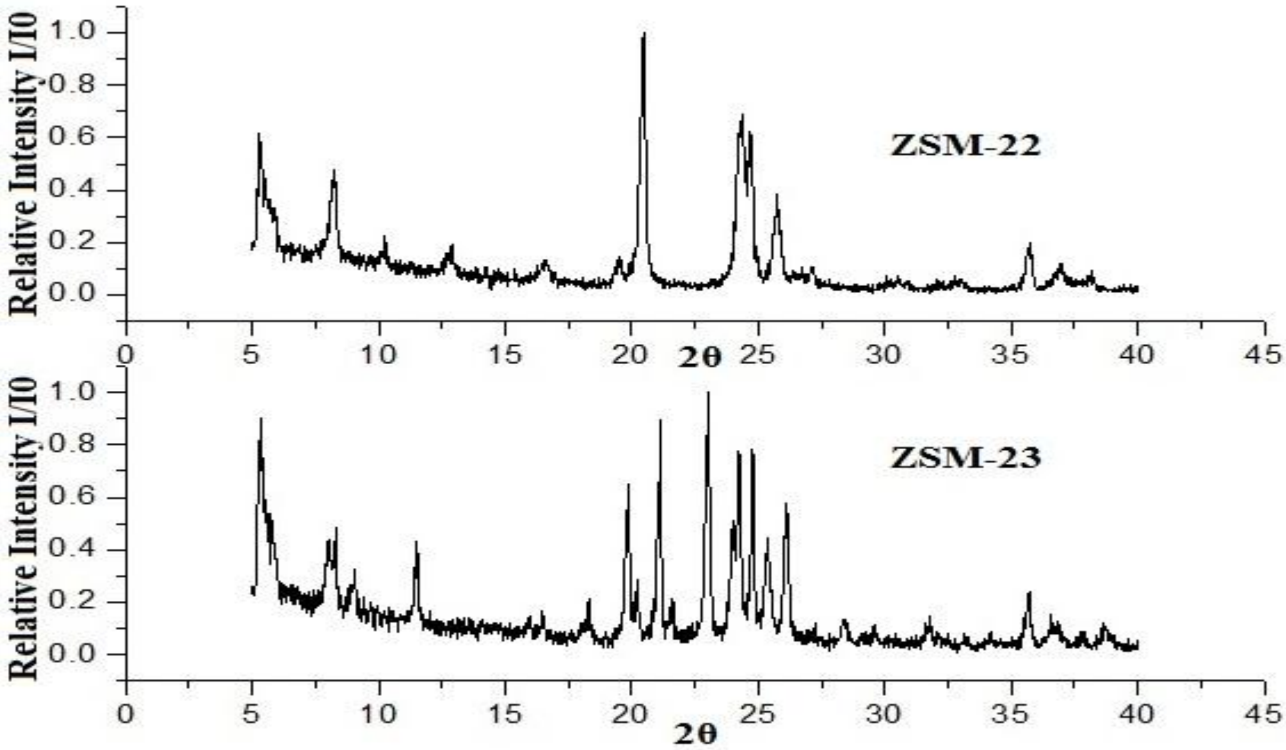

3.1.6 Pyrrolidine as structure directing agent for ZSM-23

Synthesis of ZSM-23 was done with pyrrolidine as structure directing agent (Ernst *et al.*, 1988) Synthesis temperature and stirring rate were two additional crucial factors governing the successful synthesis of zeolite ZMS-23 in addition to the usual factors like Si/Al ratio, OH/Si ratio, Na/Si ratio and R/Si ratio. ZSM-23 was successfully synthesized at Si/Al ratios of 45 and 60 for a direct comparison of performance with other zeolites (ZSM-12 and ZSM-22). Study of synthesis parameters in detail was beyond the scope of this project. Crystalline product with needle shaped crystals in the range of 1µm - 2µm were observed. A typical XRD pattern for the product was shown in figure 3.06.

3.2 RESULTS AND DISCUSSIONS – CHARACTERIZATION OF ZEOLITES

3.2.1 X-ray diffraction studies for ZSM-12 based samples

The purity of a zeolite phase could be determined by a comparison of the X-ray diffraction patterns obtained for as synthesized samples with the simulated diffraction patterns. The position of various diffraction peaks gave information about the orientation of crystallographic planes from where the reflection of X-ray beams took place. These planes were characteristic to a particular zeolite and a complete identification of the planes could be done on the basis of miller indices. The intensity of X-ray diffraction peaks was a measure of the extent of growth of the zeolite in the respective directions gives by the h, k, l indices.

A typical X-ray diffraction pattern obtained for one of the zeolite samples (sample 70) with a comparison with IZA simulated diffraction pattern with complete identification of planes was given in Figure 3.07. It was important to note that the relative intensity values in a synthesized sample differed from the relative intensity values of same peaks in a simulated diffraction pattern. The growth of zeolite planes in a synthesized sample was effected by a variety of factors thereby causing a difference in the intensity values. Figure 3.08 illustrated the XRD pattern obtained by Ernst *et al.* and Smirniotis *et al.* and indicated a XRD pattern similar to the one shown in figure 3.07. The complete XRD data for relevant peaks (I/I0 > 0.1) was tabulated in Table 3.05.

For all the synthesized ZSM-12 samples, either 100% pure ZSM-12 phase or a mixture of zeolite ZSM-5 and ZSM-12 phases was obtained. It was the aim of this project to synthesize 100% pure ZSM-12 phases. Only those synthesized samples which had a completely pure ZSM-12 composition were used to prepare ZSM-12 based hydroisomerization catalysts. As such quantification of ZSM-5 impurity in impure samples was beyond the scope of this project. However the presence of ZSM-5 impurity could be easily identified by the appearance of a shoulder to the characteristic ZSM-12 peak at a 2θ value of 7.6 degrees. Further verification could be done on the basic of comparison of the diffraction pattern in the range of 2θ values from 22.5 degrees to 25 degrees. A typical XRD pattern for a sample containing ZSM-5 as an impurity compared with a XRD pattern obtained for a commercial ZSM-5 sample were shown in Figure 3.08. The zones indicating the identification of ZSM-5 impurity were highlighted.

Figure 3.07: Comparison of XRD pattern for an as synthesized zeolite with IZA simulated diffraction pattern with complete identification of planes

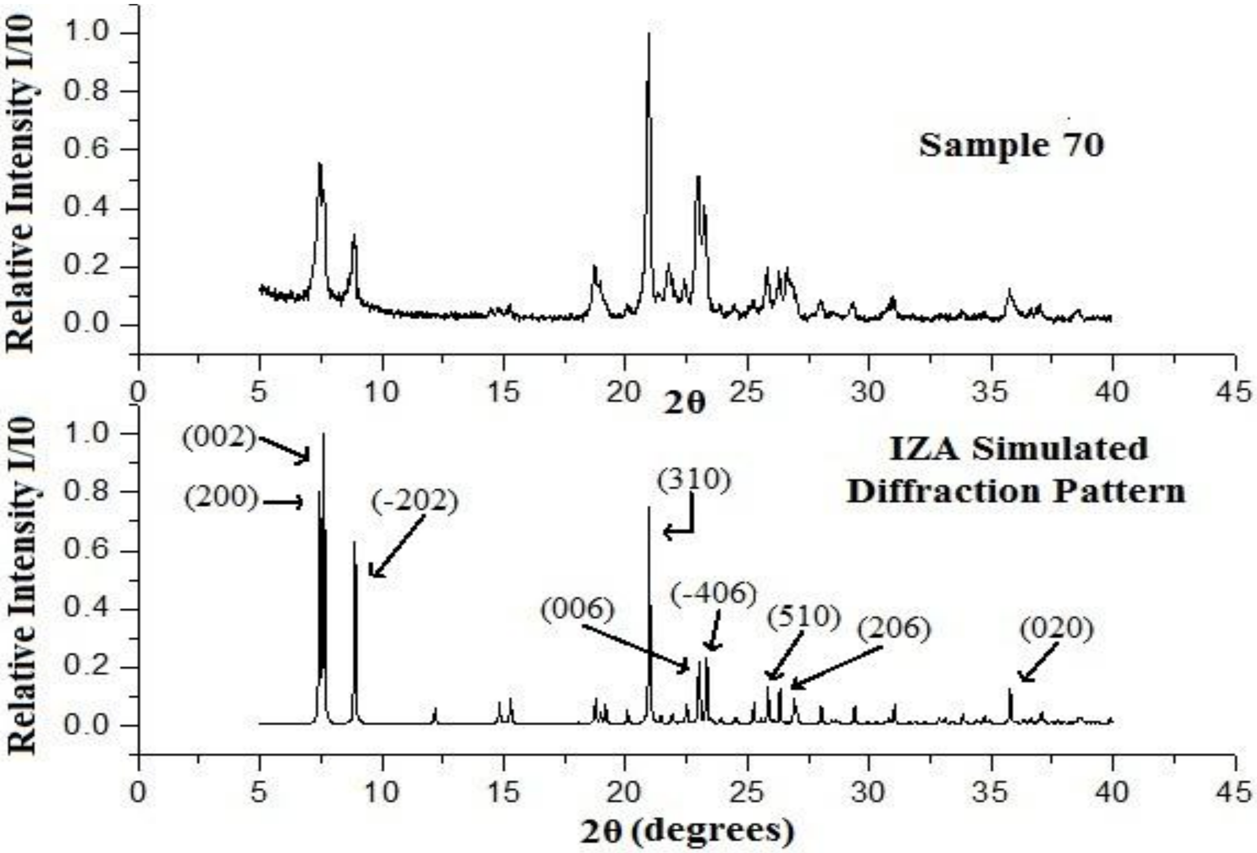

Table 3.05: Comparison of d-values and relative intensity values for as synthesized zsm-12 and IZA reported simulated data (a) Table on left hand side tabulated data for as synthesized sample70 (b) Table on right hand side tabulated data for IZA reported data.

(hkl)	d_{hkl} (A^o)	2θ (degrees)	I/I0	(hkl)	d_{hkl} (A^o)	2θ (degrees)	I/I0
(200)	11.8263	7.47	0.55	(200)	11.8417	7.459	0.78
(002)	11.5787	7.63	0.46	(002)	11.5865	7.624	1
(-202)	9.9179	8.91	0.27	(-202)	9.9292	8.899	0.64
(310)	4.2374	20.95	1	(310)	4.2315	20.977	0.76
(006)	3.8657	22.99	0.51	(006)	3.8622	23.009	0.19
(-406)	3.8231	23.25	0.41	(-406)	3.8085	23.337	0.23
(510)	3.4495	25.81	0.20	(510)	3.4427	25.858	0.10
(206)	3.3850	26.31	0.19	(206)	3.381	26.339	0.12
(020)	2.5071	35.79	0.11	(020)	2.5062	35.799	0.098

Figure 3.08: Typical XRD patterns obtained for ZSM-12 by Ernst *et al.* and Smirniotis *et al.* (Ernst *et al.,* 1987) (Smirniotis *et al.*, 2001)

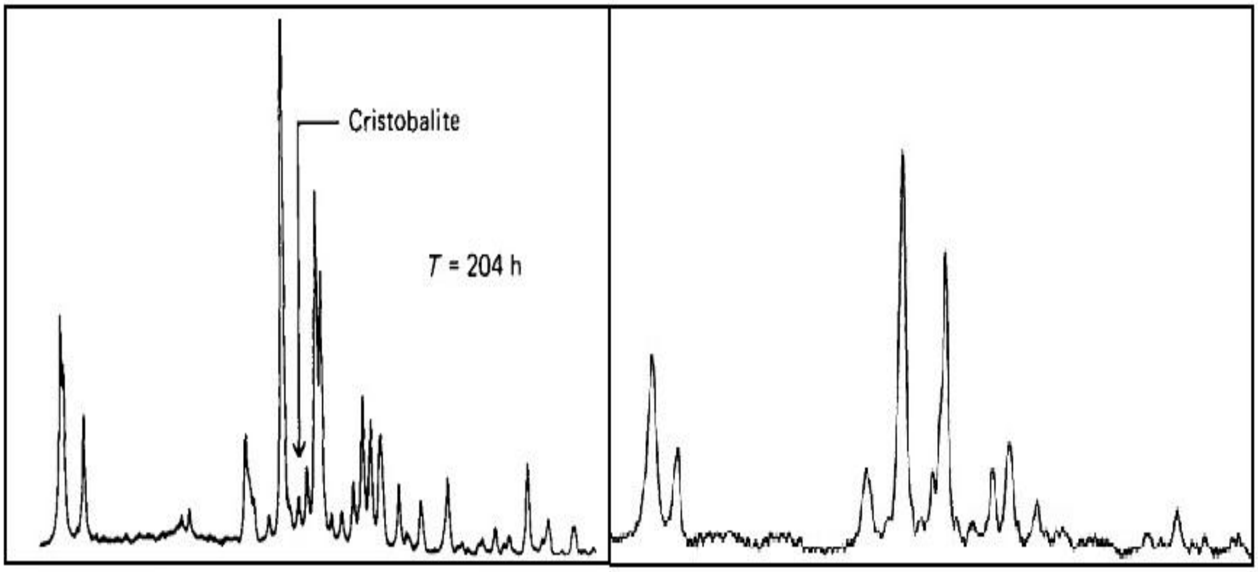

XRD Pattern Ernst *et al.*

XRD Pattern Smirniotis *et al.*

It was the objective of this project to study the synthesis of ZSM-12 from different structure directing agents such as MTEABr, TEABr, TEAOH and BTMACl. Crystalline samples were obtained only for MTEABr and BTMACl as SDA as described in the previous chapter. There was a slight difference in the X-ray diffraction pattern of ZSM-12 samples synthesized from these two templates. Figure 3.09 illustrated a comparison of XRD patterns for ZSM-12 samples prepared from MTEABr and BTMACl. The only difference in the XRD patterns was visible in the structure of peaks spread in the region of 2θ values 25 degrees to 27.5 degrees. Three peaks were visible in this region and the most prominent difference was found in the intensity values of peak at 2θ value of 26.34 degrees corresponding to the (206) plane. Sample 61 synthesized from MTEABr at a gel SAR ratio of 180 had a relative intensity value (I/I0) of 0.52 at a 2θ value of 26.34 degrees compared to a relative intensity value (I/I0) of 0.18 at the same 2θ value of 26.34 degrees for sample 69 synthesized from BTMACl at a gel SAR ratio of 180. Figure 3.09 highlighted the zone where the difference in intensities was present.

Figure 3.09: Comparison of an impure sample with ZSM-5 impurity with a commercial ZSM-5 sample

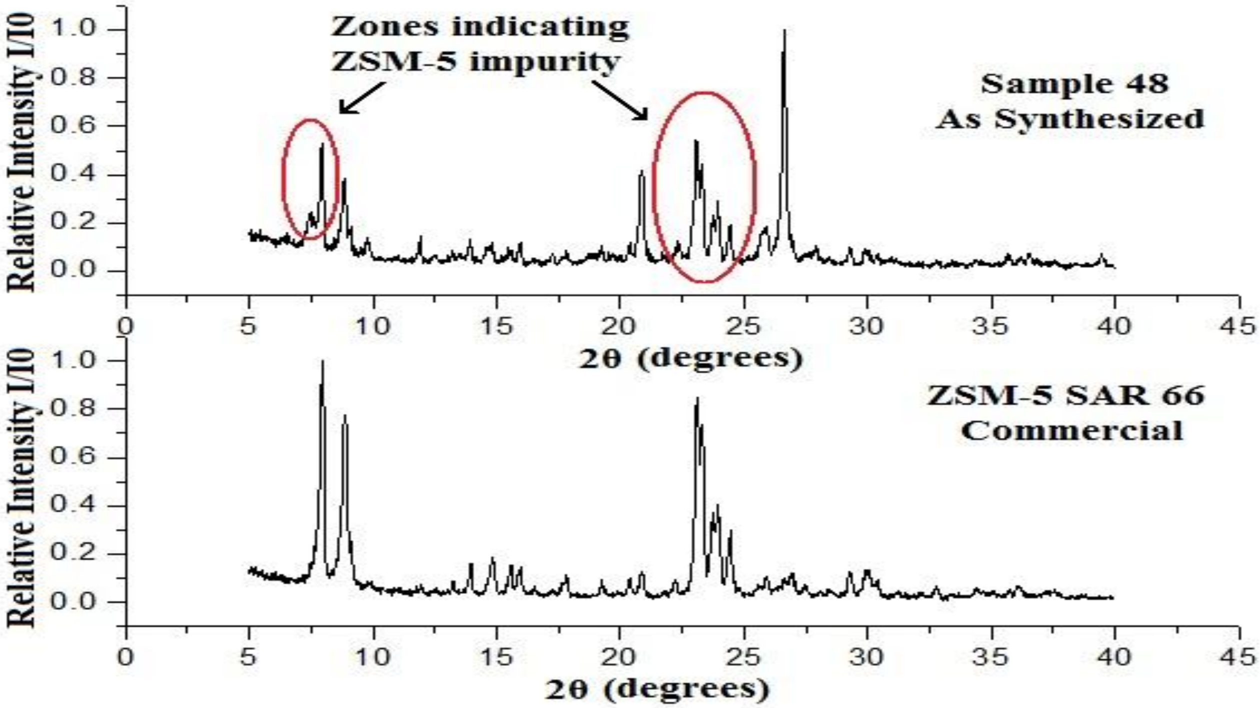

Figure 3.10: Comparison of ZSM-12 prepared from MTEABr and BTMACl as SDAs at SAR of 180

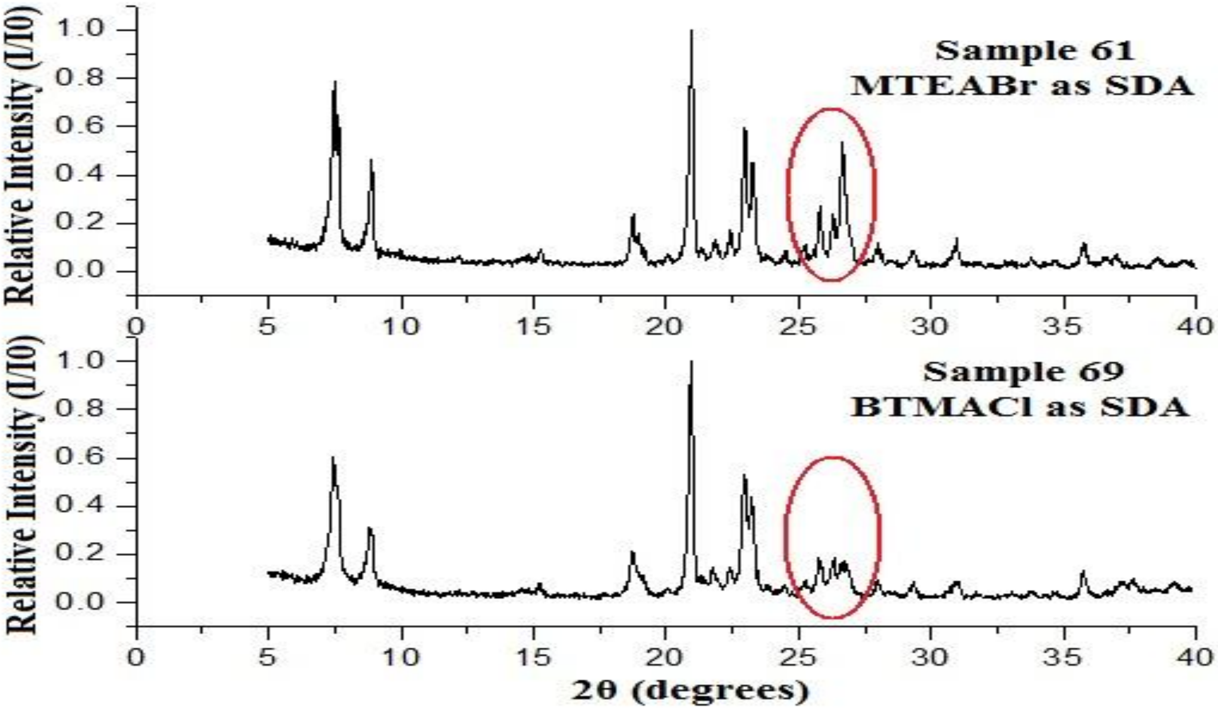

3.2.2 X-ray diffraction studies for ZSM-22 based samples

A typical X-ray diffraction pattern obtained for the as synthesized ZSM-22 sample with a comparison with IZA simulated diffraction pattern with complete identification of planes was given in Figure 3.11. Only the planes with relative intensity values greater than 0.1 were identified in terms of the miller indices. The complete XRD data for relevant peaks (I/I0 > 0.1) was tabulated in Table 3.06.

Table 3.06: Comparison of d-values and relative intensity values for as synthesized zsm-22 and IZA reported simulated data (a) Table on left hand side tabulated data for as synthesized sample (b) Table on right hand side tabulated data for IZA reported data

(hkl)	**d_{hkl} (A^o)**	**2θ (degrees)**	**I/I0**
(110)	10.7098	8.25	0.48
(020)	8.6242	10.25	0.22
(200)	6.8632	12.89	0.19
(021)	4.3356	20.47	1
(131)	3.6529	24.35	0.69
(330)	3.6090	24.65	0.62
(400)	3.4574	25.75	0.39
(002)	2.5126	35.71	0.19

(hkl)	**d_{hkl} (A^o)**	**2θ (degrees)**	**I/I0**
(110)	10.8454	8.15	1
(020)	8.7100	10.15	0.19
(200)	6.9295	12.76	0.22
(021)	4.3610	20.35	0.69
(131)	3.6695	24.23	0.49
(330)	3.6151	24.61	0.5
(400)	3.4648	25.69	0.34
(002)	2.5190	35.611	0.14

Figure 3.11: Comparison of XRD pattern for an as synthesized zeolite zsm-22 sample with IZA simulated diffraction pattern with complete identification of planes

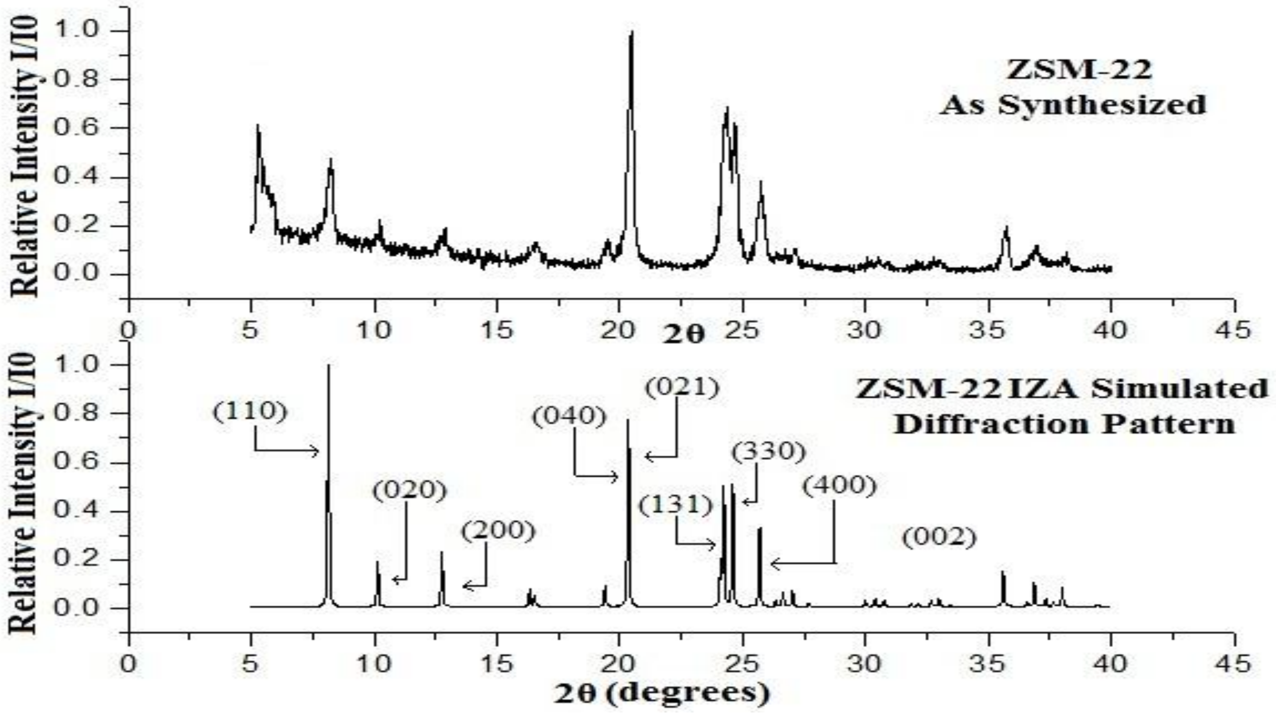

3.2.3 X-ray diffraction studies for ZSM-23 based samples

A typical X-ray diffraction pattern obtained for the as synthesized ZSM-23 sample with a comparison with IZA simulated diffraction pattern with complete identification of planes was given in Figure 3.12. Only the planes with relative intensity values greater than 0.1 were identified in terms of the miller indices. The complete XRD data for relevant peaks (I/I0 > 0.1) was tabulated in Table 3.07

Table 3.07: Comparison of d-values and relative intensity values for as synthesized zsm-23 and IZA reported simulated data (a) Table on left hand side tabulated data for as synthesized sample (b) Table on right hand side tabulated data for IZA reported data.

(hkl)	**d_{hkl} (A^o)**	**2θ (degrees)**	**I/I0**
(100)	11.0302	8.01	0.44
(002)	10.6327	8.31	0.49
(101)	9.7864	9.03	0.33
(102)	7.6827	11.51	0.43
(111)	4.4696	19.85	0.65
(112)	4.2056	21.11	0.89
(-113)	3.8624	23.01	1
(-211)	3.6707	24.23	0.77
(006)	3.5918	24.77	0.78
(-302)	3.5055	25.39	0.45
(205)	3.4079	26.13	0.57
(020)	2.5058	35.81	0.12

(hkl)	**d_{hkl} (A^o)**	**2θ (degrees)**	**I/I0**
(100)	11.1290	7.94	0.82
(002)	10.7595	8.21	1
(101)	9.8958	8.92	0.22
(102)	7.7456	11.42	0.33
(111)	4.4804	19.79	0.34
(112)	4.2156	21.05	0.31
(-113)	3.8582	23.03	0.25
(-211)	3.6735	24.208	0.25
(006)	3.5865	24.80	0.44
(-302)	3.5042	25.39	0.12
(205)	3.4087	26.12	0.18
(020)	2.5125	35.70	0.25

Figure 3.12: Comparison of XRD pattern for an as synthesized zeolite ZSM-23 sample with IZA simulated diffraction pattern with complete identification of planes

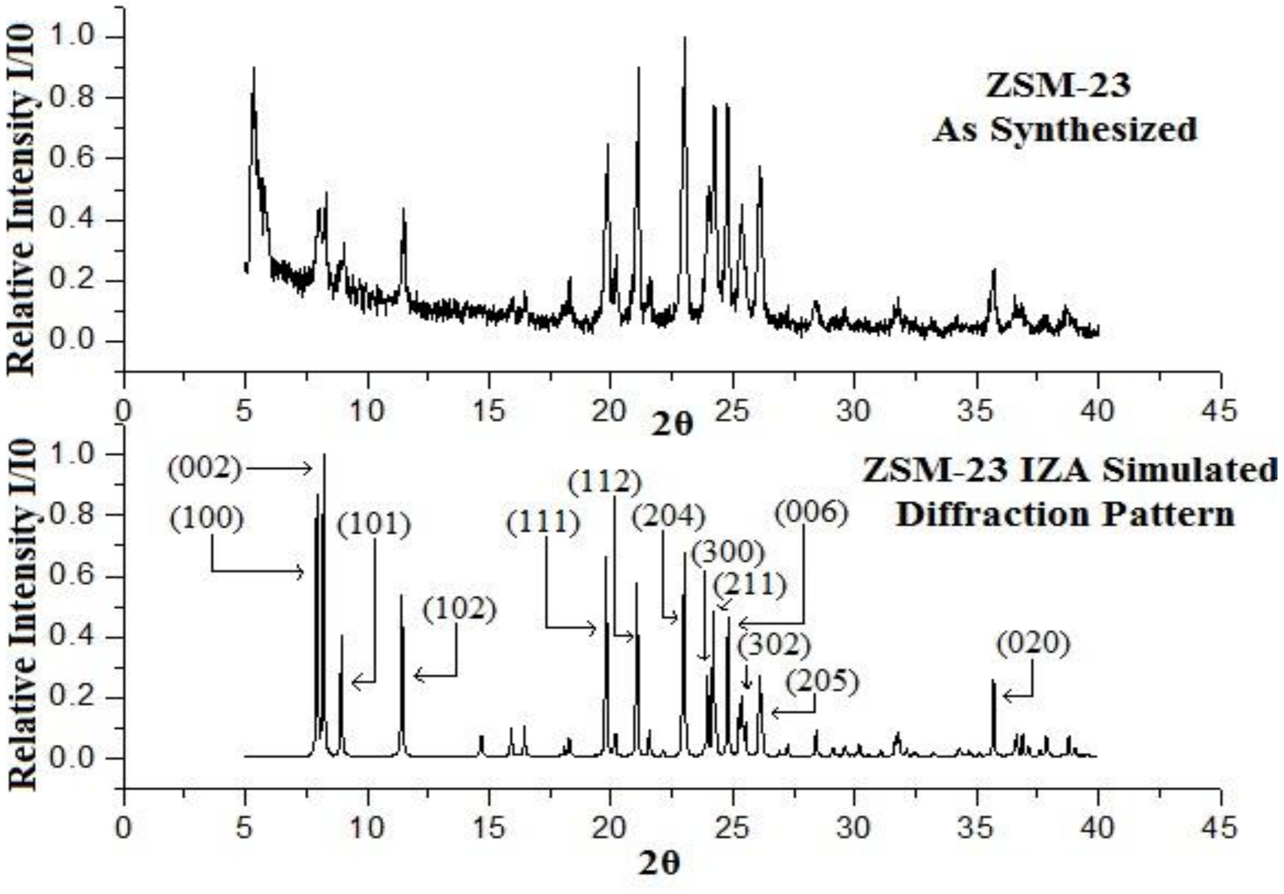

3.2.3 Scanning Electron Microscopy (SEM) Studies

Scanning electron microscopy technique used a beam of electrons to investigate the topography of sample. The beam of electrons interacted with the electrons of atoms present on the material surface and produced signal which contained information about the topography, composition and electrical conductivity of the sample. Scanning electron microscopy was used in the field of zeolite synthesis to investigate the morphology of the sample and to obtain the crystallite size of particles constituting the sample.

The microscopy studies in the course of this project were done on a TESCAN Scanning Electron Microscope. Figure 3.13 illustrated the morphology of ZSM-12 samples prepared from three different structure directing agents (MTEABr, TEABr and BTMACl). The morphology of crystals obtained from MTEABr had elongated cuboidal geometry with the size of crystals depending on the water content of the synthesis gel. A cuboidal geometry of crystals of size 2µm - 3µm was obtained for TEABr. BTMACl resulted in rice shaped crystals of size 2µm - 3 µm.

Figure 3.13: Morphology of ZSM-12 crystals obtained from 3 different SDAs

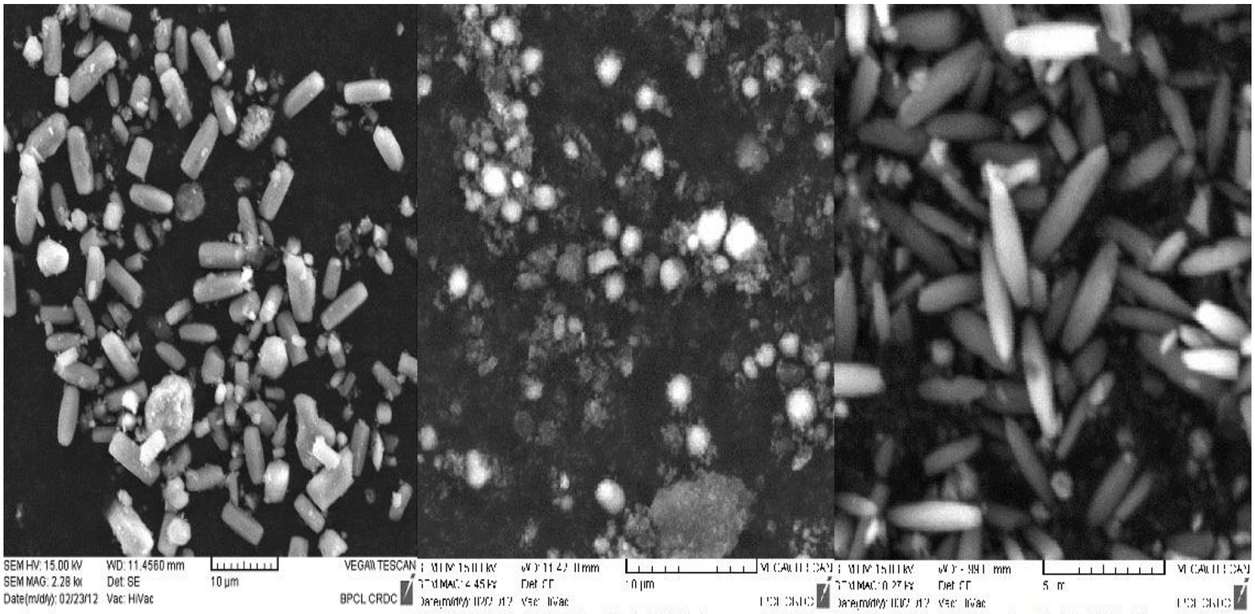

Sample 61 (MTEABr)
Crystal Size 5 µm - 6µm
Elongated Cube

Sample 60 (TEABr)
Crystal Size 2µm - 3 µm
Cuboidal Geometry

Sample 69 (BTMACl)
Crystal Size 2µm - 3 µm
Rice Shape

The crystal size of ZSM-12 samples prepared from MTEABr was dependent on the water content of the gel. The effect of increasing dilution on the size of crystals was studied for samples 48, 49 and 50. Figure 3.14 illustrated the SEM images of products obtained for two samples with difference in water content of synthesis gel. The size of the crystals increased from 14µm to 22µm on increasing the H_2O/Si values from 62 to 83.

Figure 3.15 illustrated the morphology of crystals obtained for ZSM-12 (MTEABr), ZSM-22 (DAH) and ZSM-23 (pyrrolidine). ZSM-22 was observed to have needle shaped crystals of size 2µm agglomerated into bunches of size upto 5µm. ZSM-23 also possessed needle shaped morphology of its fine crystal of size less than 1µm agglomerated into bunches of various sizes.

Figure 3.14: SEM images of two ZSM-12 samples with difference in water content of synthesis gel

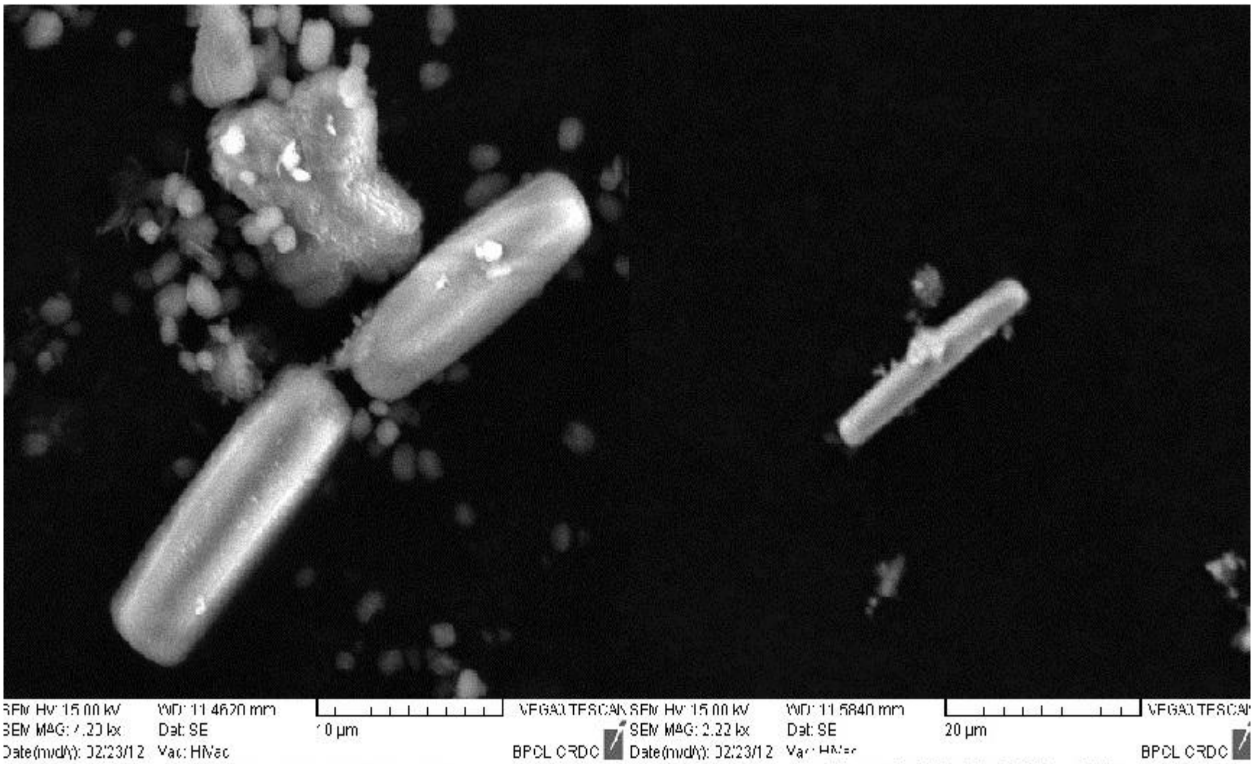

Sample 49 ($H_2O/Si = 62$)
Crystal Size 14µm

Sample 50 ($H_2O/Si = 83$)
Crystal Size 22 µm

3.2.4 Ammonia Temperature Programmed Desorption studies (NH_3 TPD)

Ammonia temperature programmed desorption technique was used to obtain the total acidity value for acidic materials. Zeolites contained both bronsted and lewis acid sites which rapidly change into each other in the presence of moisture at high temperatures. In such case ammonia TPD was an excellent method to measure the total acidity of zeolite based materials because ammonia molecule can adsorb on lewis acid sites by electron donation and bronsted acid sites by formation of NH_4^+ species.

Figure 3.15: Morphology of crystals obtained for ZSM-12, ZSM-22 and ZSM-23

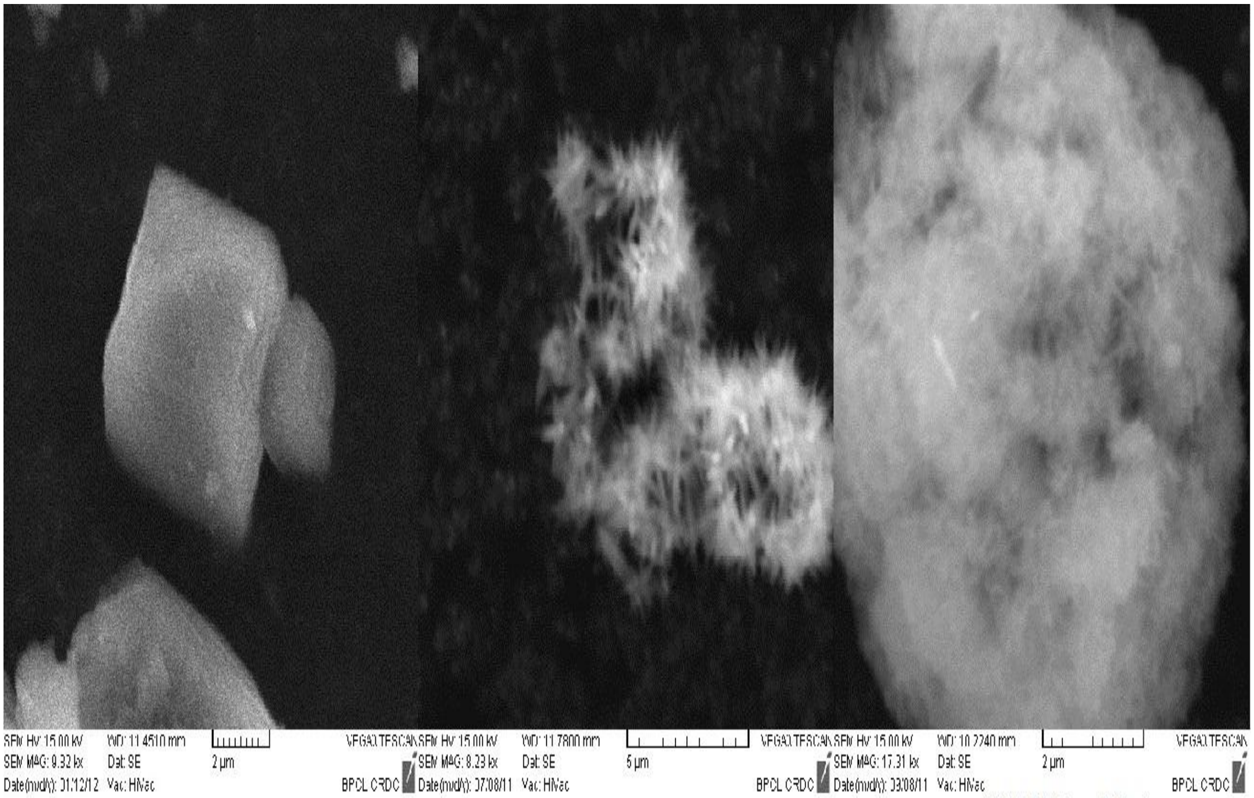

ZSM-12 (MTEABr)
Crystal Size 2µm - 3µm

ZSM-22 (DAH)
Crystal Size 2µm

ZSM-23 (Pyrrolidine)
Crystal Size < 1µm

The method for NH_3 TPD crudely consisted of two steps. NH_3 molecule was allowed to adsorb on the sample at ambient conditions. In the second step the temperature of the sample is increased linearly till a maximum temperature of 900^oC. The total ammonia desorbed from the sample in step two was the total acidity value of the zeolite sample in micro moles per gram.

The NH_3 TPD data for different zeolite samples which were used to prepare hydroisomerization catalysts was shown in table 3.08. It was important to note that NH_3 TPD technique was just a crude method of gathering information about the acidity of zeolite samples. The results varied from sample to sample because of the inherent non homogeneity of the samples in terms of the actual SAR ratio differing from the gel SAR ratio and the presence of extra framework alumina species.

Table 3.08 indicated that ZSM-23 (SAR120) was the zeolite with maximum total acidity (480 µmol/g), followed by ZSM-22 (170 µmol/g) and ZSM-12 (126 - 200 mol/g) with total acidity values in the same range. Figure 3.16 illustrated the NH_3 TPD patterns for ZSM-12, ZSM-22 and ZSM-23 all synthesized at gel SAR ratios of 120.

Table 3.08: Total acidity data for zeolite samples used to prepare hydroisomerization catalysts

Zeolite Sample	Hydroisomerization Catalyst	Total Acidity (µmol/g)
ZSM-12[79]	CAT-1	184
ZSM-12[41]	CAT-2	-
ZSM-12[43]	CAT-3	-
ZSM-12[63]	CAT-4	133
ZSM-12[61]	CAT-5	136
ZSM-12[69]	CAT6	130
ZSM-12[70]	CAT-7	124
ZSM-12[66]	CAT-8	199
ZSM-12[66]	CAT-9	184
ZSM-22 (SAR 120)	CAT-10	170
ZSM-23 (SAR90)	CAT-11	-
ZSM-23 (SAR 120, Ca)	CAT-12	480
ZSM-23 (SAR 120)	CAT-13	360

The total acidity of a zeolite was dependent on the silica alumina ratio of the zeolite. An increase in SAR ratio led to a decrease in total acidity of the zeolite. NH_3 TPD data was obtained for ZSM-12 samples at SAR ratios of 90, 120, 150, 180 and 240. Figure 3.17 illustrated the NH_3 TPD patterns obtained for ZSM-12 samples at different SAR ratios.

Figure 3.17: NH_3 TPD total acidity patterns and values for ZSM-12 samples

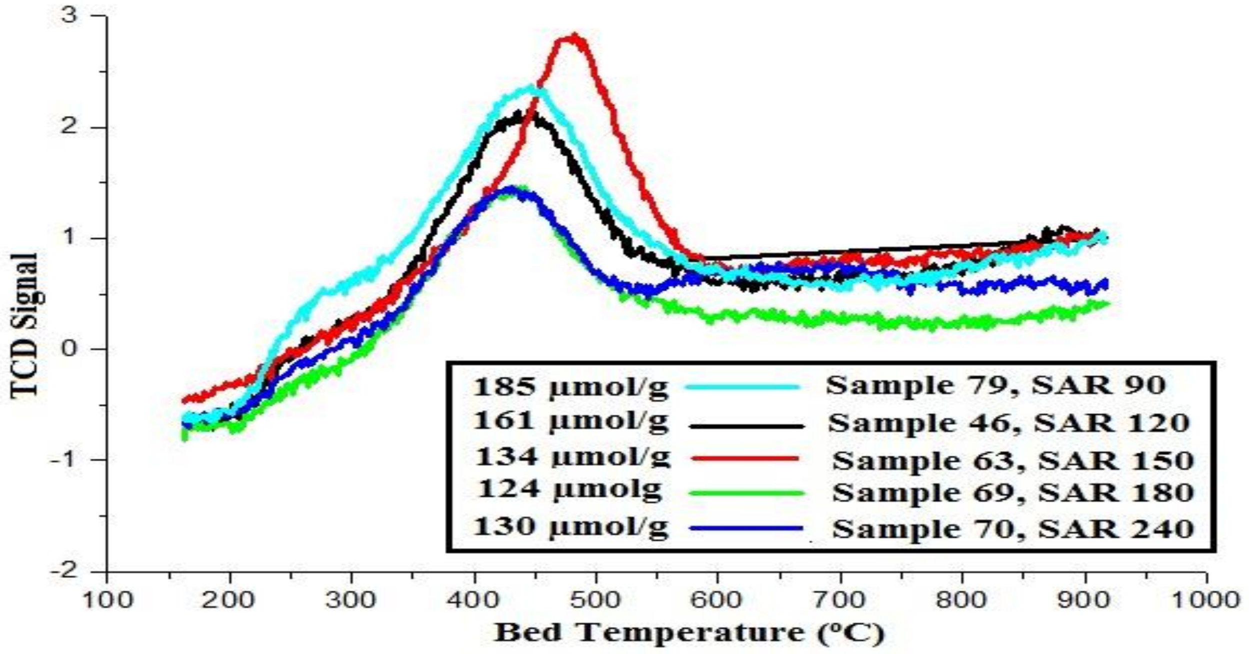

Figure 3.16: Comparison of NH_3 TPD patterns for ZSM-12, ZSM-22 and ZSM-23 zeolites synthesized at gel SAR of 120

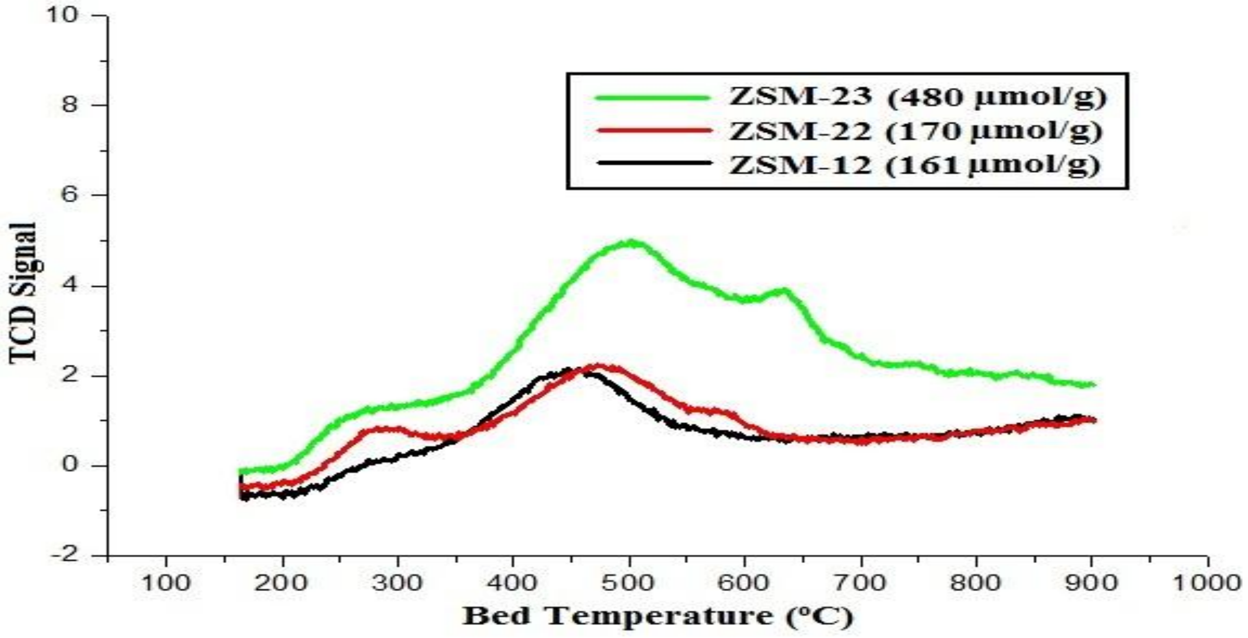

Finally, to study the effect of base metal loading, a sample (sample 66) of zeolite ZSM-12 was divided into two equal parts and each loaded with 0.35wt% calcium and 0.35wt% barium. This particular sample had a high value of total acidity (236 µmol/g) when compared to sample 46 (161 µmol/g), even though the gel SAR ratio was 120, same as sample 46. This was explained on the basis of a sample 66 actual SAR ratio less than the actual SAR ratio of sample 46 thereby having a greater total acidity. NH_3 TPD data for the calcium and barium loaded sample 66 gave total acidity values of 200 µmol/g for calcium and 185 µmol/g for barium. Figure 3.18 indicated such a comparison of the TPD patterns for these three zeolite samples. Although the height of peaks was almost same in these samples, the area under the curve varied leading to the above acidity values.

Figure 3.18: NH_3 TPD patterns for as such, calcium and barium loaded sample 66

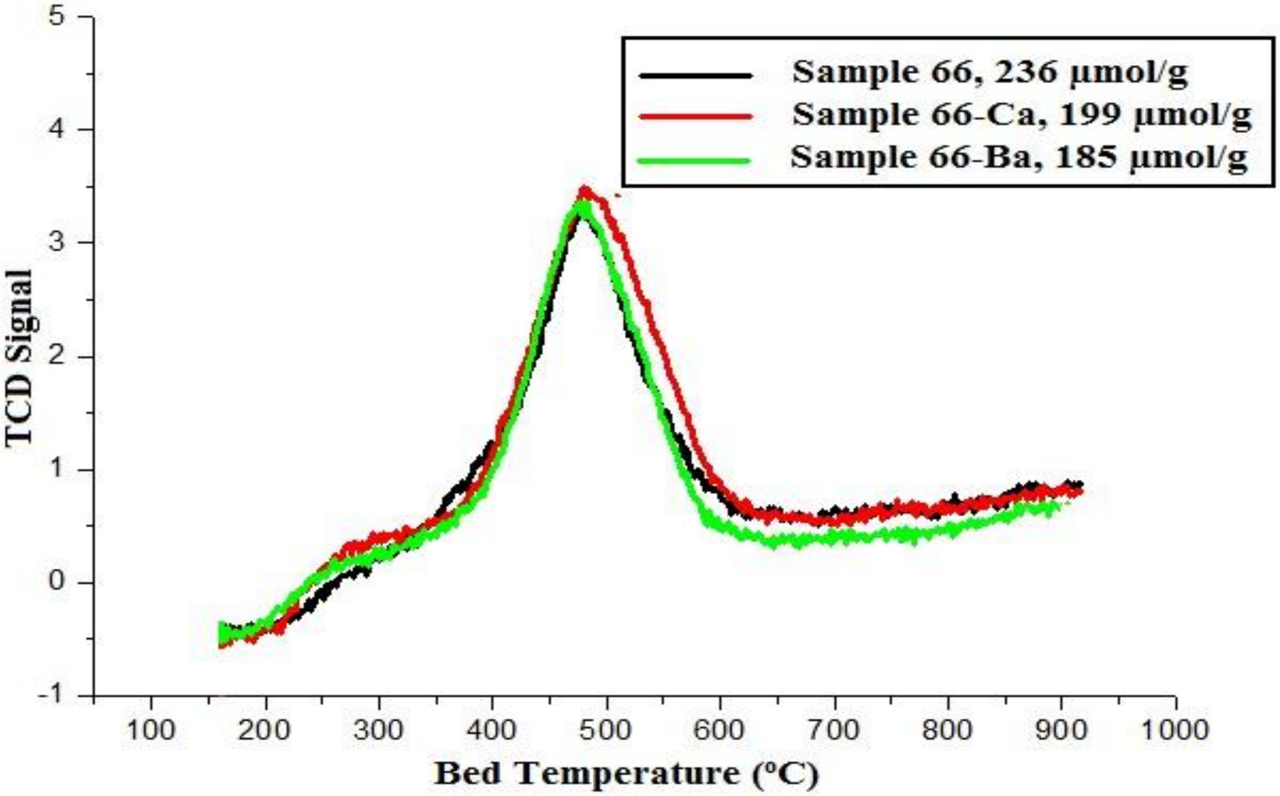

3.2.5 Nitrogen Adsorption/Desorption Studies

Nitrogen adsorption/desorption studies were performed on an Autosorb 1 – Quantachrome instrument. The degassing for all the samples was done at 300°C for at least 6 hours or longer. The instrument used the generated adsorption/desorption data to give multiple point BET surface areas using the BET equation. Figure 3.19, 3.20 and 3.21 illustrated the isotherms obtained from ZSM-12, ZSM-22 and ZSM-23 respectively. A complete collection of BET surface area data was done in table 3.08.

Figure 3.19: A typical Nitrogen isotherm for ZSM-12 zeolite

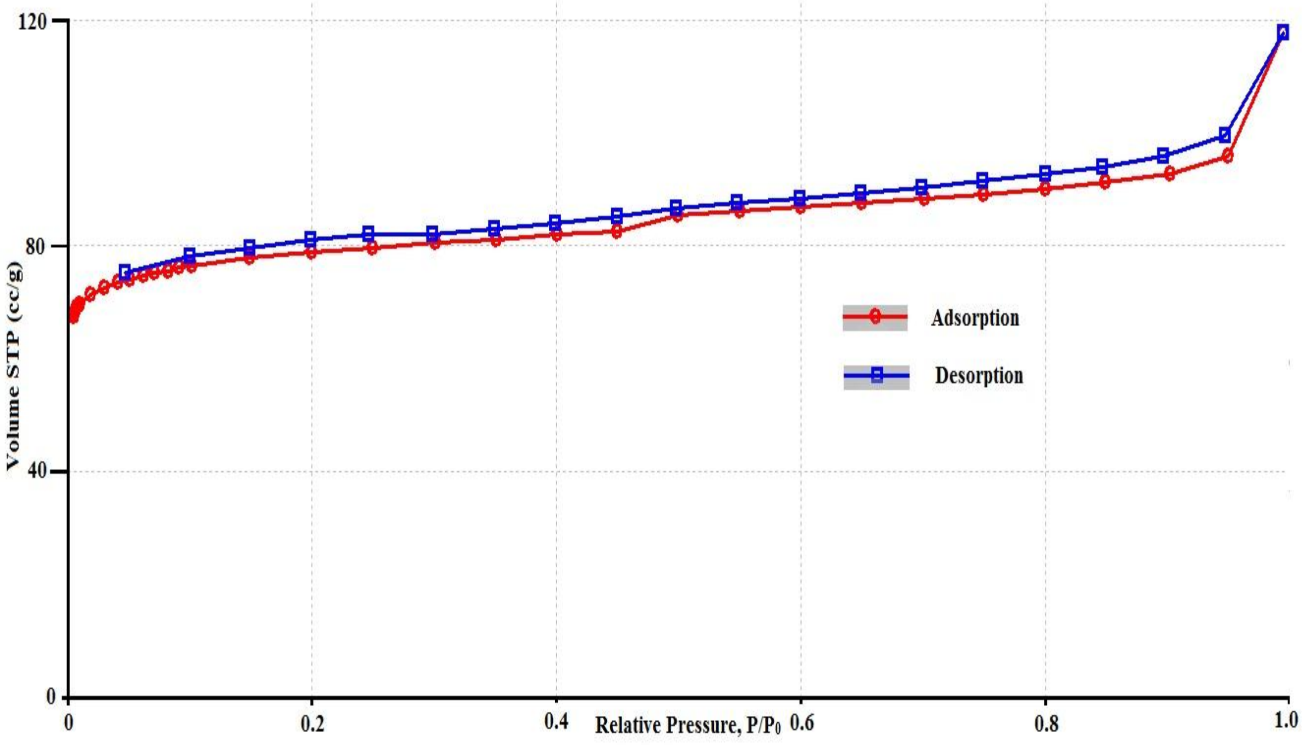

Figure 3.20: A typical Nitrogen isotherm for ZSM-22 zeolite

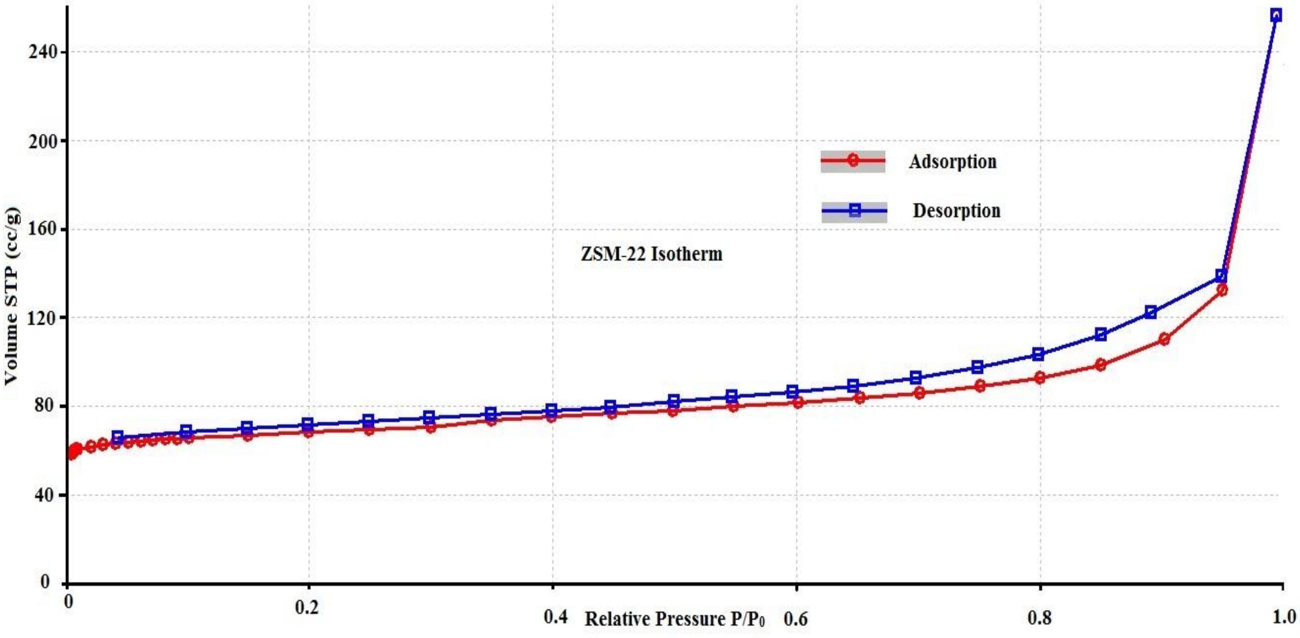

Figure 3.21: A typical Nitrogen isotherm for ZSM-23 zeolite

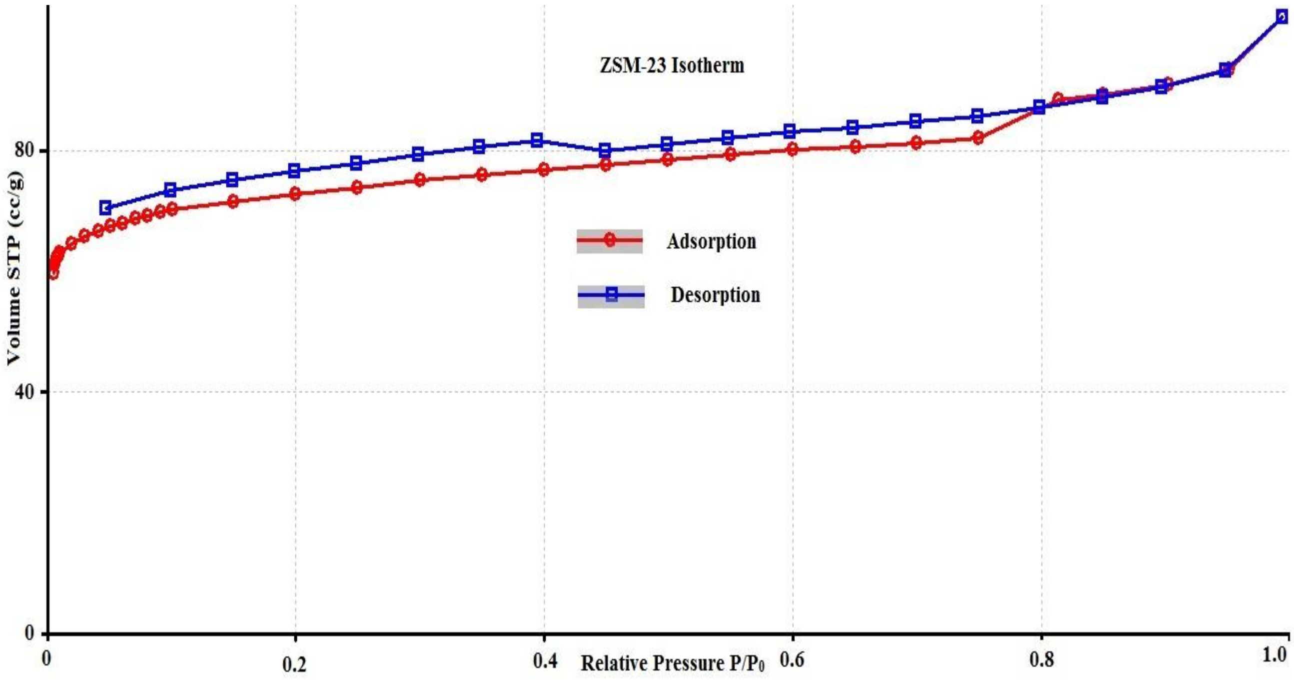

3.3 RESULTS AND DISCUSSIONS – COMPOSITION OF CATALYSTS

A hydroisomerization reaction was catalyzed by bi-functional catalyst systems with a metal function required for the hydrogenation/dehydrogenation reactions and an acid function for the isomerization of the olefinic intermediates produced during the reaction. Platinum was selected as the noble metal for use as the metal function. Literature survey supported the use of platinum metal in comparison to other noble metals nickel and palladium, as the most efficient metal function. Typically a platinum metal loading of 0.35% was recommended from literature survey. The method of platinum ion exchange was explained in detail in section 2.2.6.

Medium pore zeolites, specifically ZSM-12, ZSM-22 and ZSM-23 were selected for the acid function. Besides the usual advantages of zeolites, mentioned before in section 1.3, a zeolite based support guaranted a uniform dispersion of platinum metal on zeolite surface. Platinum metal was ion exchanged with protons on the surface of zeolites. A proton existed on the surface zeolite because of the presence of an aluminum tetrahedra surrounded by a neighborhood of silicon tetrahedra. Lowenstein’s rule forbade the presence of two aluminum tetrahedra in the immediate neighborhood. Also for high silica zeolites the aluminum tetrahedra (and therefore the protons) were vastly outnumbered by silica tetrahedra. As a result platinum metal dispersion was bound to be much better on a zeolite surface compared to other support materials. Systematic study of metal dispersion on zeolite surface was beyond the scope of this thesis.

A zeolite powder ion exchanged with platinum metal could not be used as such for the hydroisomerization reactor. Pressure drop, temperature gradient in reactor bed and solid carry over were some of the difficulties faced in using zeolite powder as catalysts. Extrudates were typically used in the industry for various reactions to overcome the shortcomings presented by using powder catalysts. The composition of extrudates, however, should be such so as to provide the necessary strength and stability under reaction environment (high temperature and pressure) without hindering the ability of the zeolite and the metal in their respective functions.

In view of the above, a finished bi-functional hydroisomerization catalyst had three important ingredients, the metal, the solid acid and the solid support. Typically a porous and neutral material which could provide the necessary strength to the extrudates would serve the purpose. Amorphous silica and amorphous alumina could fulfill the porous function but are not completely neutral. This was because of the presence of surface hydroxyl groups in case of both silica and alumina. However a high temperature calcination of these materials would sinter the solid surface thereby exterminating most of the acidity. However there was an upper limit on the temperature of calcination for the extrudates because of the presence of noble metal. Literature survey recommends a temperature of 400^{o}C for the activation of platinum loaded extrudates (Girgis *et al.*,1996). As such Puralox SCFA-230, a high temperature activated (to remove acidity) variety of pseudo bohemite (alumina) was selected as a component of the support. Puralox SCFA in itself was insufficient to provide the necessary support material to the extrudates and a minimum quantity of pseudo bohemite (as such) was required. A colloidal form of nano-alumina, Nyacol (Nyacol Nano. Tech. Inc.) diluted with 50% water was selected as the binder to bind the zeolite, SCFA-230 and bohemite into extrudates of desired strength.

In light of the above arguments, a mixture of platinum loaded zeolite powder (50 wt%) with Puralox SCFA-230 (45 wt%) and pseudo bohemite (5 wt%) was selected as the composition of the extrudates for the hydroisomerization reaction. It was important to note that there were now two sources of acidity in an extrduate, one arising out from the zeolite (50 wt%) and the other arising out from pseudo bohemite (5 wt%). Puralox SCFA-230 was assumed to impart no acidity to the extrudates. Figure 3.22 illustrated a NH_3-TPD study of the total acidity contained in pseudo bohemite calcined at 400^{o}C, 500^{o}C and 600^{o}C and a comparison with the total acidity of Puralox SCFA-230. The figure clearly illustrated almost zero acidity in SCFA-230 compared to pseudo bohemite calcined at 400^{o}C. The acidity in pseudo bohemite could be completely removed if the extrudates could be calcined at 600^{o}C. However a calcination temperature of 400^{o}C was chosen as the optimum temperature owing to the requirement of the metal function.

Table 3.09 tabulated the composition of various catalysts which were utilized for the hydroisomerization reaction. Henceforth, the catalysts would be referred to using the catalyst names given in table 3.09.

Figure 3.22:NH_3 TPD curves for pseudo bohemite calcined at different temperatures and Puralox SCFA-230

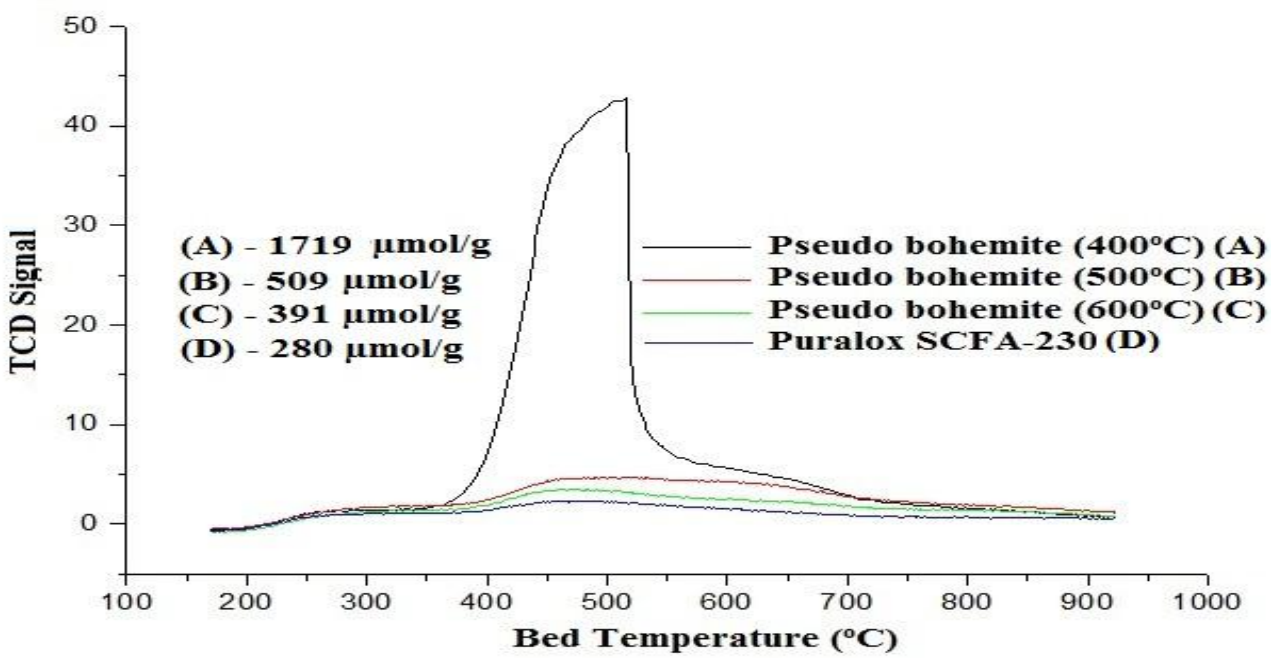

Table 3.09: Composition of various catalysts used for evaluation

Catalyst	Support[*]	Gel Si/Al	Base Metal (wt %)	Pt-loading (wt %)	Crystal Size (μm)	Acidity (μmol/g)	BET SA (m^2/g)
CAT-1	ZSM-12[79]	45	-	0.35	2 – 3	184	307
CAT-2	ZSM-12[41]	60	-	0.35	2 – 3	-	210
CAT-3	ZSM-12[43]	60	-	0.35	2 – 3	-	225
CAT-4	ZSM-12[63]	75	-	0.35	2 – 3	133	220
CAT-5	ZSM-12[61]	90	-	0.35	2 – 3	136	220
CAT6	ZSM-12[69]	90	-	0.35	2 – 3	130	266
CAT-7	ZSM-12[70]	120	-	0.35	3 - 4	124	266
CAT-8	ZSM-12[66]	60	Ca – 0.35	0.35	2 – 3	199	226
CAT-9	ZSM-12[66]	60	Ba – 0.35	0.35	2 – 3	184	226
CAT-10	ZSM-22	60		0.35	2 – 3	170	260
CAT-11	ZSM-23	45	Ca – 0.35	0.35	< 1	-	300
CAT-12	ZSM-23	60	Ca – 0.35	0.35	< 1	480	283
CAT-13	ZSM-23	60	-	0.35	< 1	360	284

3.4 RESULTS AND DISCUSSIONS – EVALUATION OF CATALYSTS

A typical hydroisomerization reaction would result into unreacted feed, monobranched isomers, multibranched isomers and cracked products. Girgis *et al.* had identified the products obtained from a hydroisomerization reaction for n-hexadecane on a similar reactor setup for the evaluation of platinum loaded zeolite based catalysts (Girgis *et al.*, 1996). The group identified the mono branched isomers, desorbing at a lesser retention time than unreacted feed, as n-methylpentadecane molecules with the value of n varying from 2 to 8 (total 7 peaks). In the GC program (described in section 2.4.1) used to identify the products, unreacted n-hexadecane appeared at a retention time of 28.4 minutes. The zone from a retention time of 27 minutes to 28.4 minutes, typically a zone with 6 or 7 peaks, was identified as the zone for mono branched isomers. The zone from a retention time of 24 minutes to 27 minutes was identified as a zone for multibranched isomers. The zone from a retention time of 8 minutes (the retention time where first peak appeared) to 24 minutes was identified as a zone for cracked products. The gaseous products were analyzed by RGA to identify the products. Methane was never observed for any of the gaseous products and ethane was observed in some of the cases but was always less than 0.15 mol%., thereby indicating no C_{15} hydrocarbons resulted from cracking to methane and C_{15} and very less C_{14} hydrocarbons (less than 0.15 mol%) resulted from cracking to ethane and $C_{14.}$ In order to characterize the products pure n-hexane (C_6), n-heptane (C_7), n-octane (C_8), n-decane (C_{10}), n-dodecane (C_{12}), n-pentadecane (C_{15}) and n-hexadecane (C_{16}) were injected in the same column used for product analysis and compared with a typical product distribution obtained from that column. Figure 3.23 showed such a comparison as well as identified the monobranched, multibranched and cracked products.

The catalysts were evaluated in terms of percentage conversion of n-hexadecane and percentage total selectivity towards isomerization products. However in order to fully convey the distribution of products into numbers three ratios, percentage monobranched, percentage multibranched and percentage cracked, were defined as the percentage of total area occupied by monobranched products to total occupied area, the percentage of total area occupied by multibranched products to total occupied area and the percentage of total area occupied by cracked products to total occupied area, respectively.

Table 3.10 tabulated the results obtained for ZSM-22 and ZSM-23 based catalysts, the compositions for which were given in table 3.09. Table 3.11 tabulated the results obtained for ZSM-12 based catalysts, the compositions for which were given in table 3.09

Table 3.10: Hydroisomerization reaction data for ZSM-22 and ZSM-23 based catalysts

CAT	**Temperature (°C)**	**Pressure (bar)**	**WHSV (sec^{-1})**	**Conversion (%)**	**Selectivity (%)**	**Mono (%)**	**Multi (%)**	**Cracked (%)**	**Yield (%)**
CAT10	287	60	0.12	57.04	90.55	0.46	0.05	0.05	51.64
CAT10	305	60	0.12	90.07	83.98	0.53	0.23	0.14	75.65
CAT10	310	60	0.12	94.57	78.53	0.42	0.32	0.2	74.27
CAT11	305	60	0.12	72.44	83	0.52	0.08	0.12	60.13
CAT11	310	60	0.12	89.25	79.85	0.54	0.17	0.18	71.27
CAT12	290	60	0.12	88.73	81.06	0.49	0.22	0.17	71.93
CAT12	300	60	0.12	96.35	66.33	0.27	0.36	0.32	63.91
CAT13	285	60	0.12	86.3	85.04	0.58	0.16	0.13	73.38
CAT13	300	60	0.12	98.83	38.95	0.08	0.3	0.6	38.49

Figure 3.23: Identification of monobranched, multibranched and cracked products in a typical chromatogram obtained for a hydroisomerization reaction of n-hexadecane

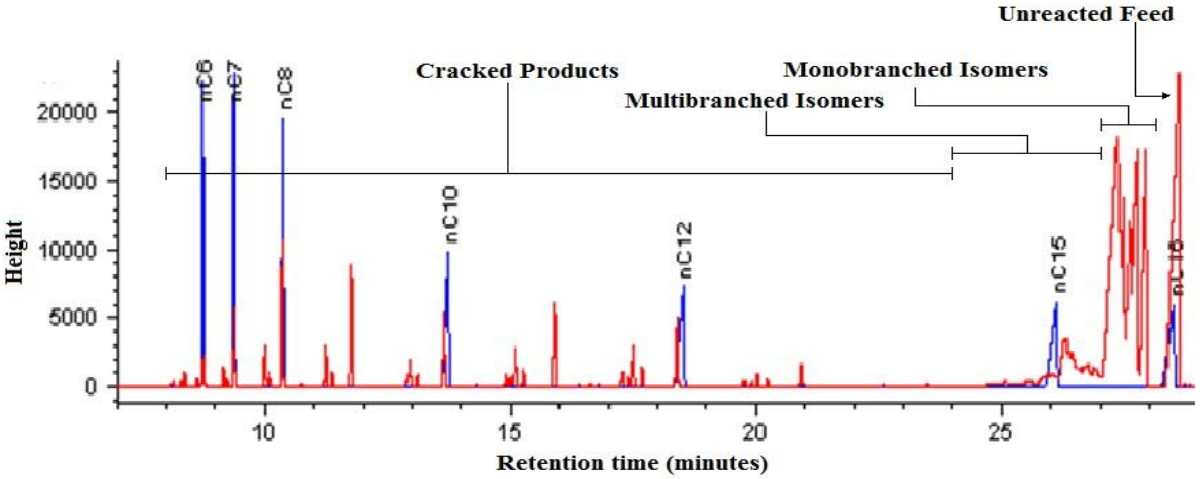

Table 3.11: Hydroisomerization reaction data for ZSM-12 based catalysts

CAT	Temperature (^oC)	Pressure (bar)	WHSV ($hour^{-1}$)	Conversion (%)	Selectivity (%)	Mono (%)	Multi (%)	Cracked (%)	Yield (%)
CAT1	295	60	1.1	95	46.23	0.094	0.36	0.51	43.92
CAT1	290	60	1.1	95.42	61.02	0.13	0.45	0.37	58.23
CAT1	280	60	1.1	80.47	79.79	0.24	0.4	0.16	64.21
CAT2	300	60	1.1	84.1	78.06	0.2	0.46	0.18	65.65
CAT2	280	60	1.1	49.3	89.9	0.23	0.21	0.049	44.33
CAT3	280	60	1.1	43.06	91.17	0.24	0.15	0.04	39.26
CAT3	300	60	1.1	82.7	80.87	0.23	0.44	0.16	66.9
CAT4	300	60	1.1	86.1	79.06	0.24	0.44	0.18	68.08
CAT4	300	40	1.1	89.17	76.48	0.19	0.48	0.21	68.2
CAT4	300	80	1.1	78.79	85.04	0.28	0.39	0.12	67.01
CAT5	300	60	1.1	35.12	57.06	0.14	0.05	0.15	20.04
CAT5	305	60	1.1	89.83	64.94	0.17	0.41	0.31	58.34
CAT5	310	60	1.1	94.18	58.62	0.13	0.42	0.39	55.21
CAT6	300	60	1.1	68.66	90.17	0.28	0.34	0.067	61.9
CAT6	315	60	1.1	81.78	87.09	0.25	0.465	0.11	71.23
CAT7	280	60	1.1	42.56	94.47	0.25	0.15	0.023	40.21
CAT7	308	60	1.1	84.59	86.43	0.25	0.49	0.11	73.1
CAT7	315	60	1.1	95.53	75.38	0.16	0.56	0.24	72
CAT8	280	60	1.1	53.57	94.29	0.3	0.2	0.03	50.51
CAT8	300	60	1.1	89.72	82.84	0.22	0.53	0.15	74.32
CAT8	290	60	1.85	54.21	94.36	0.3	0.21	0.03	51.15
CAT8	290	60	0.74	81.77	89.39	0.28	0.45	0.08	73.1
CAT8	290	60	1.48	66.5	92.95	0.32	0.3	0.04	61.82
CAT9	295	60	1.1	87.95	87.56	0.25	0.52	0.11	77.01
CAT9	290	60	1.1	81.78	90.43	0.29	0.45	0.07	73.96
CAT9	300	60	1.1	94.17	77.45	0.16	0.57	0.21	72.93

3.4.1 Effect of pressure variation

The effect of pressure variation was studied on CAT4 at reaction pressures of 40bar, 60bar and 80bar at a reaction temperature of 300°C. Theoretically, an increase in hydrogen pressure was expected to decrease the conversion with simultaneous increase in selectivity. Experimentally a similar trend was observed for the catalyst. The conversion for the catalyst decreased from 89.17% to 78.79% for an increase in pressure from 40bar to 80bar. The total selectivity towards isomerization for the catalyst increased from 76.48% to 85.04%. The total isomerization yield remained constant around 68%. This was explained on the basis of more hydrogen available at the active sites for the hydrogenation function of the catalyst at higher pressures, thereby reducing the amount of alkene intermediates that form over active sites. Due to lesser availability of alkene intermediates, the molecules that would undergo isomerization and cracking reactions would be reduced, thereby leading to a decrease in conversion.

Figure 3.24: Effect of variation in pressure over CAT4

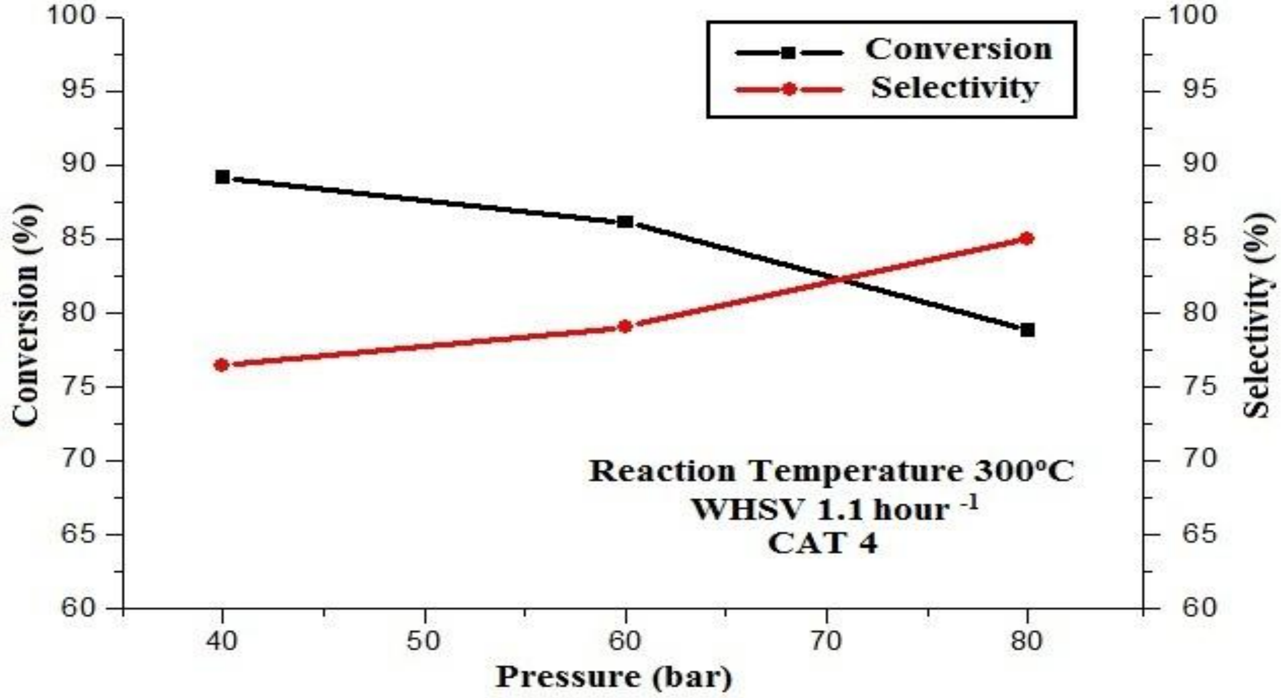

The selectivity towards isomerization showed an upward trend because selectivity was calculated on the basis of percentage of feed converted and also the fact that H_2 was a product of hydrocracking reaction. Therefore an increase in pressure would suppress the hydrocracking reaction and increase selectivity towards isomerization. Figure 3.24 illustrated the effect of variation in reaction pressure over conversion and selectivity values.

To understand the effect of pressure on the distribution of monobranched and multibranched isomers a ratio, multi/mono was defined as the ratio of percentage of multibranched isomers to the percentage of monobranched isomers. This ratio was plotted against the variation in pressure. Figure 3.25 illustrated such a variation of the multi/mono ratio with pressure. It was observed that the multi/mono ratio decreased from 2.53 to 1.39 with increase in pressure from 40bar to 60bar. It was important to note that the changes in total selectivity was due to the shift in conversion, however there was a significant variation in product distribution. Therefore a low pressure operation or conditions leading to high conversion were suitable for high selectivity towards multibranched isomers over typical zeolite based hydroisomerization catalysts. Similarly a high pressure operation or conditions leading to low conversion were suitable for high selectivity towards monobranched isomers over typical zeolite based hydroisomerization catalysts.

Figure 3.25: Effect of variation in pressure on distribution of isomers over CAT4

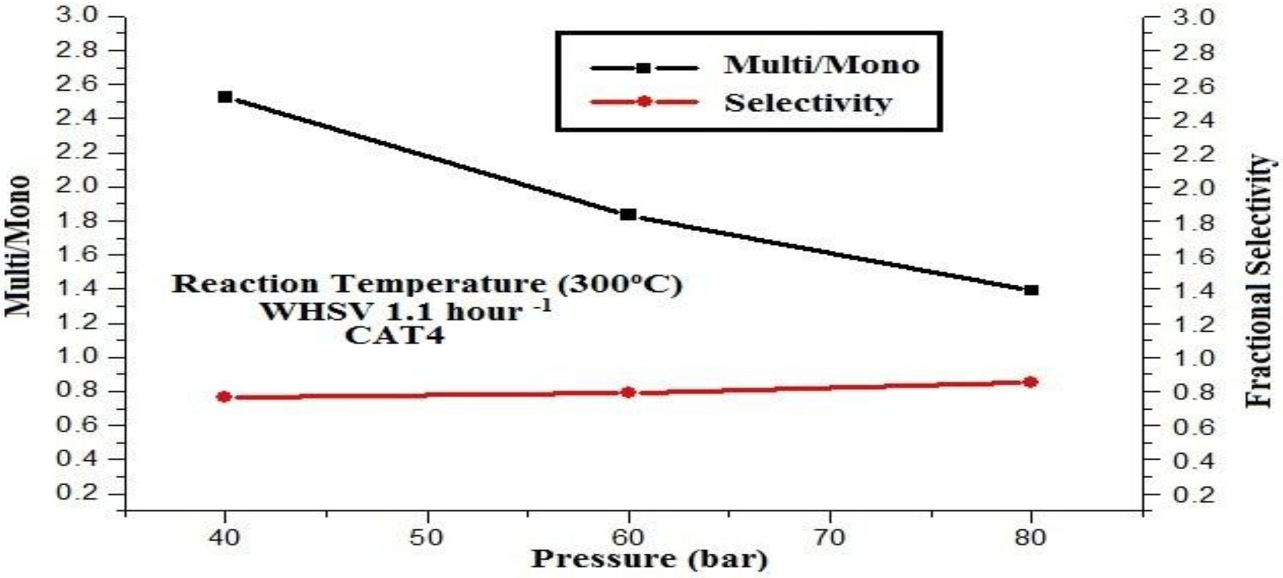

3.4.2 Effect of variation in temperature

The effect of variation in temperature was studied for all the catalysts. Typically an initial run was done at a randomly selected temperature and the product was analyzed to check for the conversion of n-hexadecane. Now the temperature of the reactor was changed accordingly so as to obtain conversion values as high as possible with good total selectivity values towards isomerization. Theoretically, an increase in temperature was expected to increase the conversion of a catalyst with a reduction in selectivity towards isomerization. A similar experimental trend was observed in all the catalysts. Figure 3.26, 3.27, 3.28 and 3.29 illustrated the effect of variation in temperature over conversion and selectivity values. The trend was explained on the basis of an increase in kinetic energy of molecule with increase in temperature and thereby leading to easy conversion to products over active sites. The decrease in selectivity values however was not only due to the effect of a bigger base on which selectivity was calculated but also because of an increase in thermal cracking which would typically be observed at higher temperatures. As a result the selectivity was expected to decrease at a faster rate at higher temperatures. Figure 3.27 and figure 3.29 clearly depicted a higher rate of decrease in selectivity of catalysts at high temperatures. The complete isomerization data for the catalysts at different temperatures is tabulated in Table 3.10 and 3.11.

Figure 3.26: Effect of variation temperature on conversion for ZSM-12 based catalysts

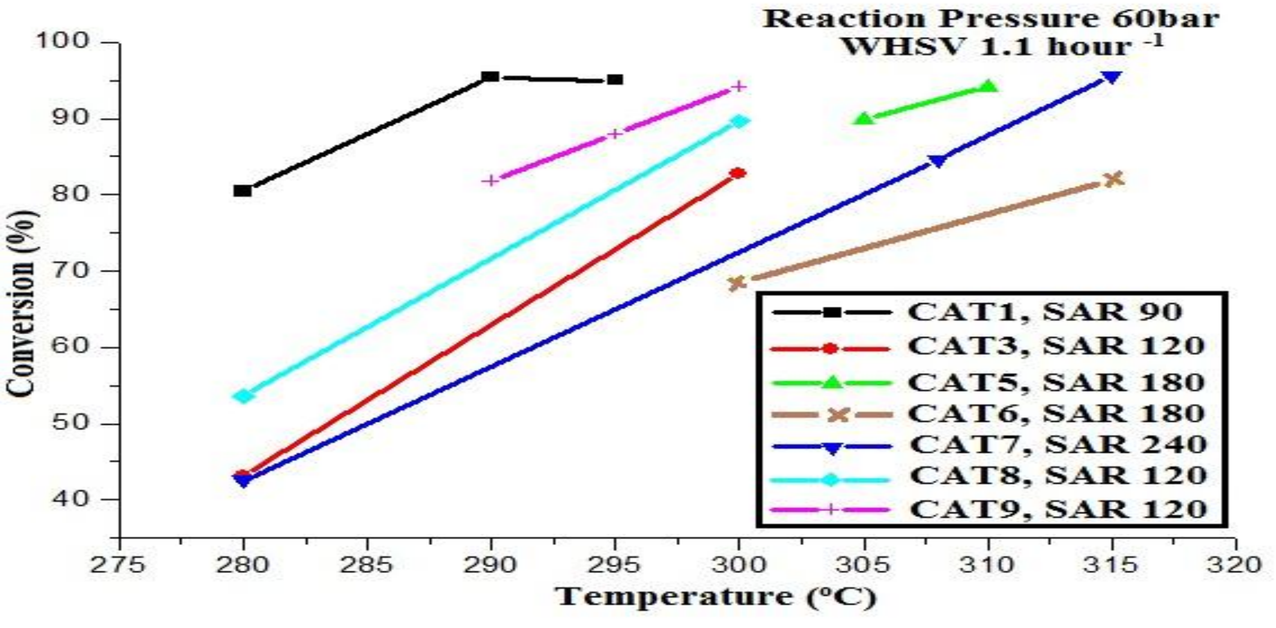

Figure 3.27: Effect of variation in temperature on selectivity over ZSM-12 based catalysts

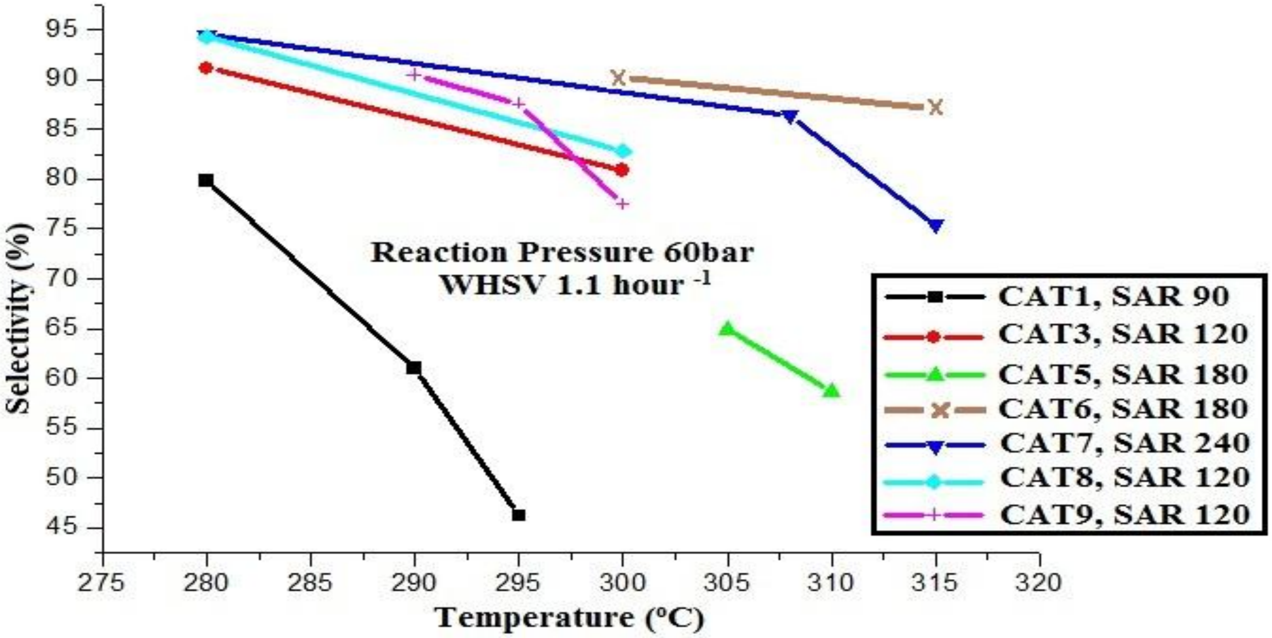

Figure 3.28: Effect of variation temperature on conversion over ZSM-22 and ZSM-23based catalysts

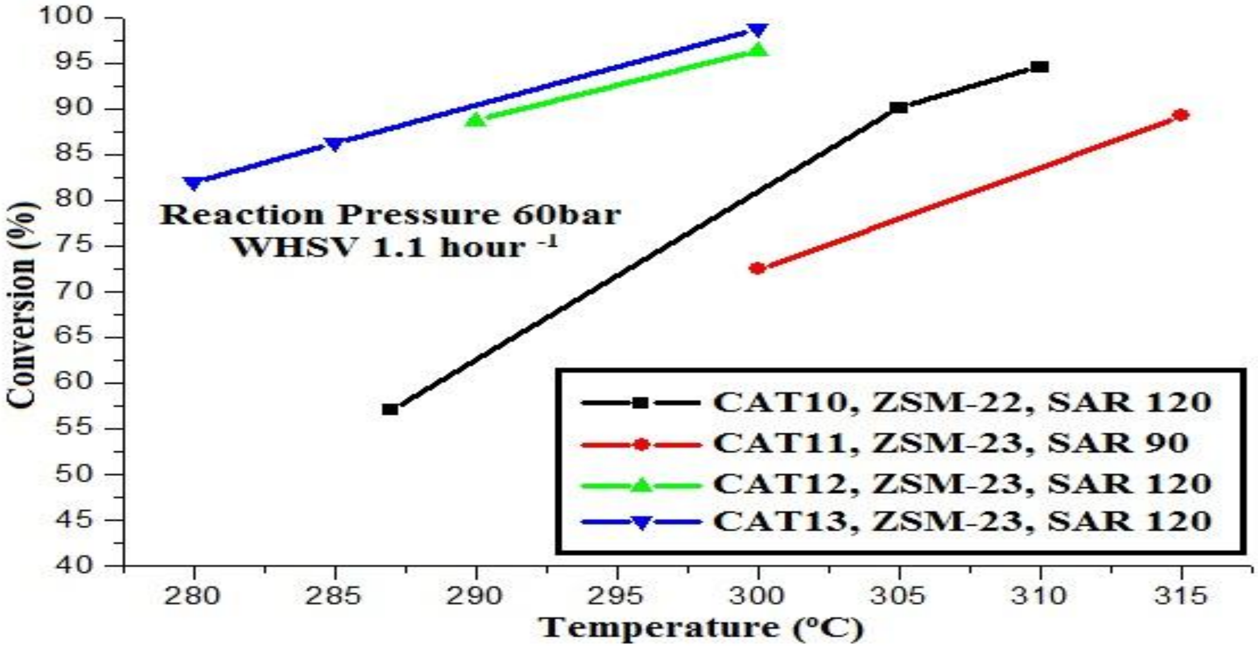

Figure 3.29: Effect of variation in temperature on selectivity over ZSM-22 and ZSM-23 based catalysts

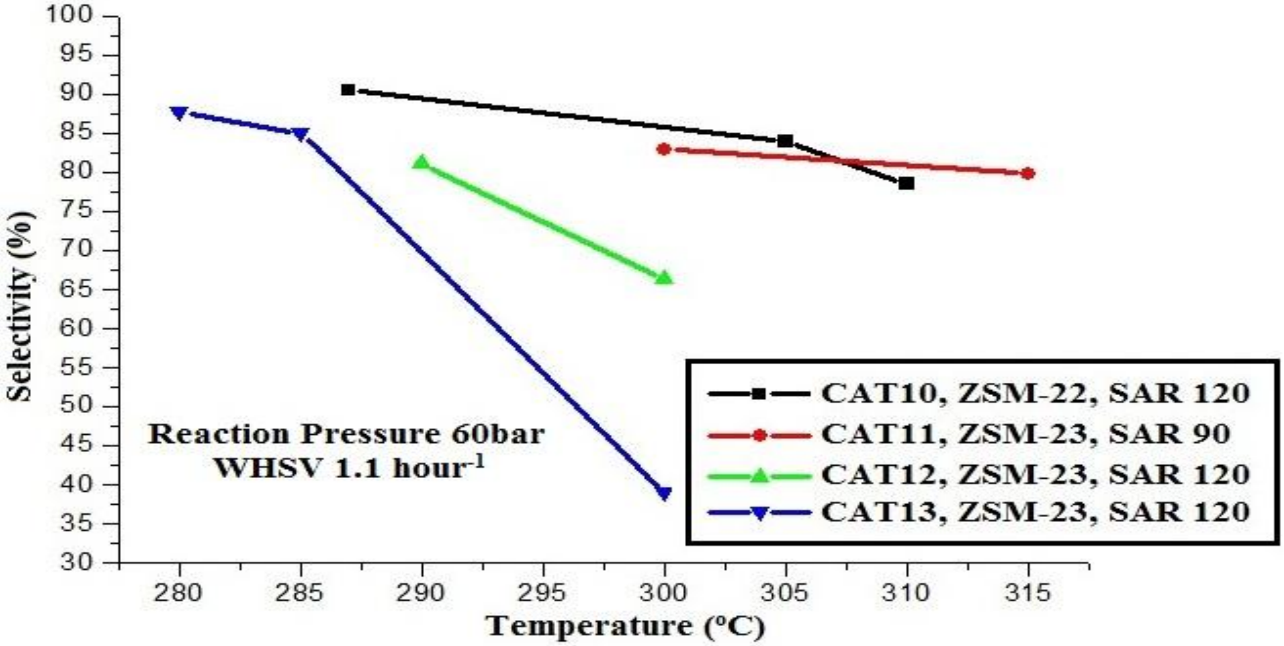

To study the effect of temperature on variation in distribution of products, the Multi/Mono ratio of some of the catalysts were plotted with temperature. Figure 3.30 illustrated a significant variation in Multi/Mono ratio of the different catalysts with variation in temperature. It was observed that Multi/Mono ratio increased with temperature for all the catalyst except CAT9. Also the rate of increase in Multi/Mono ratio was higher at high temperatures except in case of CAT1. This happened because cracking started at the higher temperature for CAT1 owing to the high activity of this catalyst due to a low SAR ratio of 90. The figure also illustrated very low (less than 1) Multi/Mono ratio values for ZSM-22 and ZSM-23 based catalysts, indicating their preference towards monobranching compared to multibranching. Finally, it was concluded that a high temperature operation or conditions leading to high conversion were suitable for high selectivity towards multibranching. Similarly, a low temperature operation or conditions leading to low conversion were suitable for high selectivity towards monobranching.

Figure 3.30: Effect of variation in temperature over distribution of isomers

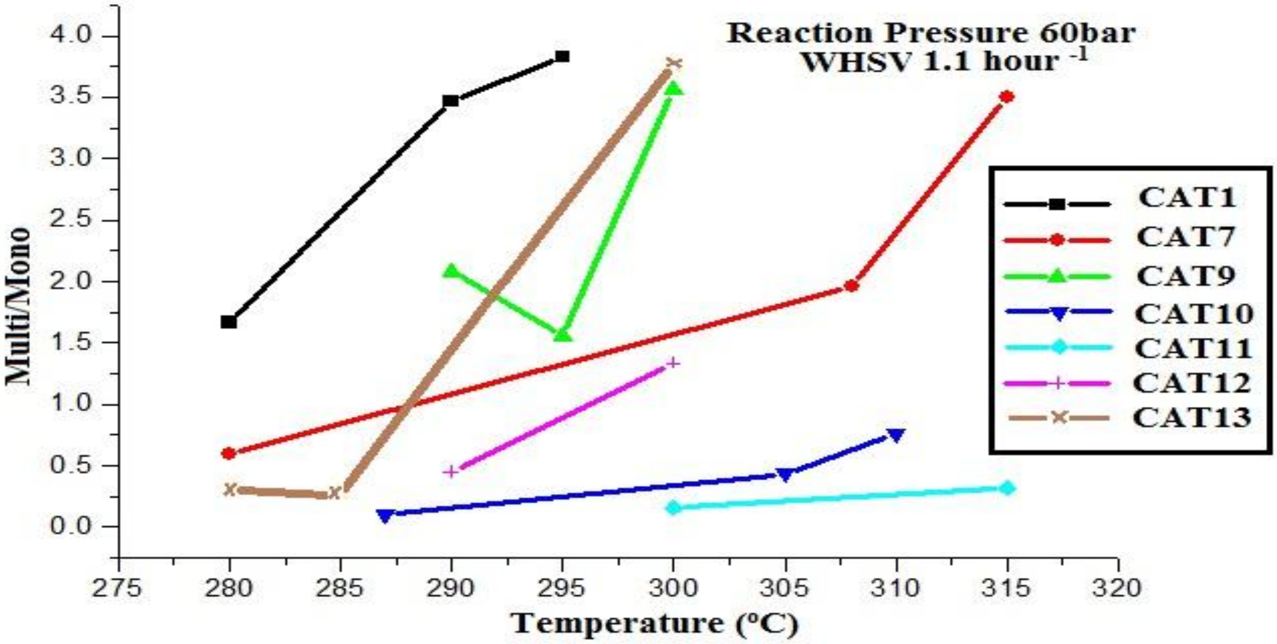

3.4.3 Effect of variation in WHSV

Weight hour space velocity (WHSV) was a measure of the time spent by molecules in contact with the catalyst, because the reciprocal of WHSV gave the contact time. The effect of WHSV variation was studied on CAT7 at a reaction temperature of 290^{o}C and a reaction pressure of 60bar. Theoretically for a single step reaction, conversion would be a linear function of WHSV till a particular value (100% conversion) beyond which an increase in WHSV would have no effect on conversion. However for a series reaction like hydroisomerization where monobranched isomers appeared first followed by multibranched isomers with cracked products forming as the last step, the effect of an increase in WHSV on conversion was expected to imitate the effect of decrease in temperature, thereby leading to a decrease in conversion. A similar trend was observed experimentally for CAT8 where an increase in WHSV from 0.74 hour^{-1} to 1.85 hour^{-1} led to a decrease in conversion from 81.77% to 54.21%. This was explained on the basis of molecules spending more time on active sites at low WHSV values, thereby leading to high conversion values. Figure 3.31 illustrated the effect of variation in WHSV over conversion.

The effect of variation in WHSV over selectivity pattern was a little difficult to comprehend because at high contact times the molecules were expected to covert as a certainty but towards which type of product would be governed by the pore structure of the zeolites owing to molecular shape selectivity effects. Also the selectivity values would be effected by a change in conversion owing to the shift in base on which selectivity is calculated. Experimentally an increase in WHSV from 0.74 hour^{-1} to 1.85 hour^{-1} led to an increase in selectivity from 89.39% to 94.36%. However it was important to note that the decrease in conversion was much rapid as compared to the increase in selectivity. This was explained on the basis of cracking reactions being preferred at high contact times or low WHSV values owing to the sequential nature of the hydroisomerization reaction. Only those n-hexadecane molecules which converted to monobranched isomers were available for further conversion to multibranched isomers and so on. Thus at low contact times most of n-hexadecane molecules would be converted only to monobranched isomers before they were flushed away by a flow of fresh n-hexadecane molecules. Due to high concentration of monobranched isomers compared to multibranched isomers in the equilibrium mixture, cracked products were expected to decrease, thereby leading to an increase in selectivity. Figure 3.31 illustrated the effect of variation in WHSV over selectivity values. The selectivity increased linearly with an increase in WHSV.

To study the effect of variation in WHSV over the distribution of products, the Multi/Mono ratio was plotted against WHSV. Figure 3.32 illustrated a significant variation in Multi/Mono ratio of the different catalysts with variation in WHSV. It was observed for all the catalysts that Multi/Mono ratio decreased with increase in WHSV. Therefore, a low WHSV operation or conditions leading to high conversion were suitable for high selectivity towards multibranching. Similarly, a high WHSV operation or conditions leading to low conversion were suitable for high selectivity towards monobranching.

Figure 3.31 Effect of variation in WHSV on conversion and selectivity over CAT8

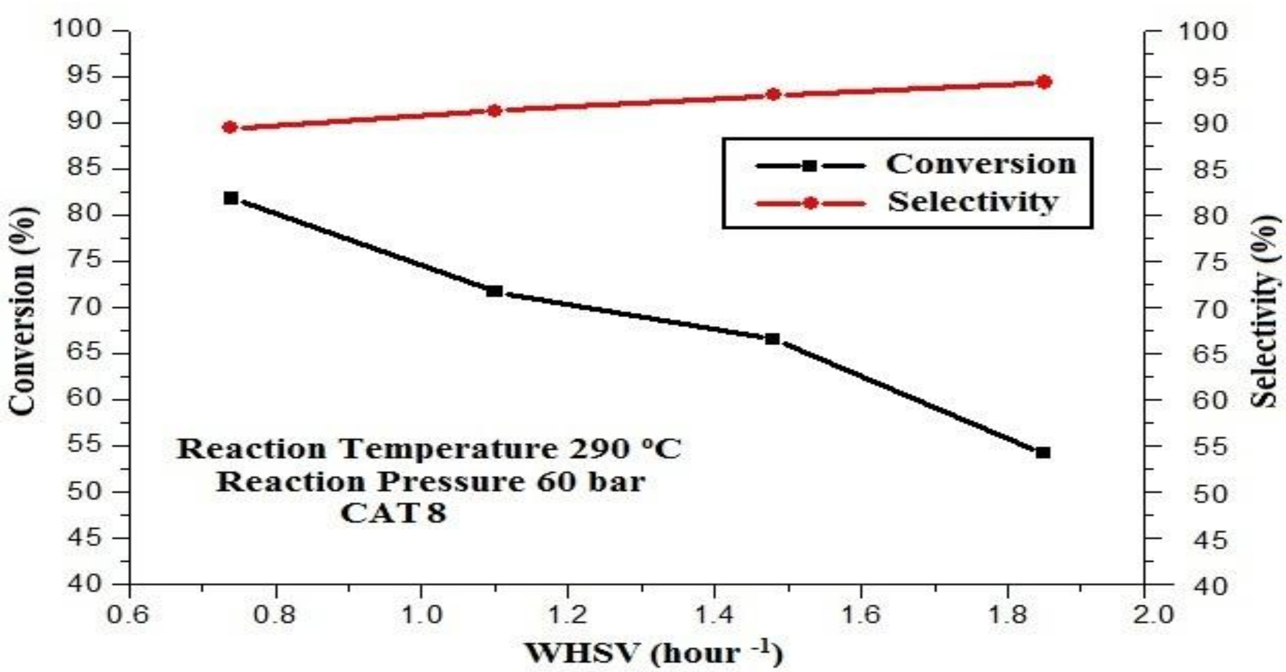

Figure 3.32: Effect of variation in WHSV over distribution of isomers over CAT8

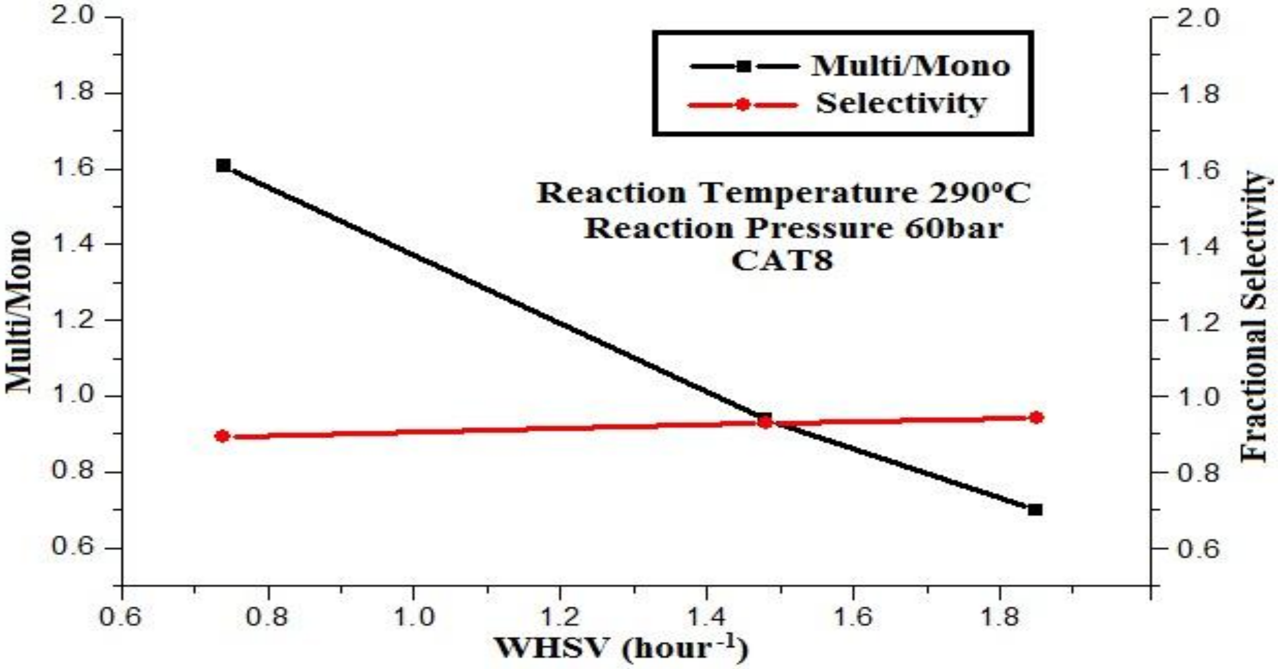

3.4.4 Effect of variation in SAR of zeolite used in the catalyst

SAR ratio of a zeolite was directly related to the strength and number of acid sites present in the zeolite. An increase in SAR ratio led to a decrease in total acidity of the zeolite. However it was essential to note that gel SAR ratios differed from actual SAR ratios at which zeolite crystallized. The actual SAR ratios could be obtained using X-ray Fluorescence (XRF) studies. However a XRF study of the synthesized zeolite samples could not be done in the limited span of the project. As such a variation in conversion and selectivity data would be best explained on the basis of variation in total acidity of the zeolite samples. The total acidity of zeolite samples was obtained using NH_3 temperature programmed desorption technique. The total acidity values of zeolite samples were tabulated in Table 3.09. Theoretically, an increase in total acidity of a zeolite sample was expected to increase the activity of the catalyst, thereby leading to an increase in conversion. The selectivity pattern obtained would depend on the type of zeolite and the composition of catalyst owing to molecular shape selectivity effects.

Among the various factors governing the selectivity towards isomerization, an important factor was the percentage of cracked products formed over a particular catalyst. Theoretically the percentage of cracked products was expected to increase with an increase in total acidity of a zeolite sample. However it was important to understand the sequential nature of reactions taking place inside a zeolite porous network. N-hexadecane molecule was reported to first convert to mono branched isomers followed by conversion to multibranched isomers and finally to cracked products in this exact sequence. The concept was discussed in detail in section 1.2. Therefore the distribution of cracked products was dependent on total acidity of the zeolite as well as the percentage of multibranched isomers which was controlled by the pore structure of the zeolite.

In order to understand the observed selectivity patterns over various catalysts it was important to understand the pore structure of the corresponding zeolites. Theoretically a medium pore zeolite with pore size just big enough to allow n-hexadecane and methyl branched iso-pentadecane molecules to pass through it would lead to high amount of monobranched isomers. Multibranching would be disfavored in such a pore network as further methyl branches would be sterically hindered and as a result kinetically disfavored during the transition state. Pore dimensionality and pore size data for zeolites ZSM-12, ZSM-22 and ZSM-23 were tabulated in section 1.6. ZSM-22 and ZSM-23 with pore size in the range of $4.6A^o$-$5.7A^o$ and $4.5A^o$-$5.2A^o$

respectively were therefore expected to show high selectivity towards monobranched isomers and less selectivity towards multibranched isomers. A similar experimental trend was observed for these two zeolites. Typical Multi/Mono ratio values for ZSM-22 based catalyst varied from 0.11 to 0.43 depending upon conversion. Similarly Multi/Mono ratio values for ZSM-23 based catalysts varied from 0.15 to 0.3 depending upon conversion.

A medium pore zeolite with pore size big enough to allow n-hexadecane as well as methyl branched isopentadecanes to pass through it but presenting hindrance to ethyl branches was expected to result in a comparatively low selectivity towards monobranched isomers and a high selectivity towards multibranched isomers. However it was important to note that in such a zeolite based catalyst a fine balance between the acid and the metal function was even more essential because a high strength of acid sites would immediately convert multibranched isomers to cracked products. In such a zeolite based catalyst the total acidity had to be controlled to the desired extent by utilizing an optimum SAR ratio. ZSM-12 with a pore size of 5.7 A^o to 6.1 A^o was such a zeolite expected to show high selectivity towards multibranched isomers. It was an objective of this research to find such an optimum SAR ratio for zeolite ZSM-12 which maximized the total selectivity towards isomerization. Another method of controlling the total acidity of a zeolite based catalyst was to use base metal loading prior to platinum loading. The detailed method and discussion for base metal loading is given in section 2.2.5. Experimentally, zeolite ZSM-12 showed high selectivity towards multibranched isomers. Typical Multi/Mono values obtained for ZSM-12 based catalysts varied from 3.6 to 2.5 for high conversion runs and 0.5 to 1.5 for low conversion runs.

On careful observation of variation of conversion with temperature in figure 3.26, it was found that catalysts prepared from zeolites of high SAR ratios (180 and 240) were located in the right hand side portion of the plot indicating the need of high reaction temperatures to reach desired conversion values. Similarly on observation of variation of selectivity with temperature in figure 3.27, it was found that highest selectivity values (among no base loaded catalysts) were obtained for zeolites with high SAR ratios (240 and 180) at the high temperatures required for desired conversion values. Therefore the selectivity towards isomerization was dependent on the mild nature of acid sites.

3.4.5 Effect of group (II) base metal loading

The concept behind the base metal loading and loading methods was described in section 2.2.5. It was important to note that there were two advantages of using a base metal loading. The first was the neutralization of partial acidity of the zeolite which was expected to have a same kind of effect as increasing the SAR ratio of zeolite. The partial neutralization was a method of controlling the much desired fine balance between acid and metal functions. The second advantage was the effect of such metal loadings on zeolite pore structure. When a proton was exchanged by atoms of much bigger size like calcium and barium the pore size of a zeolite was expected to shrink a little. As such, base metal loading provided a method of controlling the pore structure of zeolite. Finally a typical base metal loading procedure was performed before platinum ion exchange and therefore was bound to have some effect on the platinum dispersion on zeolite surface. Study of such an effect was beyond the scope of this project.

Theoretically, a base metal loading was expected to decrease the activity of a catalyst with an increase in total selectivity towards isomerization. On the same principle a catalyst with calcium loading was expected to have better activity than a catalyst with barium loading when all other factors were kept at the same level. To study the effect of base metal loading on ZSM-12 a same zeolite sample (sample 66) was divided into two parts and each loaded with equal amount of calcium and barium, finally ending up in catalysts CAT8 (calcium) and CAT9 (barium). Figure 3.26 illustrated the effect of base metal loading on CAT8 and CAT9. Surprisingly, CAT9 with 0.35wt% barium loading showed a higher conversion as well higher selectivity when compared with CAT8 with 0.35wt% calcium loading. This result was unexpected because barium loaded sample 66 had a total acidity of 185 µmoles/g compared to 200 µmoles/g for calcium loaded sample 66 (Table 3.09). The higher selectivity of CAT9 could be explained on the basis of molecular shape selectivity effects in a constricted channel as well as the mild acidity of active sites resulting mostly in isomerized products and very less cracked products.

The study of effect of base metal loading for ZSM-23 was done on two different samples prepared at same gel SAR ratio of 120. One sample (CAT12) was loaded with 0.35wt% calcium and no base loading was done on the other sample (CAT13). CAT13 with no calcium loading was expected to show a better activity than CAT12. Figure 3.33 illustrated the reactivity patterns on these two catalysts. Once again it was observed that CAT12 with a calcium loading showed both higher activity as well as selectivity towards isomerization. The higher selectivity of CAT12 could be explained on the basis of molecular shape selectivity effects in a constricted channel as well as the mild acidity of active sites resulting mostly in isomerized products and very less cracked products.

Therefore it was observed that in spite of a reduction in total acidity of a zeolite sample by a base metal loading their corresponding catalysts showed a better conversion of n-hexadecane molecules with high selectivity towards isomerization at the same time for both ZSM-12 and ZSM-23 based catalysts. This unexpected behavior might have originated from a favorable shift in metal acid balance on metal loading. A better platinum dispersion resulting from base metal loading could also have an effect towards such a trend.

To understand the effect of base metal loadings toward product distribution, the Multi/Mono ratio was plotted against temperature for CAT8, CAT9, CAT12 and CAT13 (figure 3.34). It was observed that a Multi/Mono ratio increased with temperature except for CAT13 where the decrease was only nominal. For zsm-12 based catalysts there was only marginal difference between Multi/Mono ratios in the temperature range of 290°C to 295°C. This indicated that distribution of monobranched and multibranched isomers was almost similar for both of these metals (calcium and barium). No suitable conclusions could be drawn for ZSM-23 based catalysts because of variation of too many factors to pin point the effect of calcium loading.

Figure 3.33: Effect of base metal loading on ZSM-12 based catalysts

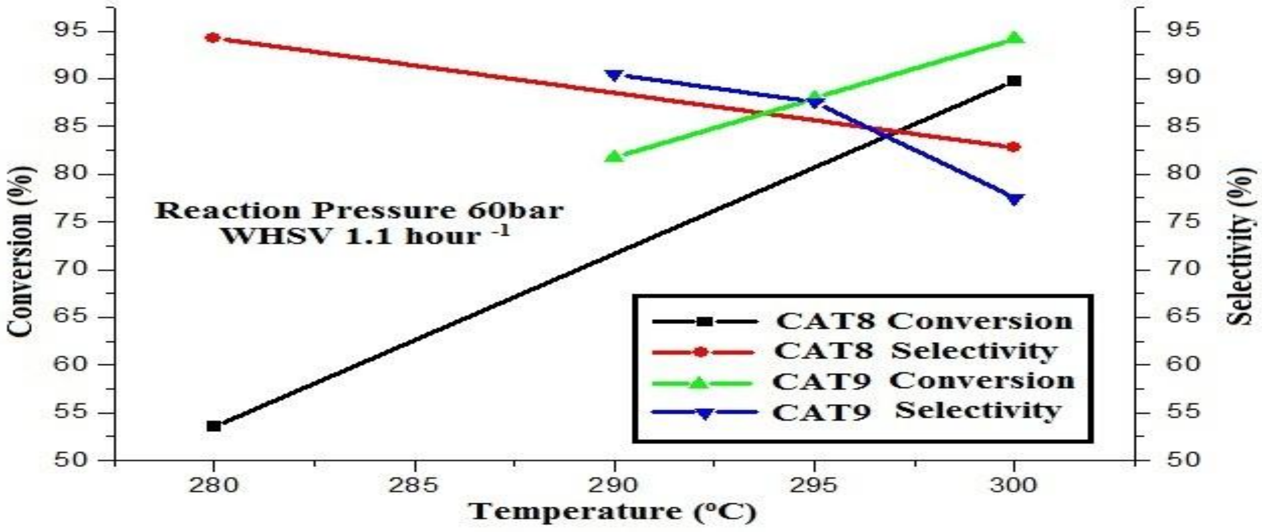

Figure 3.34: Effect of base metal loading on ZSM-23 based catalysts

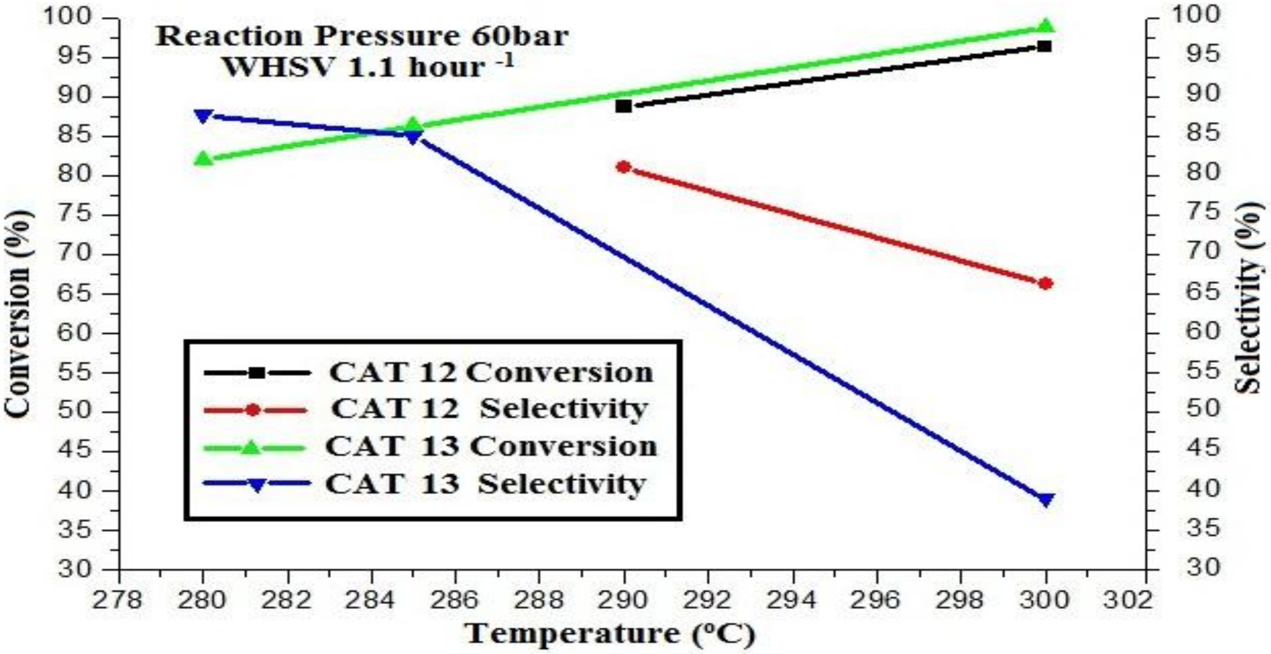

Figure 3.35: Effect of base metal loading on distribution of isomers for ZSM-12 and ZSM-23 based catalysts

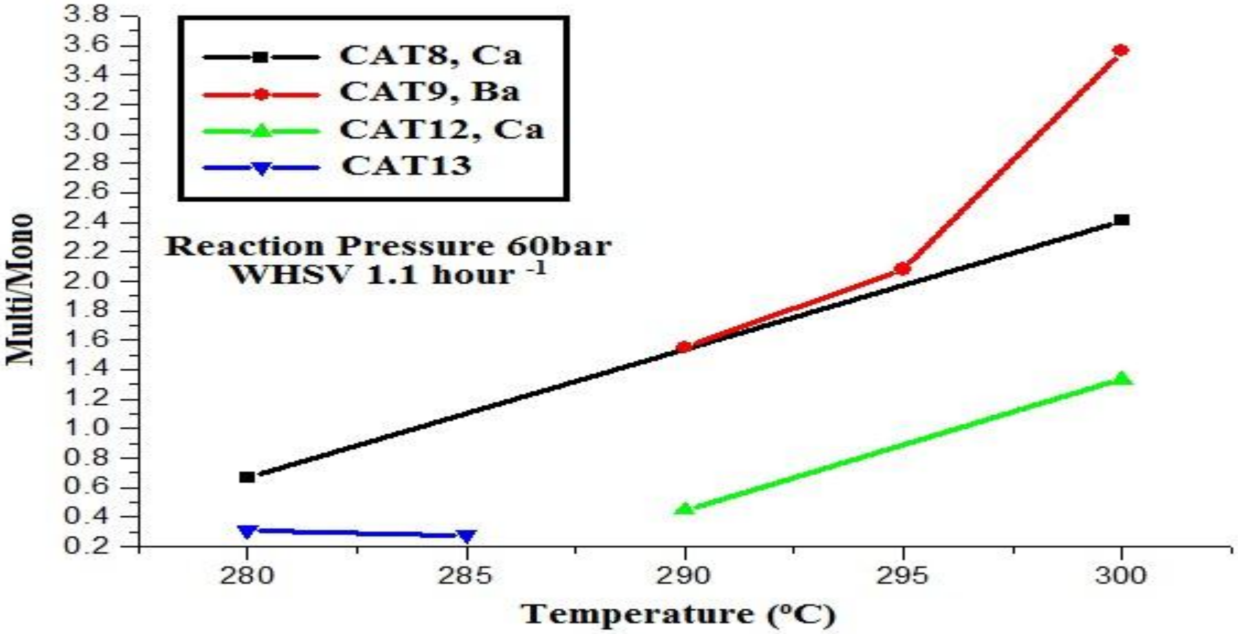

CHAPTER 4

SUMMARY AND CONCLUSIONS

4.1 SUMMARY

100% pure zeolite ZSM-12 was successfully synthesized from methyltriethylammonium bromide (MTEABr) and benzyltrimethylammonium chlorides as structure directing agents at 160°C. ZSM-12 at gel silica alumina ratios (SAR) of 90, 120, 180 and 240 was synthesized using MTEABr whereas ZSM-12 at SAR ratios of 150, 180 and 240 was obtained using BTMACl. Effect of changing the alkalinity, changing the concentration of SDA and increasing dilution of the synthesis gel was studied for MTEABr as SDA. The synthesis of ZSM-12 using tetraethylammonium bromide (TEABr) and tetraethylammonium hydroxide (TEAOH) as SDA was found to be highly sensitive to the pH and SAR ratio of the synthesis gels. An elongated cuboidal geometry of crystals with crystal size increasing with water content was observed for MTEABr, a cuboidal geometry of crystals with crystal size in the range of 2 – 3 µm was obtained for TEABr and rice shaped crystal morphology with crystal size in the range of 2 – 3 µm was obtained for BTMACl.

100% pure zeolites ZSM-22 and ZSM-23 were successfully synthesized from 1,2 diaminohexane and pyrrolidine respectively at synthesis temperatures of 160°C and 150°C respectively. Besides the usual synthesis parameters like gel SAR ratio, alkalinity, concentration of SDA, concentration of base metal, synthesis temperature and stirring rate were found as important parameters for the synthesis of both ZSM-22 and ZSM-23 zeolites. Needle shaped crystals of size 1 – 2 µm agglomerated into crystallites of size 4 – 5 µm were obtained for ZSM-22 and needle shaped crystals of size less than 1 µm agglomerated into crystallites of size 4 – 5 µm were obtained for ZSM-23.

Zeolites ZSM-12, ZSM-22 and ZSM-23 were characterized by X-ray diffraction, Scanning Electron Microscopy, ammonia temperature programmed desorption and nitrogen adsorption/desorption studies.

Hydroisomerization catalysts were prepared using platinum loaded zeolites ZSM-12, ZSM-22 and ZSM-23 as support (50 wt%) along with pseudo bohemite (5 wt%) and Puralox SCFA-230 (45 wt%). Cylindrical extrudates of diameter 1.6mm and length ~ 3mm were prepared using Nyacol (50 vol%) and water (50 vol%). The evaluation of zeolites was done for the hydroisomerization of model feed n-hexadecane in fixed bed up-flow reactor at high pressures.

Hydroisomerization reaction data was generated to study the effect of variation in pressure, variation in temperature and variation in WHSV on conversion of hexadecane, total selectivity towards isomerization and distribution of products.

4.2 CONCLUSIONS

MTEABr was found to be a flexible structure directing agent for the synthesis of crystalline ZSM-12 in terms of variation in SAR. The advantages of using MTEABr as SDA were a relatively simple synthesis procedure and flexibility towards a wide range of SAR ratios. The disadvantages of using MTEABr as SDA were the high cost of MTEABr and variation in growth in [206] direction (observed by variation in intensity of peak at 2θ value of 26.34).

BTMACl was found to be a suitable structure directing agent for the synthesis of crystalline ZSM-12 at high SAR (>150). The advantages of using BTMACl as SDA were the relatively very low cost of BTMACl and high crystallinity of product ZSM-12.

TEABr and TEAOH were found to be SDAs highly sensitive to the pH and SAR of synthesis gels.

Zeolites ZSM-22 and ZSM-23 based hydroisomerization catalysts were found to be suitable for lubricant oil dewaxing applications. The catalysts showed high isomerization selectivity towards monobranched isomers, marked by very low Multi/Mono ratios (0.15 – 0.45). The activity of zeolite ZSM-22 at a gel SAR of 120 was found to be less than the activity of ZSM-23 at a gel SAR of 120. High isomerization yields above 70% for more than 80% conversion of n-hexadecane were obtained for ZSM-22 and ZSM-23 based hydroisomerization catalysts.

Zeolite ZSM-12 based hydroisomerization catalysts were found to be suitable for renewable and conventional diesel oil dewaxing applications. The best ZSM-12 catalysts showed high total isomerization selectivity with preference towards multibranched isomers. Typically high Multi/Mono ratios (1.5 – 3.5) were obtained for ZSM-12 based catalysts. BTMACl was found to be the preferred SDA for the synthesis zeolite ZSM-12 (CAT6, SAR 180) owing to better results towards hydroisomerization for catalyst when compared with ZSM-12 obtained from MTEABr (CAT5, SAR 180). CAT7 synthesized from ZSM-12 at a gel SAR of 240 was found to be the best hydroisomerization catalyst (with no base loading) for isomerization of n-hexadecane showing a total isomerization selectivity of 86.43% at a conversion of 84.59%. However a high temperature of operation (308^{o}C) was required for this catalyst owing to its low activity.

A group (II) base metal loading was found to increase the activity and selectivity of hydroisomerization catalysts. The effect was more pronounced for ZSM-12 based catalysts when compared with ZSM-23 based catalyst. Barium loaded ZSM-12 catalyst showed better results than calcium loaded ZSM-12 catalyst. CAT9 with a barium loading of 0.35 wt% was found to be the best hydroisomerization catalyst showing a total isomerization selectivity of 87.56% at a conversion of 87.95%. The advantage of using a base metal loading was to get high isomerization yields, comparable to high SAR ratio ZSM-12, even at low temperatures of operation (299^{o}C). Therefore a base loading procedure was highly recommended for hydroisomerization catalysts.

A temperature range of 290 – 320^{o}C was found suitable for the hydroisomerization of n-hexadecane at high reaction pressure (60bar). The activity of all hydroisomerization catalysts was found to increase with an increase in temperatures leading to a simultaneous decrease in total selectivity towards isomerization. The rates of decrease of selectivity were higher at higher temperatures. Multi/Mono ratio of products also increased with an increase in temperature.

A reaction pressure of 60bar was found suitable to study the isomerization reaction of n-hexadecane. An increase in pressure led to a decrease in conversion and increase in total isomerization selectivity with total isomerization yield remaining constant (studied for CAT4). However a significant variation of Multi/Mono ratio was observed with variation in pressure. Low pressure conditions led to high Multi/Mono ratios. Therefore high pressure conditions favored lubricant oil dewaxing applications whereas low pressure (till a certain limit) conditions favored diesel dewaxing applications.

A WHSV of 1.1 hr^{-1} was selected to evaluate the various hydroisomerization catalysts. A decrease in WHSV was found to lead to a decrease in conversion with a simultaneous increase in selectivity. However the rate of decrease of conversion was faster than the rate of increase in selectivity. As a result highest isomerization yields were obtained at the lowest WHSV value (0.74 hr^{-1}) (CAT8). The Multi/Mono ratio was found to decrease with an increase in WHSV. Therefore a low WHSV run was suitable for diesel dewaxing applications owing to high Multi/Mono ratio and high isomerization yields. On the contrary a trade-off existed between high isomerization yields and obtaining low Multi/Mono ratios. Therefore an optimum WHSV was suitable for lubricant oil dewaxing applications.

Finally, a mild acidity of zeolites samples was discovered as the most essential criteria for obtaining high isomerization yields. Results obtained over high SAR ZSM-12 (240) and barium loaded ZSM-12 (120) strengthened the above logic.

4.3 SCOPE FOR FURTHER WORK

The role of pore structure towards molecular shape selectivity effects was made evident by the Multi/Mono ratios obtained for ZSM-12 and ZSM-22/ZSM-23 based catalysts. Therefore the effect of controlled silylation of porous networks of ZSM-12 zeolite towards a shift in the nature of Multi/Mono ratio (a shift towards high selectivity for monobranched isomers, lubricant dewaxing applications) can be investigated.

Crystallite size of prepared zeolite materials is an important parameter governing the selectivity towards isomerization. The crystal size of zeolite ZSM-12 obtained from MTEABr was dependent on the water content of the synthesis gel. Therefore crystals of ZSM-12 zeolite at same SAR ratios but different crystal sizes can be obtained. The crystal size can be further reduced by the use of surfactant molecules. Therefore an effect of changing the crystal size of a zeolite towards hydroisomerization selectivity can be investigated.

Excellent hydroisomerization results were obtained for barium loaded ZSM-12 based catalyst. The effect of such a barium loading on isomerization selectivity for lubricant oil dewaxing catalysts like ZSM-22, ZSM-23, ZSM-48 and SSZ-32 can be investigated. Strontium and zinc also appear as interesting candidates for achieving the mild acidity required for isomerization.

REFERENCES

1. **Akhmedov, V.M., Al-Khowaiter**, **S.H.** Recent Advances and Future Aspects in the Selective Isomerization of High n-Alkanes. *Catalysis Reviews*, **49** (2007) 33.
2. **Barrer, R.M. Munday, B.M**. Cation exchange in the synthetic zeolite K-F. *J. Chem. Soc.* (1948) 127.
3. **Barrer, R.M., Denny**, **P.J.** Hydrothermal chemistry of the silicates. Part IX. Nitrogenous aluminosilicates. *J. Chem. Soc.* (1961) 971.
4. **Barton, D.G., Soled, S.L., Meitzner, G.D., Fuentes, G.A., Iglesia, E.** Structural and Catalytic Characterization of Solid Acids Based on Zirconia Modified by Tungsten Oxide. *J. Catal*. **181** (1999) 57.
5. **Blasco, T., Chica, A., Corma, A., Murphy, W.J., Rodriguez, A., Pérez-Pariente J.** Changing the Si distribution in SAPO-11 by synthesis with surfactants improves the hydroisomerization/dewaxing properties. *J.Catal.* **242** (2006) 153.
6. **Burton, A.W., Zones, S.I., Rea, T., Chan, I. Y.** Preparation and characterization of SSZ-54: A family of MTT/TON intergrowth materials. *Micro. Meso. Mater.* **132** (2010) 54.
7. **Claude, M.C.** and **Martens**, **J.A.** Monomethyl-Branching of Long n-Alkanes in the Range from Decane to Tetracosane on Pt/H-ZSM-22 Bifunctional Catalys.*J. Catal.* **190** (2000) 39.
8. **Claude, M.C., Vanbutsele, G. and Martens**, **J.A.** Dimethyl Branching of Long n-Alkanes in the Range from Decane to Tetracosane on Pt/H–ZSM-22 Bifunctional Catalyst. *J. Catal.* **203** (2001) 213.
9. **Deldari**, **H.** Suitable catalysts for hydroisomerization of long-chain normal paraffins. *Applied Catalysis A* **293** (2005) 1 – 10
10. **Deville**, **H.C.** Compt. Rend. *Se´ances Acad. Sci*. **54** (1862) 324.
11. **Elangovan, S.P., Bischof, C. M., Hartmann**, Isomerization and Hydrocracking of n - Decane over Bimetallic Pt–Pd Clusters Supported on Mesoporous MCM-41 Catalysts. *Catal. Lett.* **80 (1/2)** (2002) 35.
12. **Ernst, S., Jacobs, P.A., Martens, J.A., Weitkamp, J.** Synthesis of zeolite ZSM-12 in the system $(MTEA)_2O$-Na_2O-SiO_2-AI_2O_3-H_20. *ZEOLITES*, **7** (1987), 458.

13. **Ernst, S., Kumar, R., Weitkamp J.** Synthesis and catalytic properties of zeolite ZSM-23. *Catalysis Today* **3 (1)** (1988) 1

14. **Ernst, S., Weitkamp, J., Martens, J.A., Jacobs, P.A.** Synthesis and shape-selective properties of ZSM-22. *Appl. Catal. A* **48** (1989) 137.

15. **Fang, K., Wei, W., Ren, J. Sun, Y.** n -Dodecane Hydroconversion over Ni/AlMCM-41 Catalysts. *Catal. Lett.* **93 (3/4)** (2004) 235.

16. **Geng, C.H., Zhang, F., Gao, Z.X., Zhao, L.F., Zhou, J.L.** Hydroisomerization of n-tetradecane over Pt/SAPO-11 catalyst. *Catal. Today* **93-95** (2004) 485.

17. **Giordano**, **G.** *Synthesis Commision, IZA*, http://www.iza-online.org/synthesis/default.htm

18. **Girgis, M.J., Tsao, Y.P.,** Impact of catalyst metal-acid balance in n-hexadecane hydroisomerization and hydrocracking, *Ind. Eng. Chem. Res*., **35** (1996), 386 – 396.

19. **Gopal, S.,Yoo, K., Smirniotis, P.G**. Synthesis of Al-rich ZSM-12 using TEAOH as template. *Microporous and Mesoporous Materials* **49** (2001), 149.

20. **Hino, M., Arata, K.** Synthesis of solid superacid catalyst with acid strength of H_0–16.04. *J. Chem. Soc. Chem. Comm.* **18**, (1980) 851.

21. **Huang, X., Wang, L., Kong, L., Li, Q.** Improvement of catalytic properties of SAPO-11 molecular sieves synthesized in H2O–CTAB–butanol system. *Appl. Catal. A* **253** (2003) 461

22. **Huybrechts, W., Vanbutsele, G., Houthoofd, K.J., Bertinchamps, F., Laxmi N.C. S., Gaigneaux, E.M, Thybaut, J. W., Marin, G.B., Denayer, J.F.M., Baron, G.V., Jacobs, P.A., Martens**, **J.A.** *Catal. Lett.***100** (2005) 235.

23. **Keogh, R.A., Sparks, D., Hu, J., Wender, I., Tierney, J.W.** Hydroisomerization and Hydrocracking of n-Hexadecane over a Platinum-Promoted Sulfated Zirconia Catalyst *Energy Fuels* **8** (1994) 755.

24. **Keogh, R.A., Davis, B.H.,** Hydroconversion of n -hexadecane with Pt-promoted monoclinic and/or tetragonal sulfated zirconia catalysts. *Catal. Lett.* **57** (1999) 33.

25. **Kerr, G.T., Kokotailo**, **G.T.** Sodium Zeolite Zk-4, A New Synthetic Crystalline Aluminosilicate *J. Am. Chem. Soc*. **83** (1961) 4675.

26. **Kresge, C.T., Leonowicz, M.E., Roth, W.J., Vartuli, J.C., Beck, J.S.** Ordered mesoporous molecular sieves synthesized by a liquid-crystal template mechanism. *Nature* **359** (1992) 710.

27. **Kuehl, G.H.** Synthesis of ZSM-12 Zeolite. *US Patent No* **4482531** (1984)
28. **Kuehl, G.H.** Synthesis of ZSM-12 Zeolite. *US Patent No* **4559213** (1985)
29. **Lin, S., Ning, H., Wan-Fu, S., Wei-Min, L., Qun-Ji, X.** Preparation of Pd/Al-MCM-41 catalyst and its hydroisomerization properties for long chain alkane compounds. *Stud. Surf. Sci. Catal.* **141** (2002) 517.
30. **Maesen, Th.L.M., Schenk, M., Vlugt, T.J.H., de Jonge, J.P., Smit, B.** The Shape Selectivity of Paraffin Hydroconversion on TON-, MTT-, and AEL-Type Sieves. *J. Catal.* **188** (1999) 403.
31. **Martens, J.A., Souverijns, W., Verrelst, W., Parton, R., Froment G.F.** and **Jacobs, P.A.** Selective Isomerization of Hydrocarbon Chains on External Surfaces of Zeolite Crystals (pages 2528–2530). *Angew. Chem. Int. Ed. Engl.* Vol. **34,** Issue 22 (1995) 2528
32. **Moini, A.** and **Valyocsik, E.W.** Synthesis of Crystalline Silicate ZSM-12. *US Patent No* **5192521** (1993)
33. **P. Leprince**, *Conversion Processes*, **Vol. 3**, Editions TECHNIP, (2001) 229.
34. **Rosinski, E.J., Rubin, M.K.** Synthesis of Crystalline ZSM-12. *US Patent No* **3832449** (1974)
35. **Rosinski, E.J., Rubin, M.K.** Preparation of ZM-12 Type Zeolites. *US Patent No* 4391785 (1983)
36. **Rubin, M.K.** Synthesis of Crystalline Silicate ZSM-12. *US Patent No* **4585637** (1986)
37. **Rubin, M.K.** Synthesis of Crystalline Silicate ZSM-12 using Dibenzyldimethyl Cations and the Product Produced. *US Patent No* **4636373** (1987)
38. **Rubin, M.K.** Synthesis of Crystalline ZSM-12 Type Structure. *US Patent No* **2021141** (1991)
39. **Sequeira, A., Jr.**, *Lubricant Base Oil and Wax Processing* Marcel Dekker, Inc., Chemical Industries Series, 1994.
40. **Sinha, A.K., Sivasanker, S., Ratnasamy, P.** Hydroisomerization of n-Alkanes over Pt−SAPO-11 and Pt−SAPO-31 Synthesized from Aqueous and Nonaqueous Media. *Ind. Eng. Chem. Res.* **37** (1998) 2208,
41. **S.J. Miller**, U.S. Patent application **0077209** (2005).

42. **Souverijns, W., Martens, J.A., Froment, G.F., Jacobs, P.A.** Hydrocracking of Isoheptadecanes on Pt/H–ZSM-22: An Example of Pore Mouth Catalysis. *J. Catal*. **174** (1998) 177

43. **Subotic, B., Bronic, J., Antonic, T., Treacy, M.M.J., Marcus, B.K., Bisher, M.E., Higgins J.B.,** *Proc. 12th Int. ZeoliteConf., Materials Research Society*, Warrendale, PA, 1999, p. 2057.

44. **Sugi, Y**., Shape Selective Alkylation of Polynuclear Aromatics. *Catalysis Today*, 1994, **19**, 187-212.

45. **Szostak, R.** Preparation of crystalline Silicate ZSM-12. *US Patent No* **4585639** (1986)

46. **Szostak**, **R.** *Molecular Sieves: Principles of Synthesis and Identification*, Van Nostrand Reinhold, New York, 1989;

47. **Szostak**, **R.** *Handbook of Molecular Sieves*, Van Nostrand Reinhold, New York.

48. **Trap, M., van Bokhovan, J.A., Oostenbrink, M.T.G., Bitter, J.H., deJong, K.P., Koningsberger**, **D.C.** Influence of the Generation of Mesopores on the Hydroisomerization Activity and Selectivity of n-Hexane over Pt/Mordenite. *J.Catal.* **190** (2000) 209.

49. **Valyocsik, E.W.** Synthesis of Crystalline Silicate ZSM-12. *US Patent No* **5137705** (1992)

50. **Wen, M.Y., Wender, I., Tierney, J.W.** Hydroisomerization and hydrocracking of n-heptane and n-hexadecane on solid superacids. *Energy Fuels* **4** (1990) 372.

51. **Yadav, G.D.** and **Nair, J.J.** Sulfated zirconia and its modified versions as promising catalysts for industrial processes. *Micro. Meso. Mater.*, **33** (1999), 1.

52. **Yoo, K., Kashfi, R., Gopal, S., Smirniotis, P.G., Gangoda, M., Bose, R.N.** TEABr directed synthesis of ZSM-12 and its NMR characterization. *Microporous and Mesoporous Materials* **60** (2003), 57

53. **Zhang, S., Zhang, Y., Tierney, J.W., Wender, I.** Hydroisomerization of normal hexadecane with platinum-promoted tungstate-modified zirconia catalysts. *Appl. Catal. A* **193** (2000) 155.

54. **Zones Jr., S., Burton, A.W.**, Zeolite SSZ-54 composition of matter and synthesis thereof. US Patent **6,676,923** (2004).